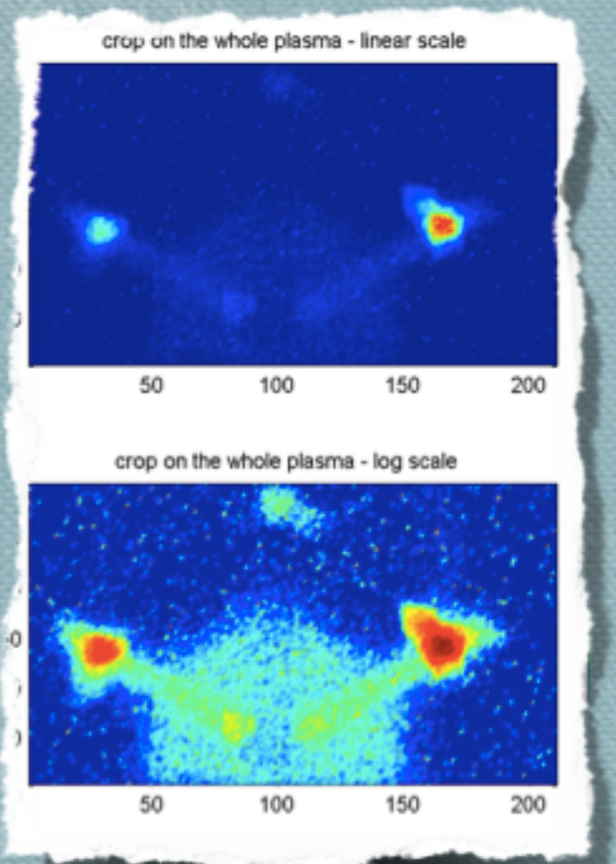

INFN
Istituto Nazionale di Fisica Nucleare

ICIS2015
16th International Conference on Ion Sources
August 23-28, 2015
New York City

MTA atomki

David Mascali, G. Castro, S. Biri, R. Rácz, J. Pálinkás, C. Caliri, L. Celona, L. Neri, P. Romano, G. Torrisi, and S. Gammino

Electron Density and Temperature measurements in Electron Cyclotron Resonance Ion Source plasma by means of X-ray spectroscopy and X-ray imaging

Outline

- Introduction
- Experimental set-up
- Volumetric measurements
- Space-resolved measurements
- Modeling and discussion

Some questions...

- Does exist an "ECRIS fine structure" with respect to magnetic field and RF frequency tuning?

O. Tarvainen et al. Plasma Sour. Sci. Tech. 2014

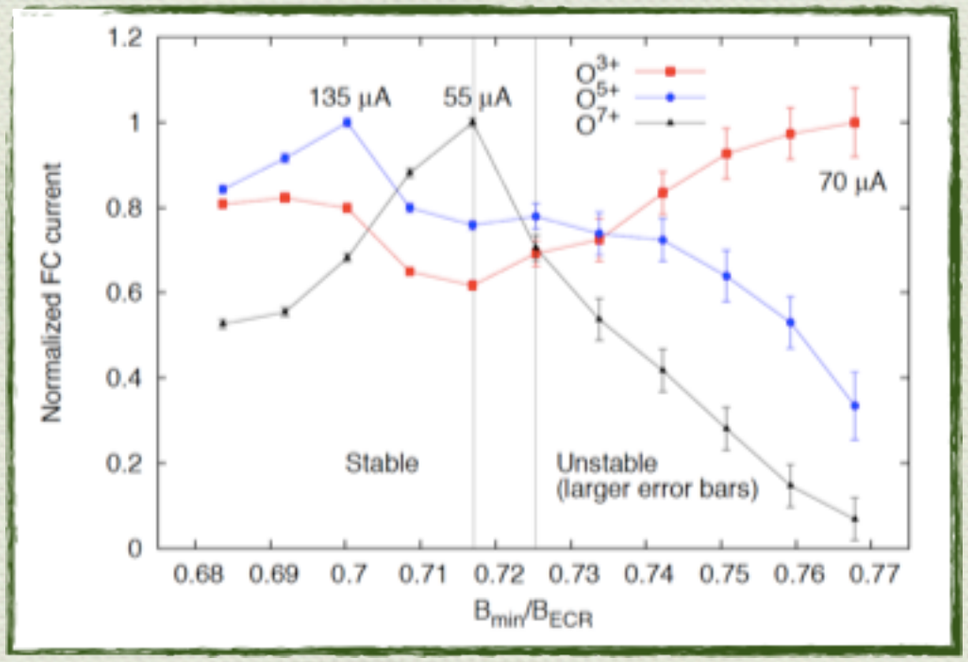

Evidences of plasma instabilities when tuning B

D. Mascali et al., Rev. Sci. Instrum. 2014

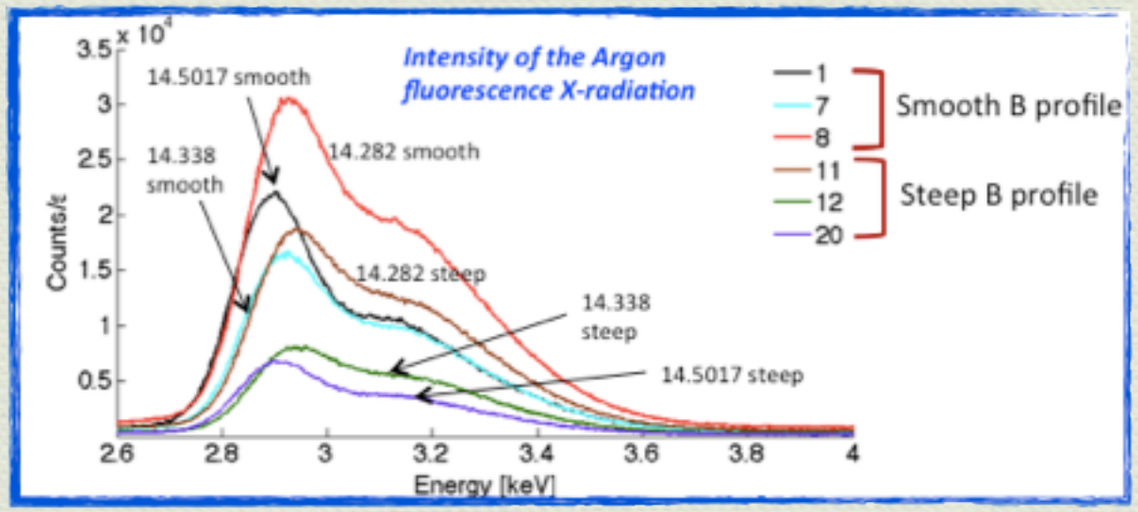

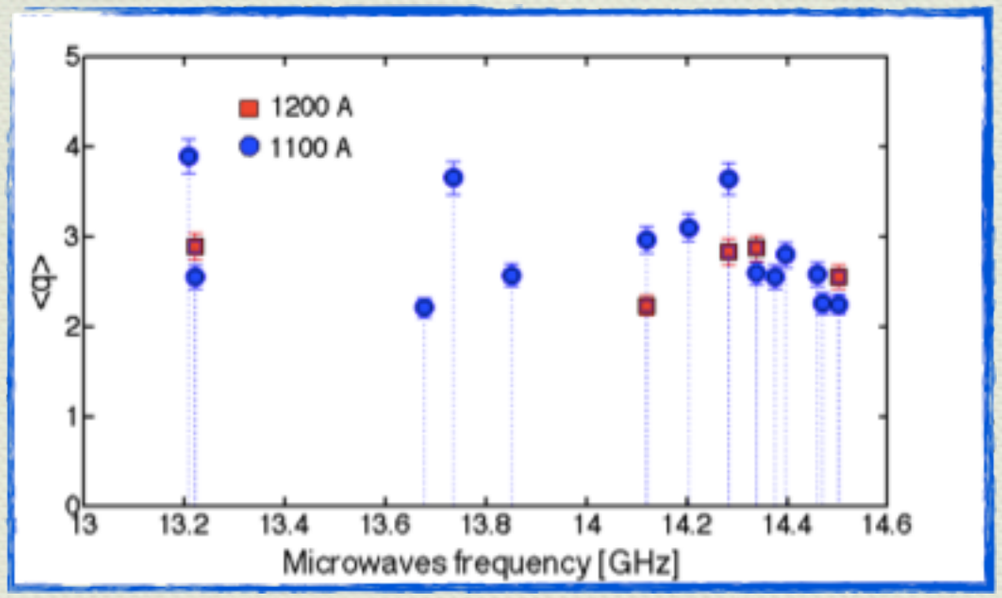

Evidences of strong fluctuations with the RF frequency correlated to X-ray emission

Some questions....

- Does exist an INTERPLAY between the plasma structure and the beam shape, brightness, emittance?

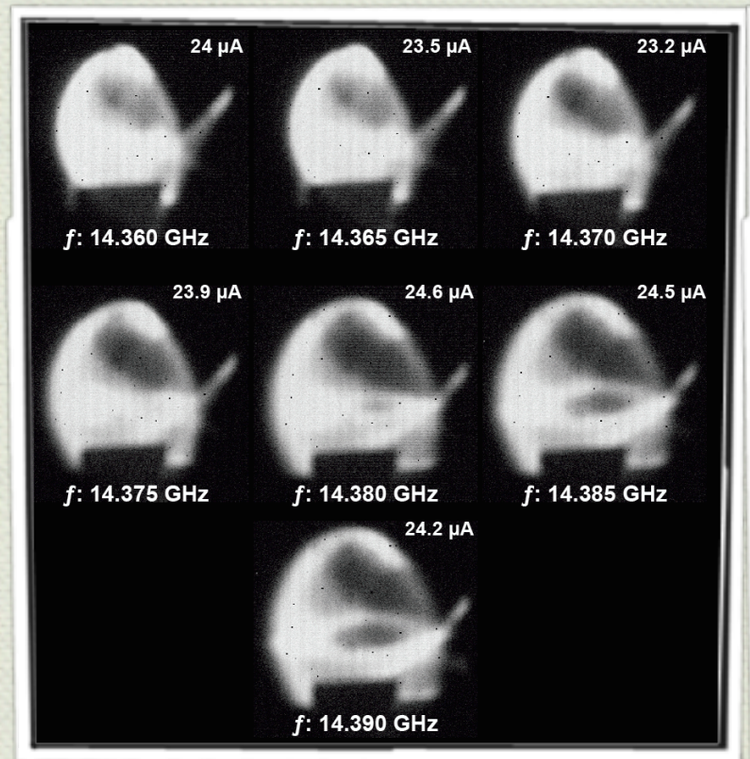

D. Nicolosi et al. This conference

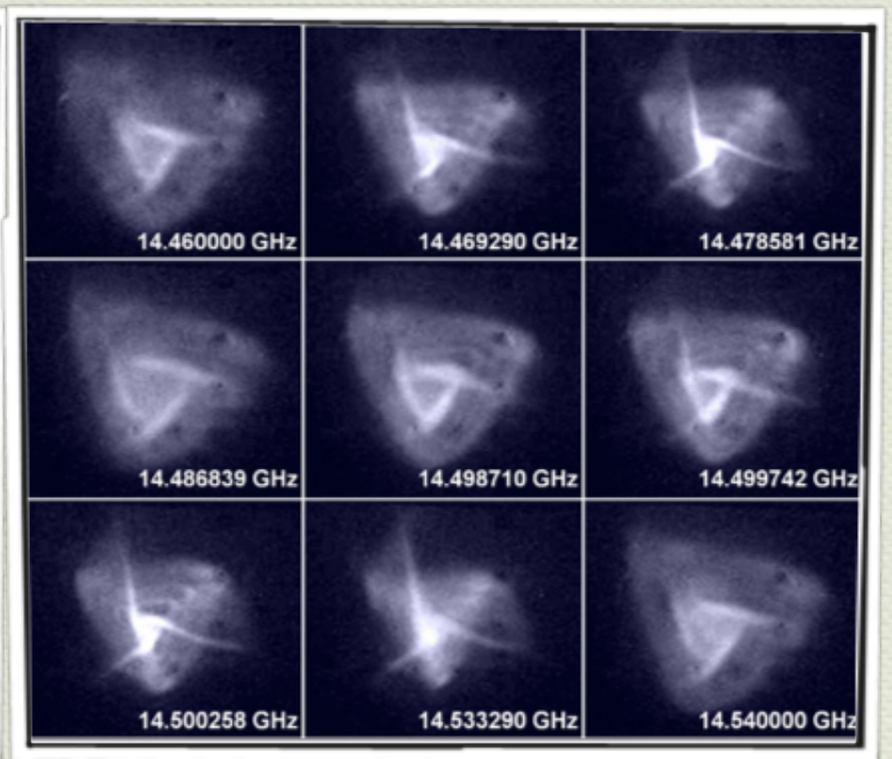

L. Celona et al., Rev. Sci. Instrum. 2008

sim. density

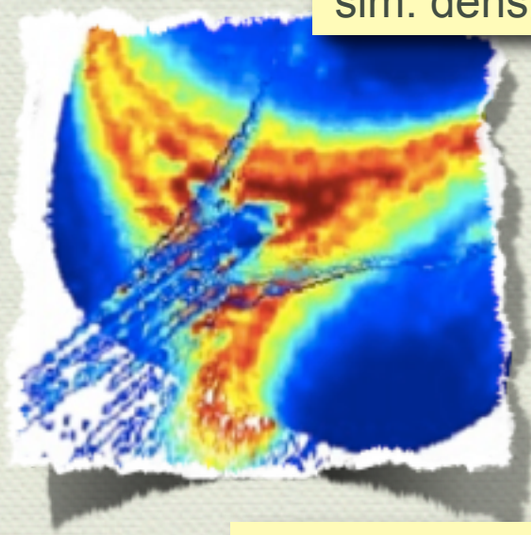

single mode distrib.

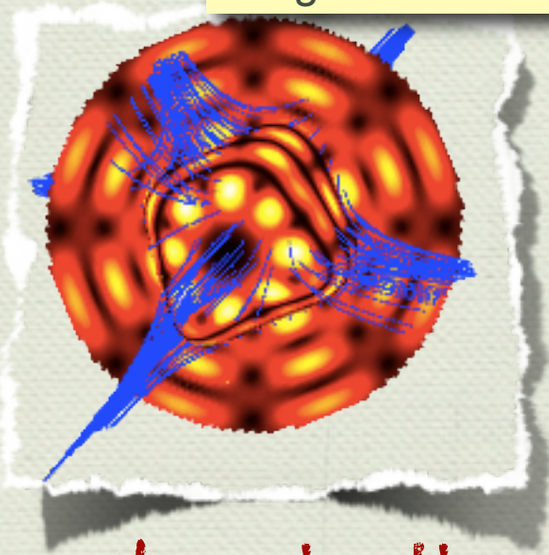

- Does the plasma distribute uniformly?
- Are electrons of different energy domains merged each other or not?

Non-intrusive plasma diagnostics methods

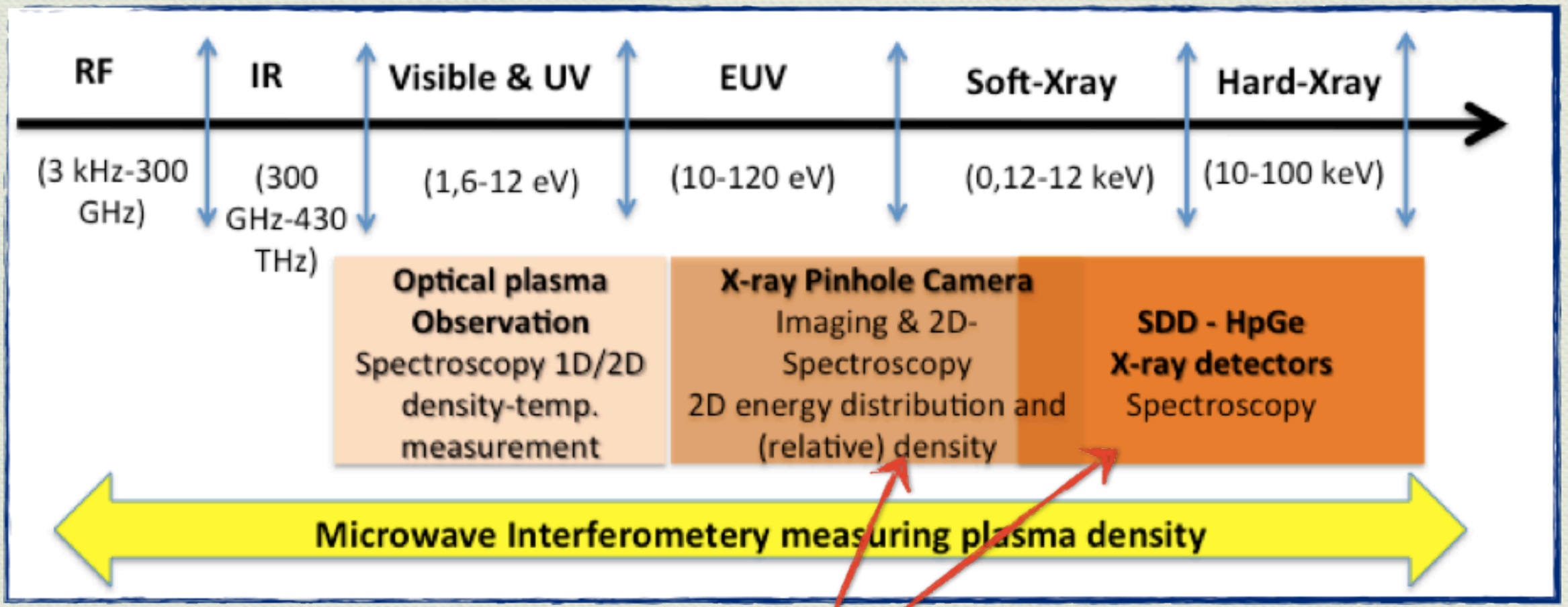

Measuring the plasma density in different energy regimes: density, temperature and plasma structure evaluation under different operative parameters

Exploring plasma structure: pionereering experiment in Atomki-Debrecen (2002-03)

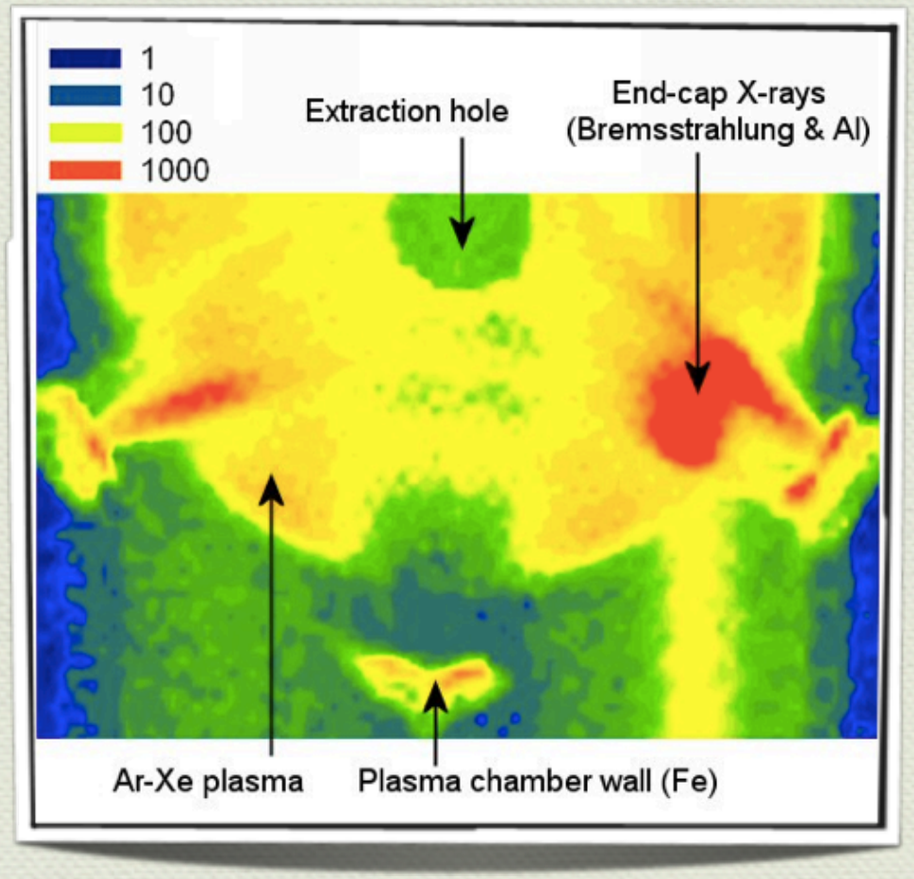

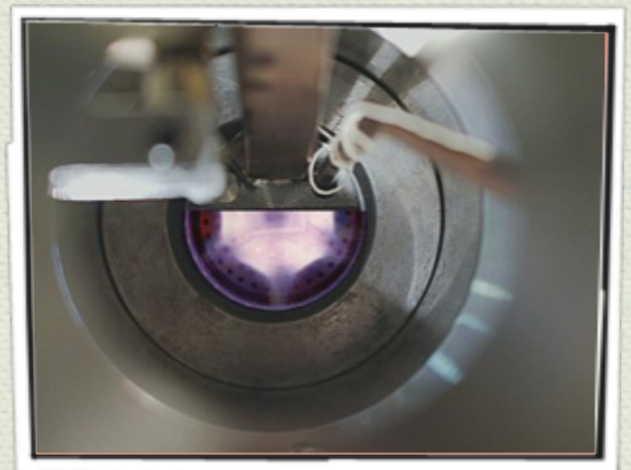

Plasma at optical inspection

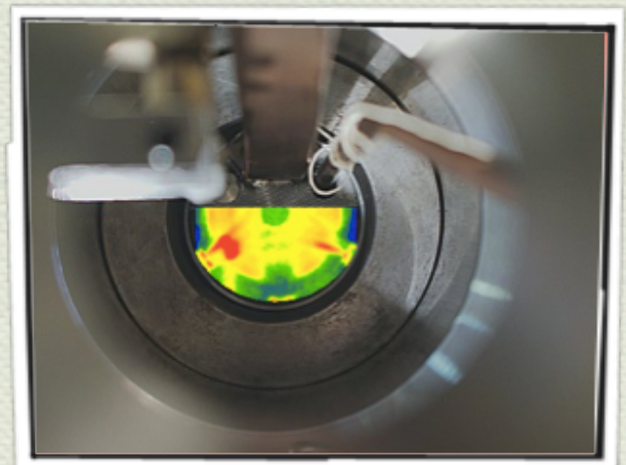

Plasma at X-ray inspection

- Full-size images (LCI plasmas) show the spatial placement of different X-ray sources (energetic electrons hit the chamber wall, plasma ions)

Experimental setup for simultaneous measurement of density, temperature and CSD

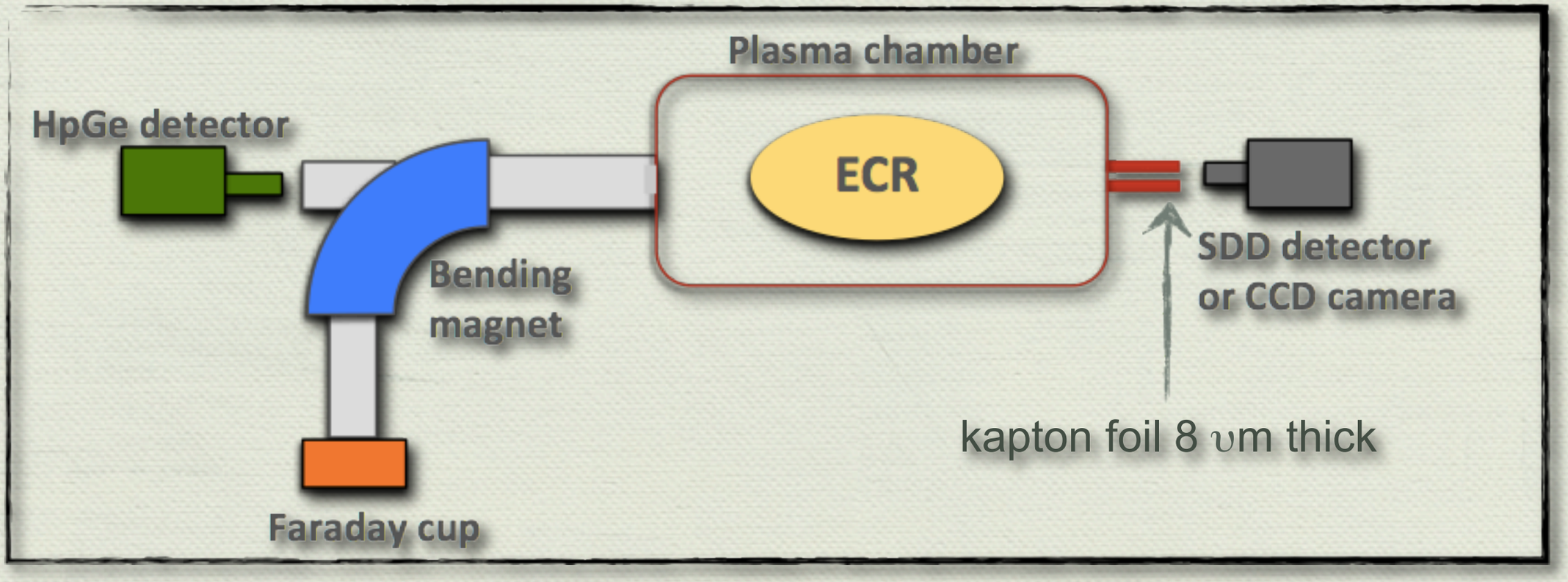

- Three detectors were used for a broad characterization of the EEDF:
  - HpGe for "hot electrons" E>30 keV
  - SDD for "warm electrons" 2<E<30 keV
  - CCD camera for imaging and 2D resolved spectroscopy 1<E<10keV

SDD - Setup

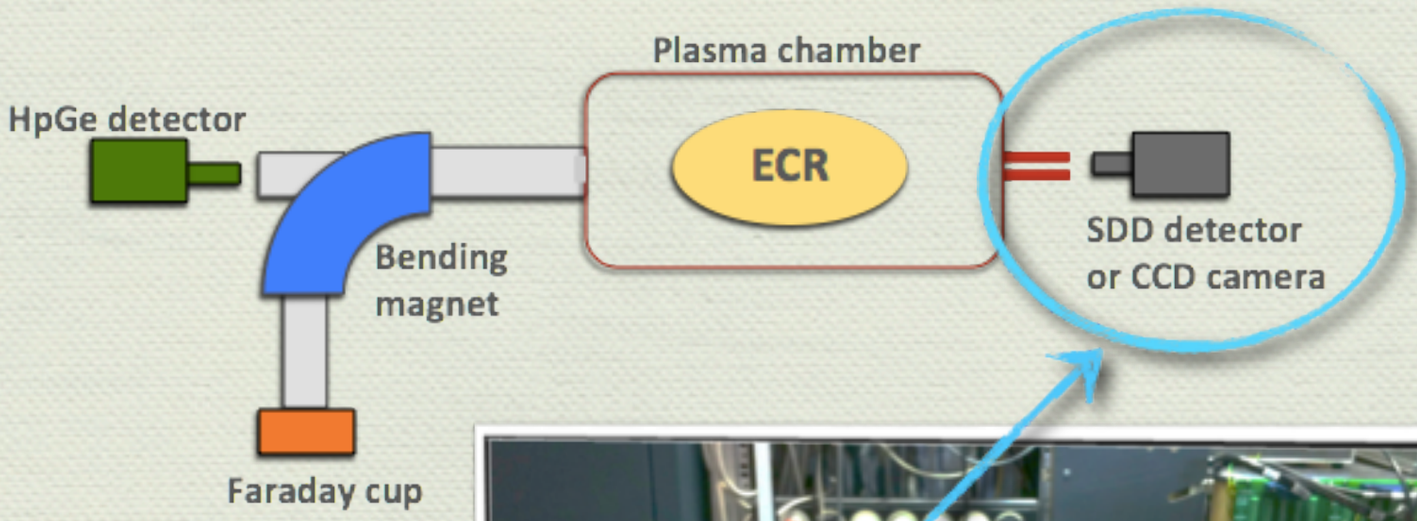

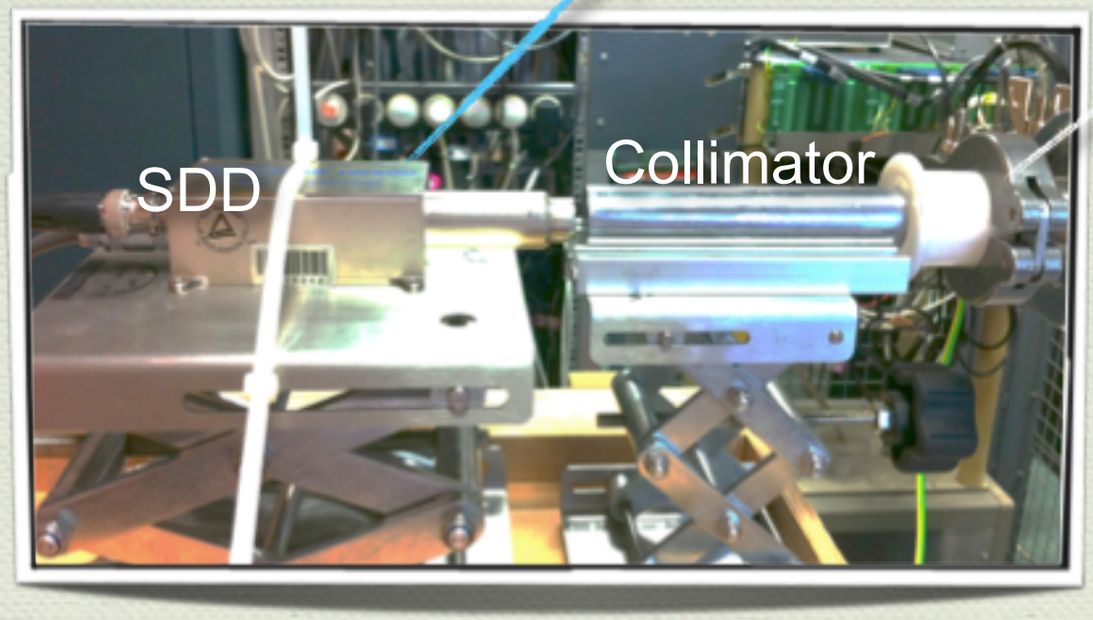

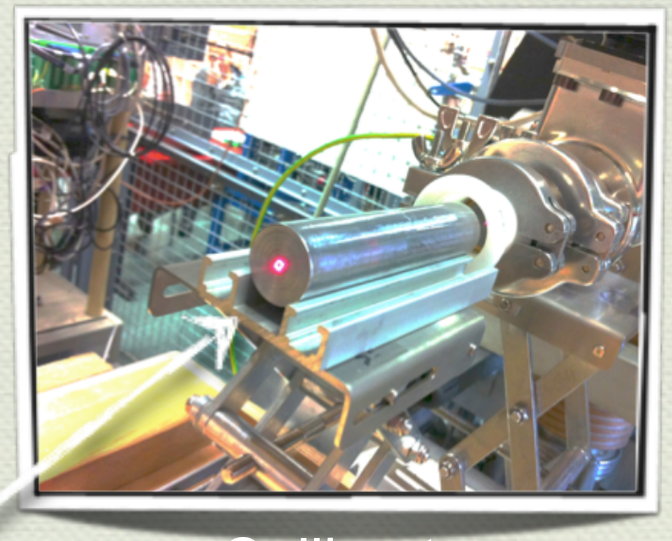

Collimator alignement

Bulk lead 155 mm long drilled collimator for near axis inspection

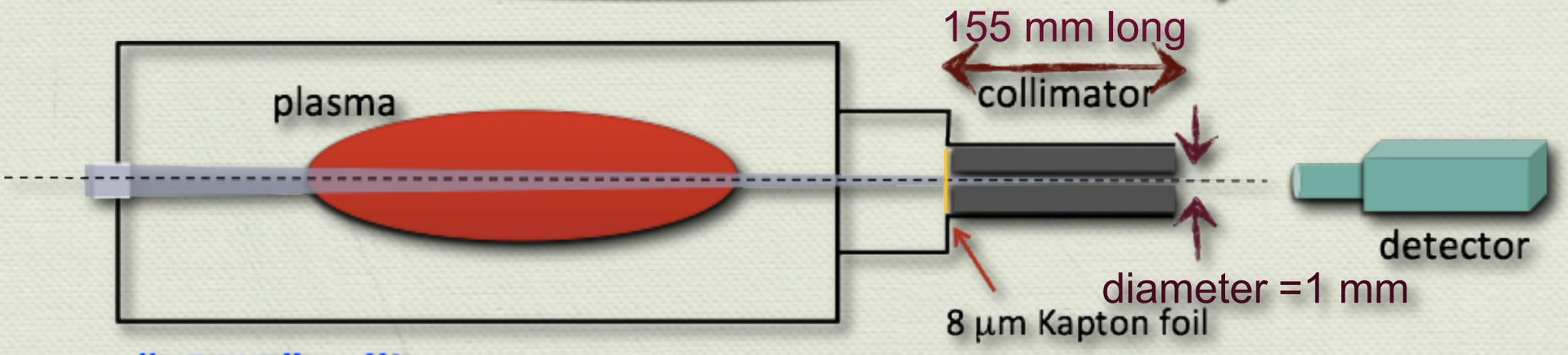

"LONG" collimator

SDD - Data Analysis

*Analysis procedure consists in evaluating the **Experimental Emissivity** after ε_g calculation, that must be then compared to the **Theoretical Emissivity** by fitting procedure.*

Exp. Emissivity

$$J(h\nu) = h\nu \frac{N^{ch}(h\nu)}{\varepsilon_g t} \frac{4\pi}{\Delta E V_p \Omega_{Tot}}$$

Theor. Emissivity

$$J_{M-K}(h\nu) = N_i N_e (Z\hbar)^2 \left(\frac{4\alpha}{\sqrt{6m_e}}\right)^3 \left(\frac{\pi}{kT_{Mw}}\right)^{1/2} e^{(-h\nu/kT_{Mw})}$$

$N_i N_e$: **Plasma density**

kT_{Mw}: **Plasma temperature**

SDD/HpGe - Parameters space

Freq. [GHz]
12,8
12,84
12,88
12,92
12,96
13
13,04
13,08
13,12
13,16
13,2
13,24
13,28
13,32
13,36
13,4

RF power
30 W

Ext. Voltage
10 kV (beam ON)

Coils (inj/mid/ext)
100% each
80% each
60% each

gas pressure
3,50E-06 mbar

Gas type
Argon
Argon+Oxygen

Observation of spectral density and temperature variation in the low/high energy part of the spectrum (warm electrons 1<E<30 keV; hot electrons 50<E<300 keV) versus RF frequency, coils setup (high/low mirror ratio), gas mixing.

Observation of the plasma structure by CCD based – pin-hole camera

(SDD) F.T.E. study

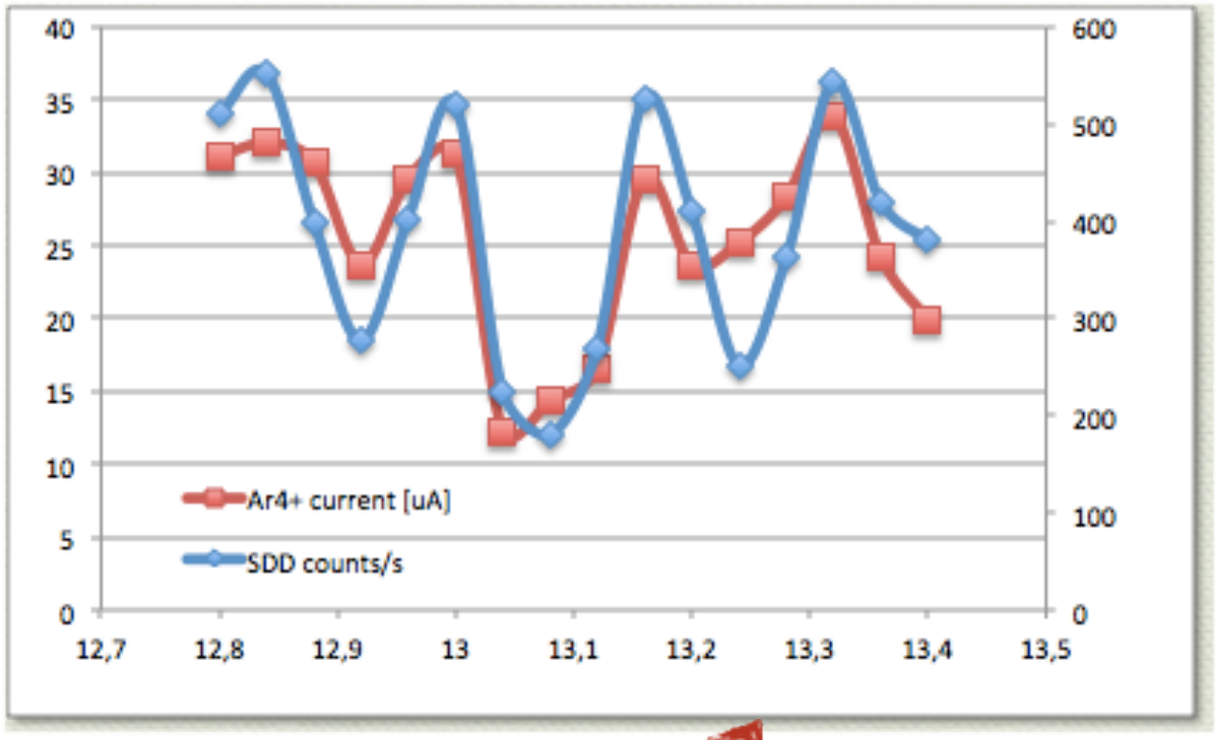

- Very Strong correlation (!!!) between Ar4+ current, X-ray flux and modal density
- Same number of "peaks", but with upshifted frequency (plasma effect).

Strong correlation among:
(i) Ar4+ current,
(ii) SDD counts/sec. and
(iii) e.m. modal density distribution

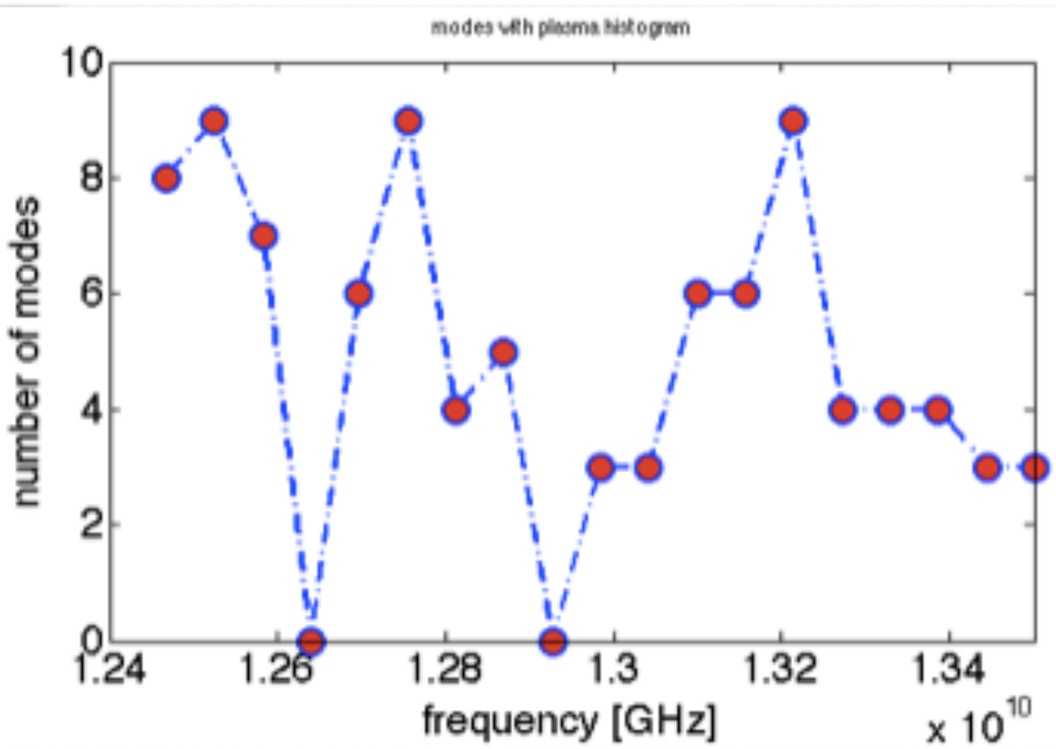

(SDD) F.T.E. study

<q>

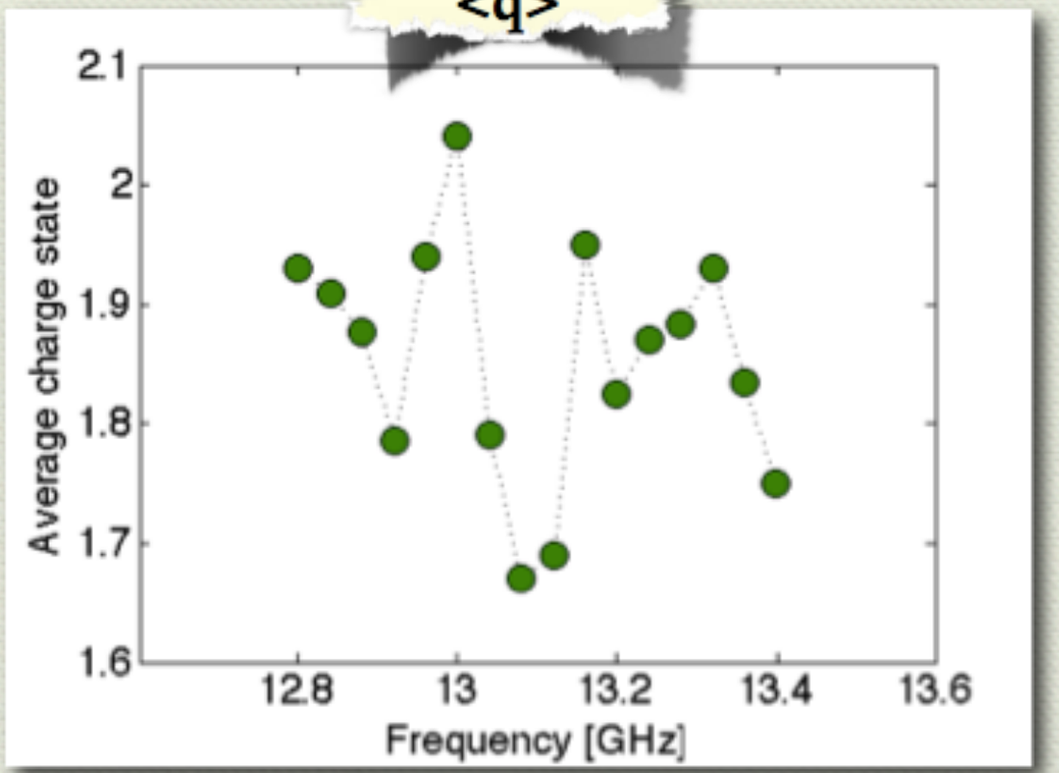

n_e

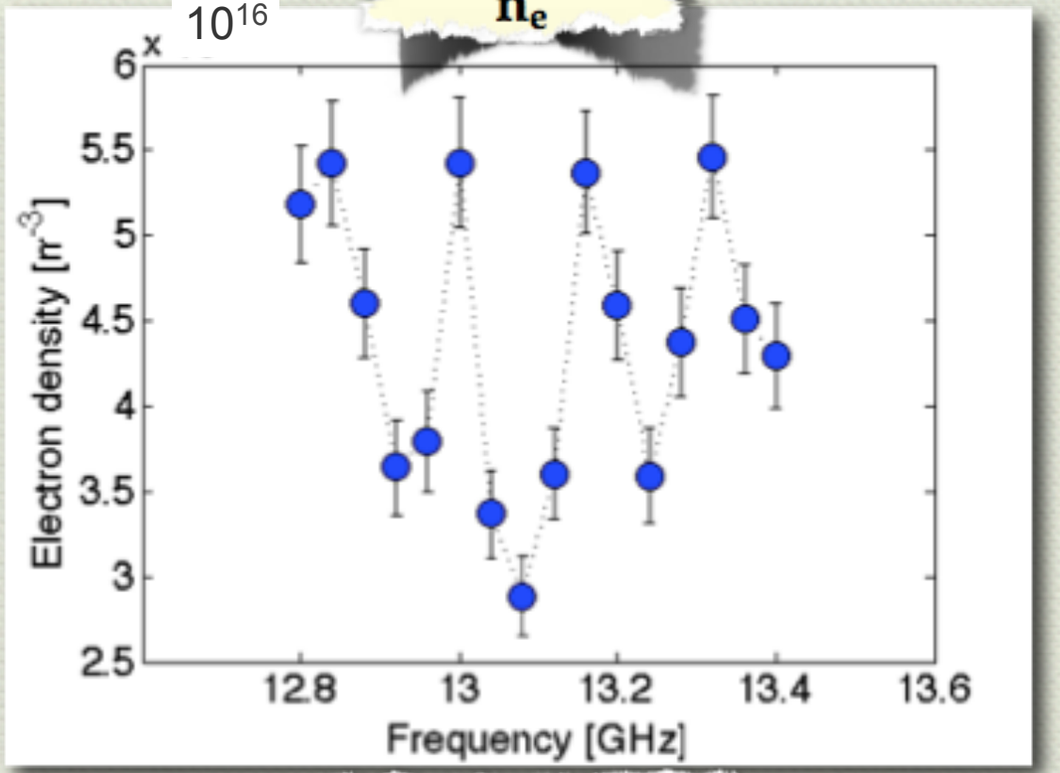

T_e

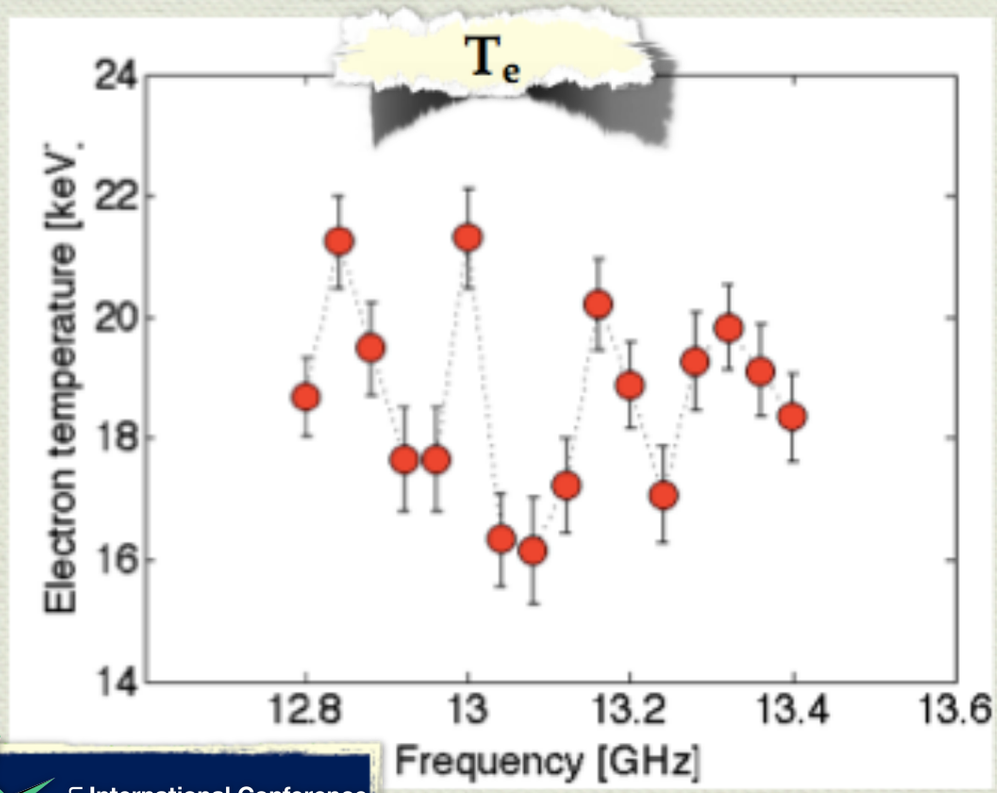

Modal density

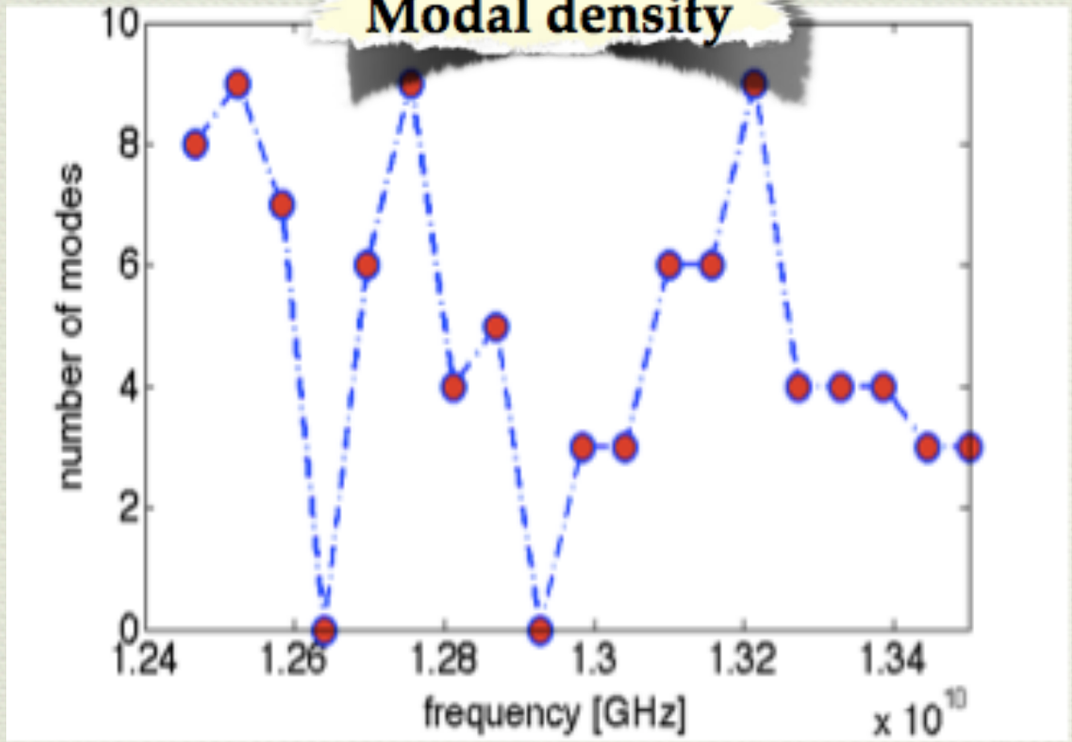

(SDD) F.T.E. study

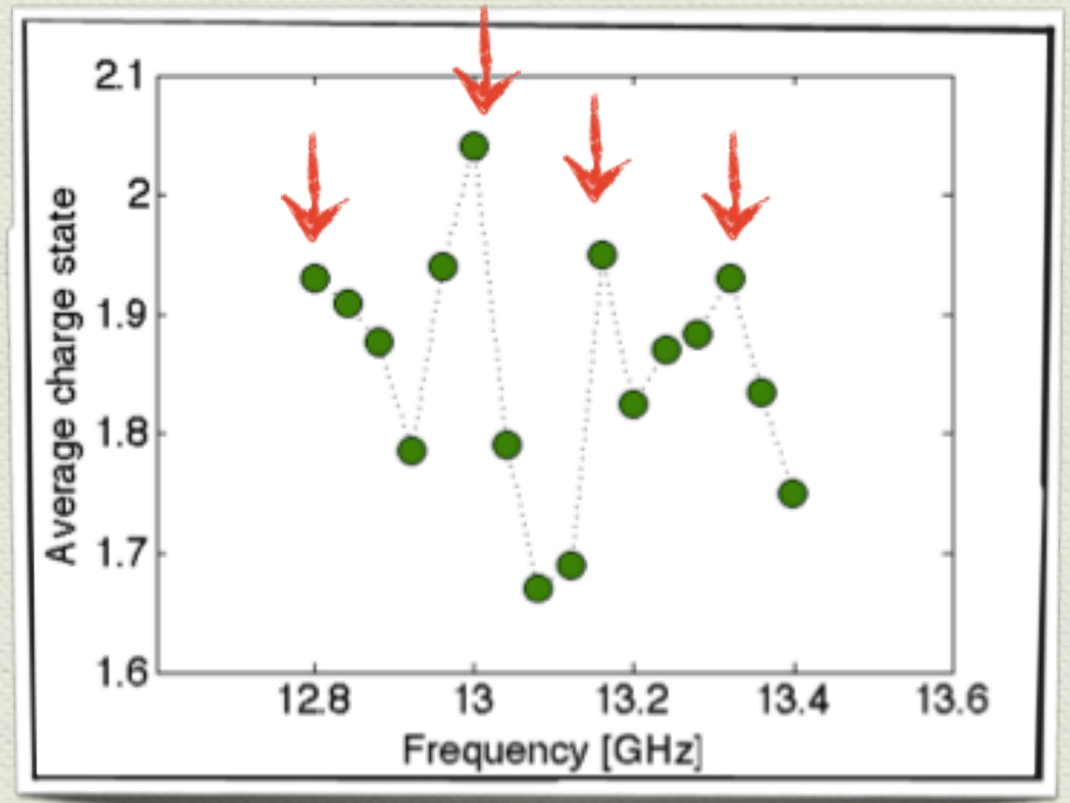

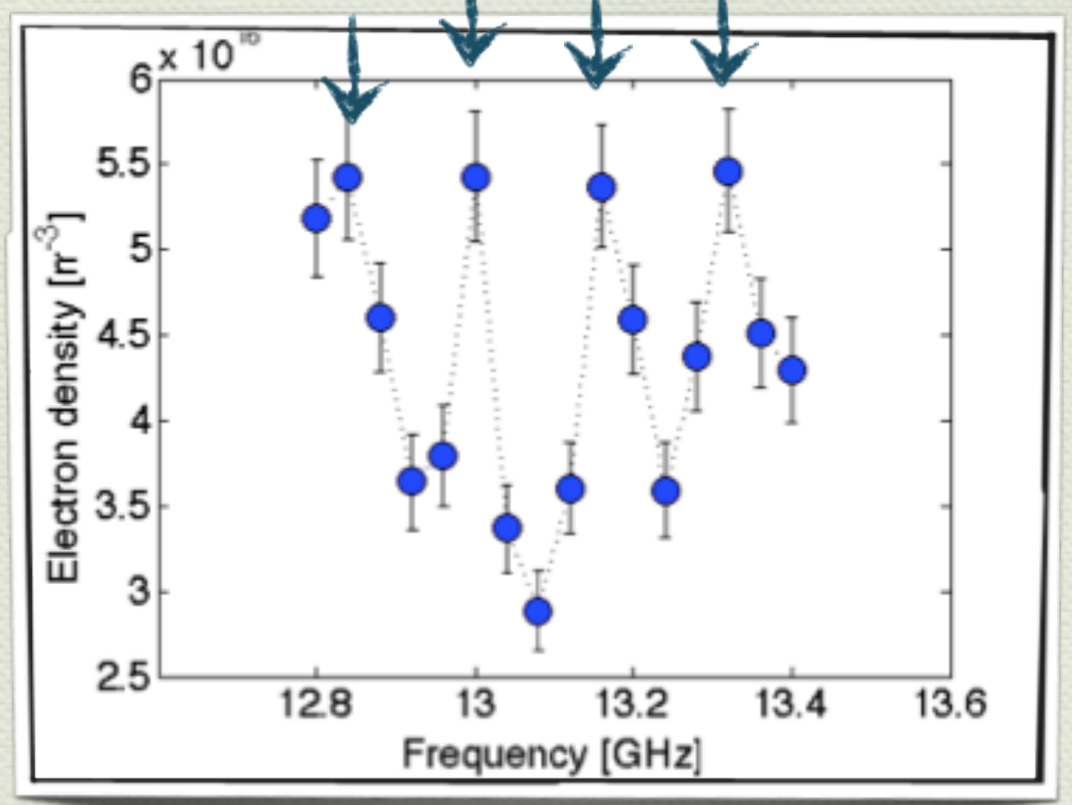

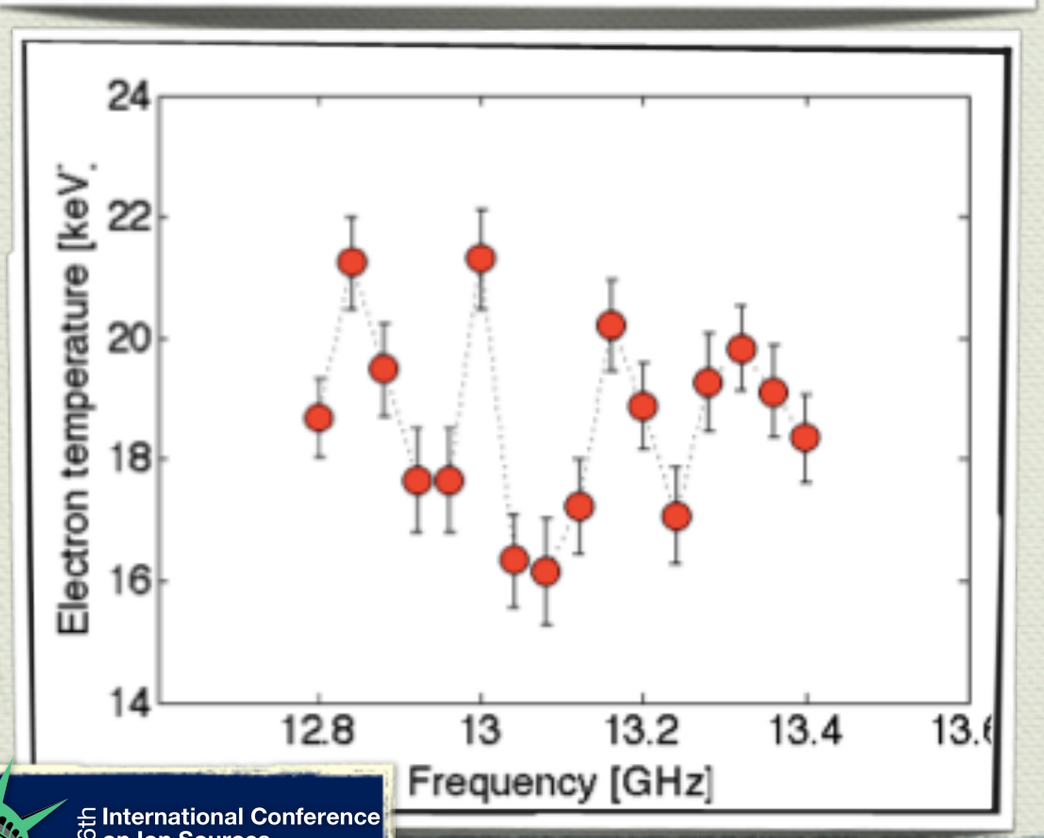

- Warm electron density
  range 2.5 - 5.5·10^{16} m^{-3}
- Warm el. temperature
  range 13-22 keV

CCD camera Set-up

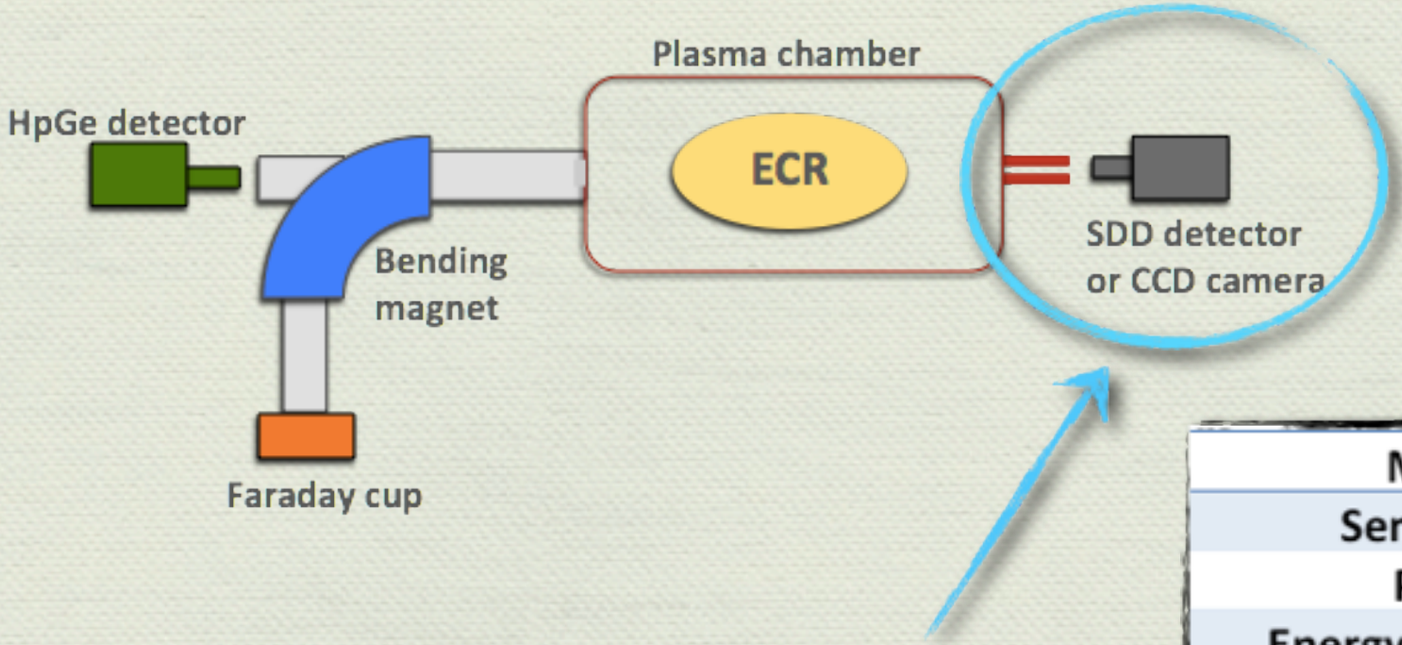

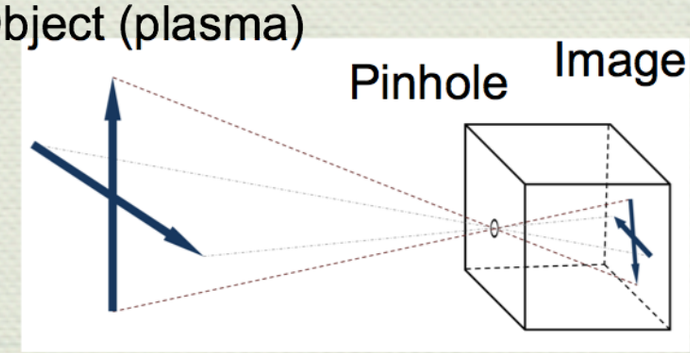

Model	Andor Technology - Newton
Sensor size	27.6 mm x 6.9 mm
Pixels	1024 x 255 (0.3 MP)
Energy Resolution	150 eV
Energy range	1-10 keV
Magnification	0.082-0.124-0.158
Pin-hole diameters	75 um and 100 um (W and Pb)

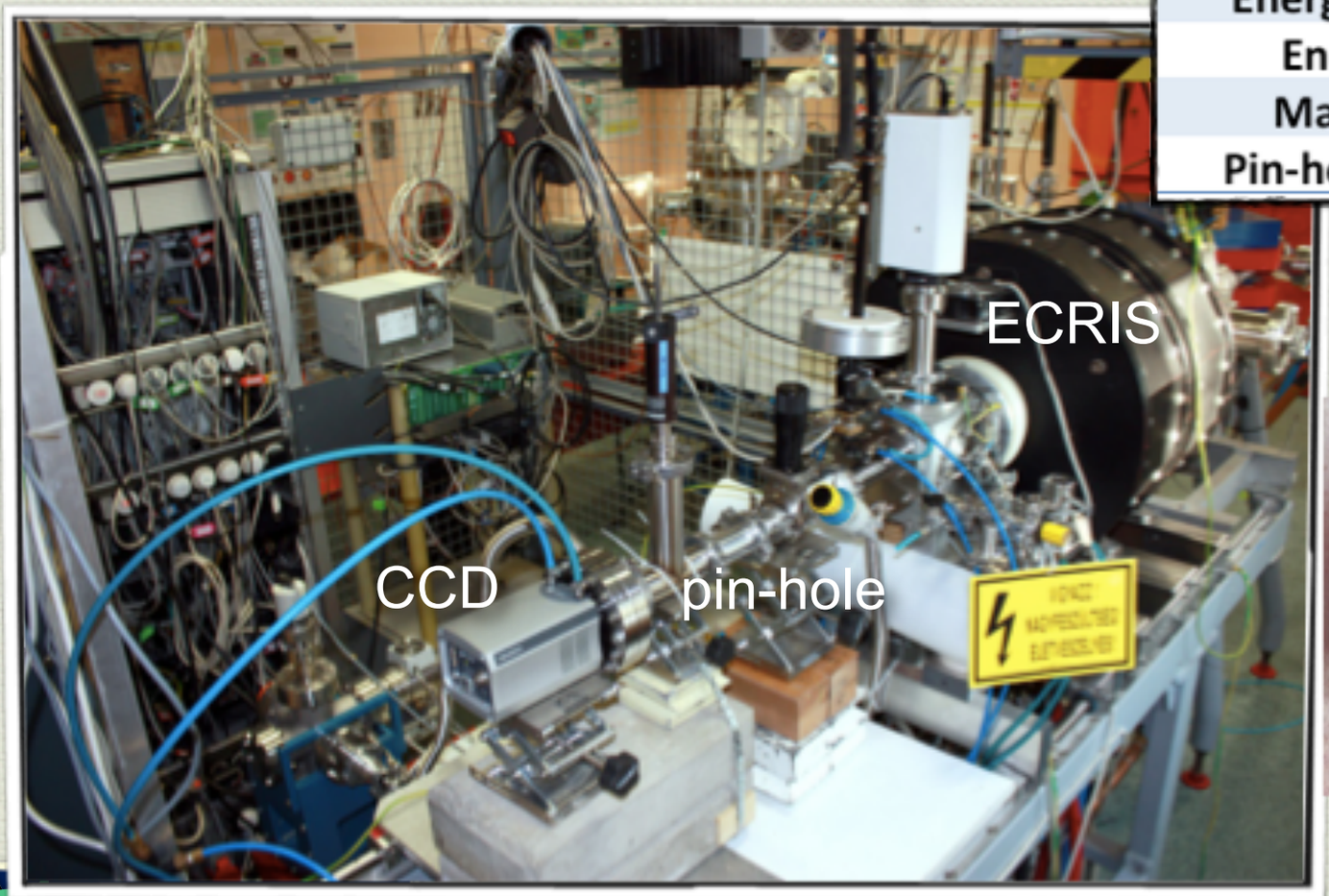

Pin-hole holder

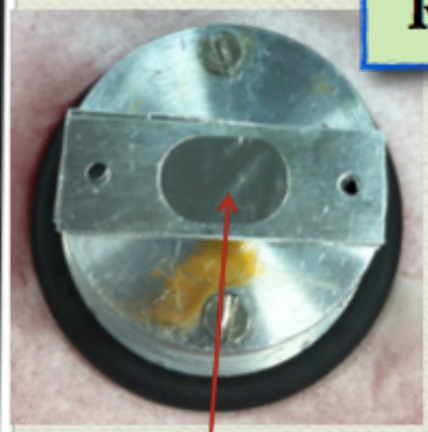

Aluminum Window

For more details see R. Rach et al. ThuPS09

X-ray imaging

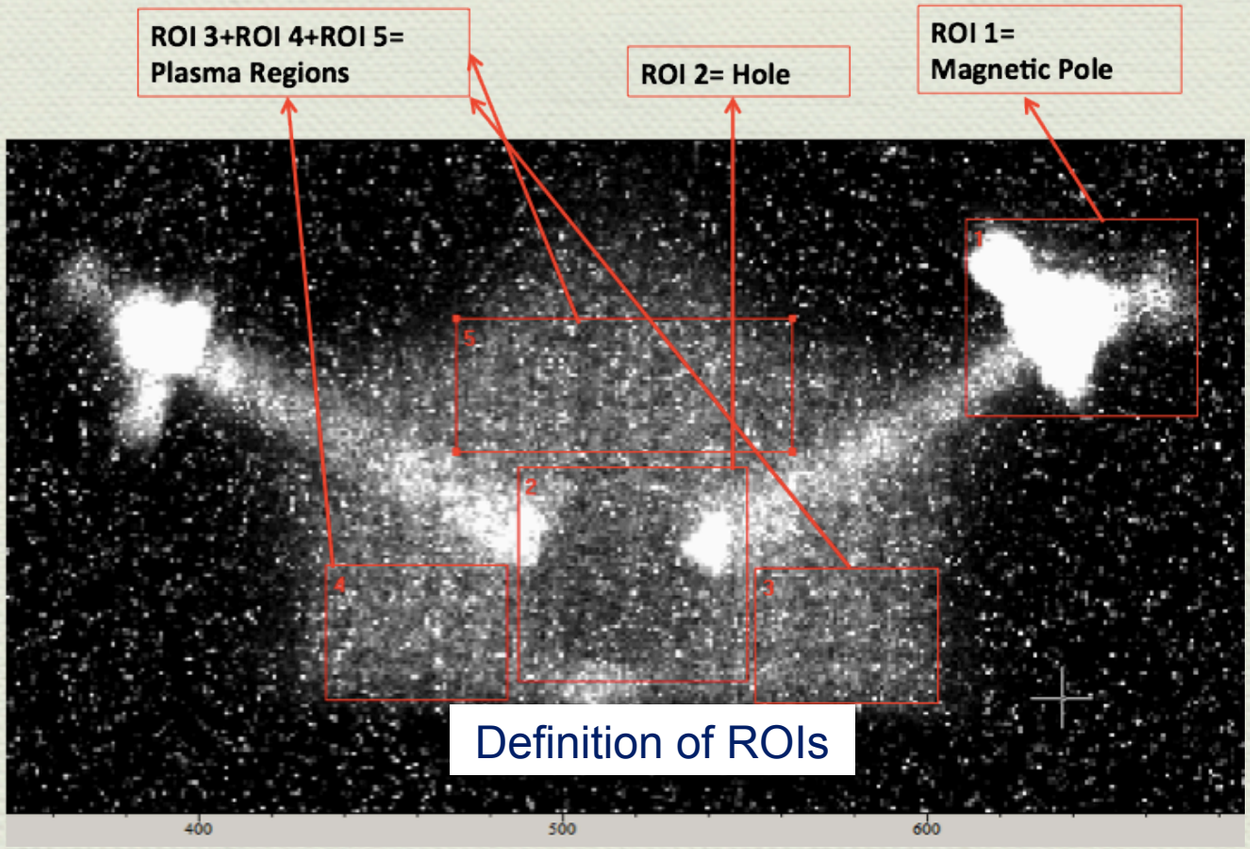

Definition of ROIs

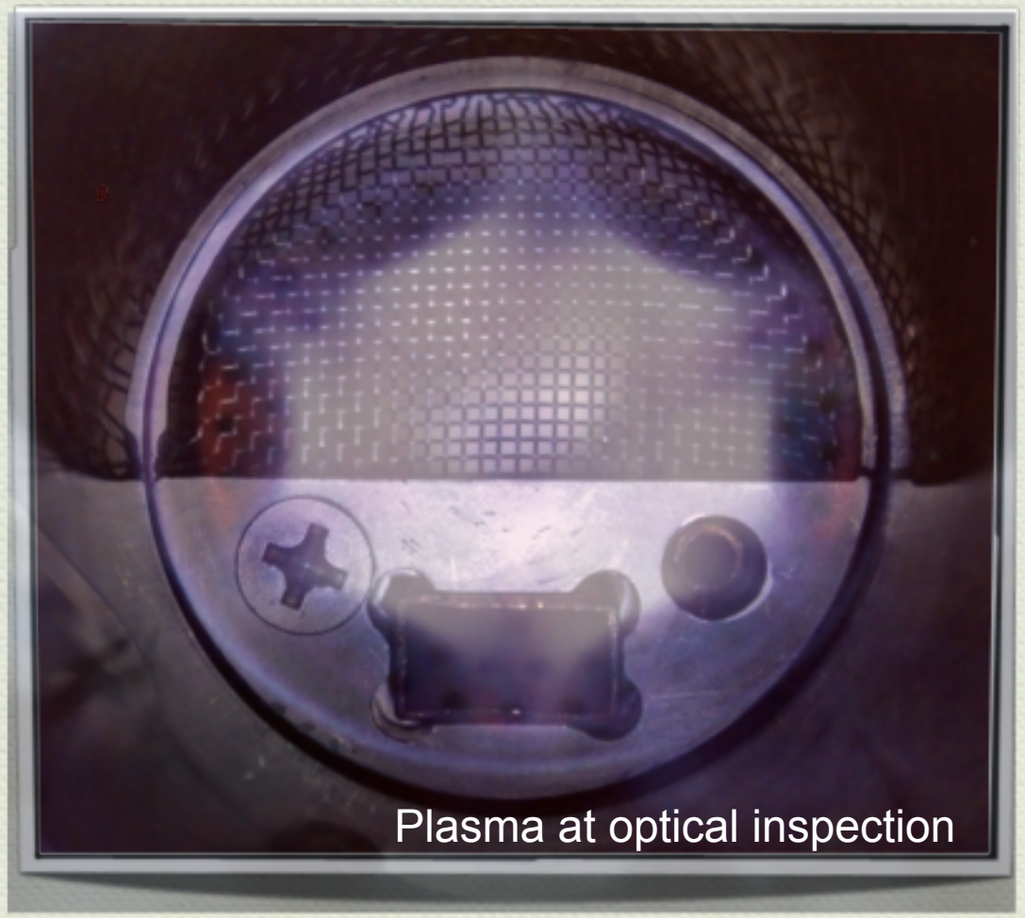
Plasma at optical inspection

- X-ray imaging: single frame acquisition, up to 30-40 sec. needed, no energy information;
- Photon Counting mode: from 10^{-5} to 0.3 sec., depending on the ROI.

- A Stainl-Steel grid was placed at injection edplate allowing plasma inspection
- Spatial resolution is high enough to find the mesh in X-ray images

X-ray imaging

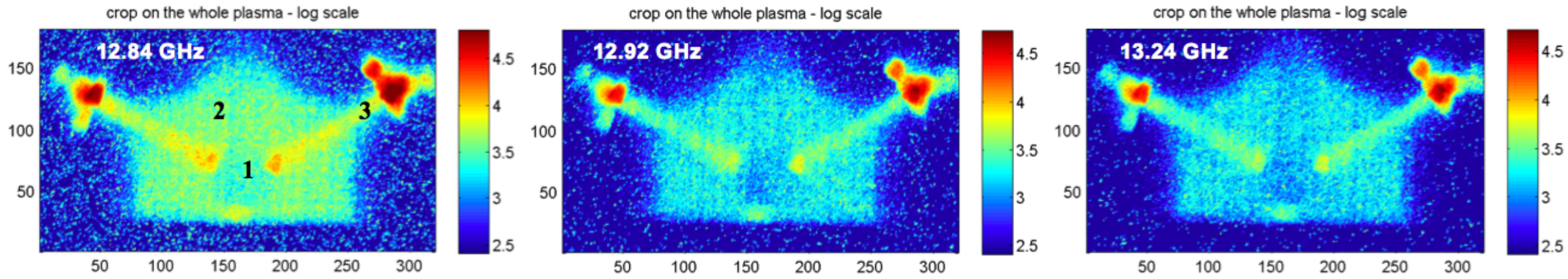

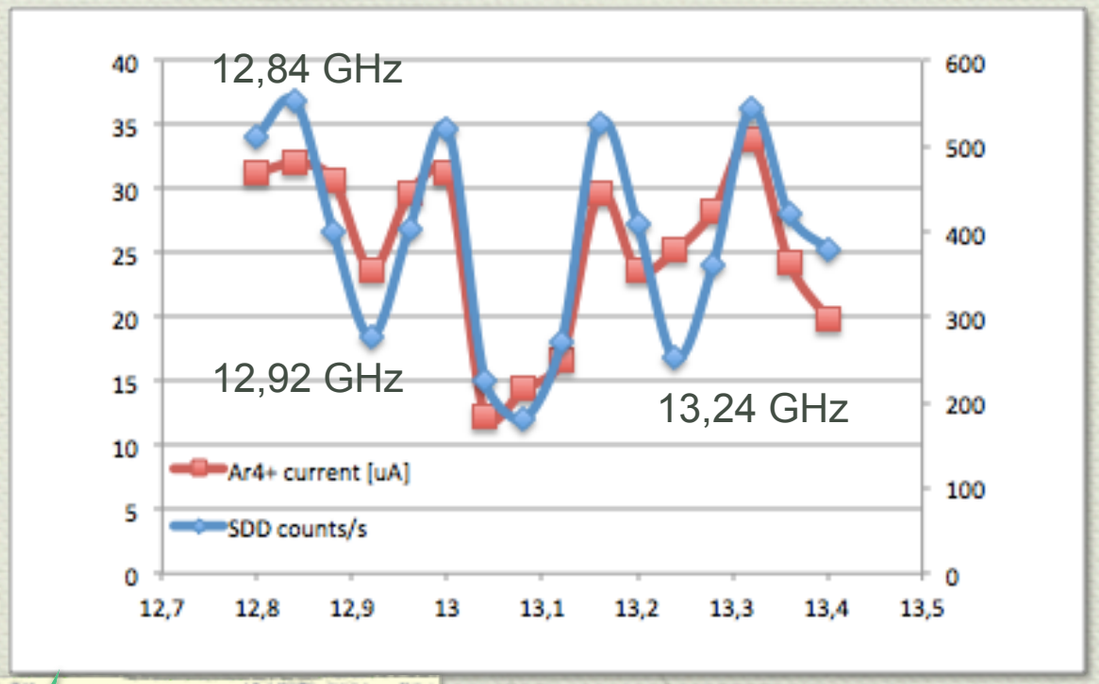

- From a general inspection of the pictures, it is clearly visible the structure of the plasma:
  - the hole in the near axis region
  - the branches due to the electrons escaping from the confinement
  - he hot spots due to lost electrons producing bremsstrahlung radiation when impinging on the chamber walls.

X-ray imaging

RF power [W]	Coils (inj/mid/ext)	gas pressure
30	100% each	3,30E-06

Acquisition Time 15 sec Gas: Argon

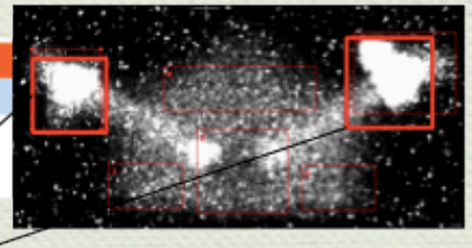

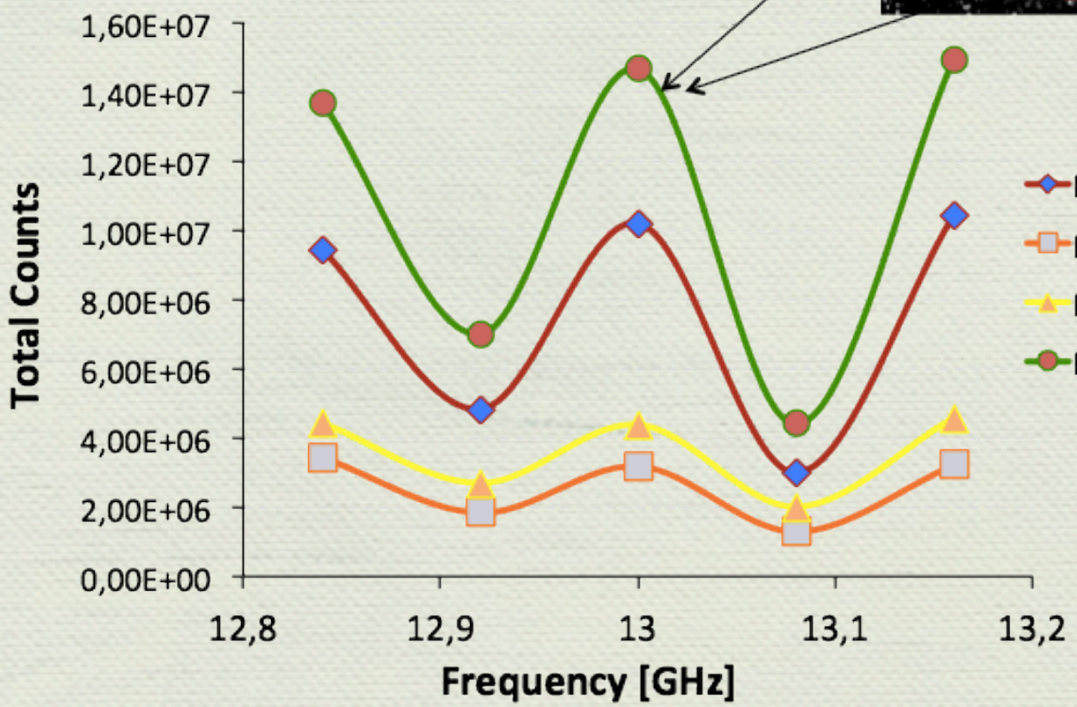

Rough evaluation of
X-ray E.C./ROI
where the energy content is
n-ph.el=flux x energy.

TRAP-Cad code was used to investigate the number of lost electrons vs. frequency, comparing them to exp. results

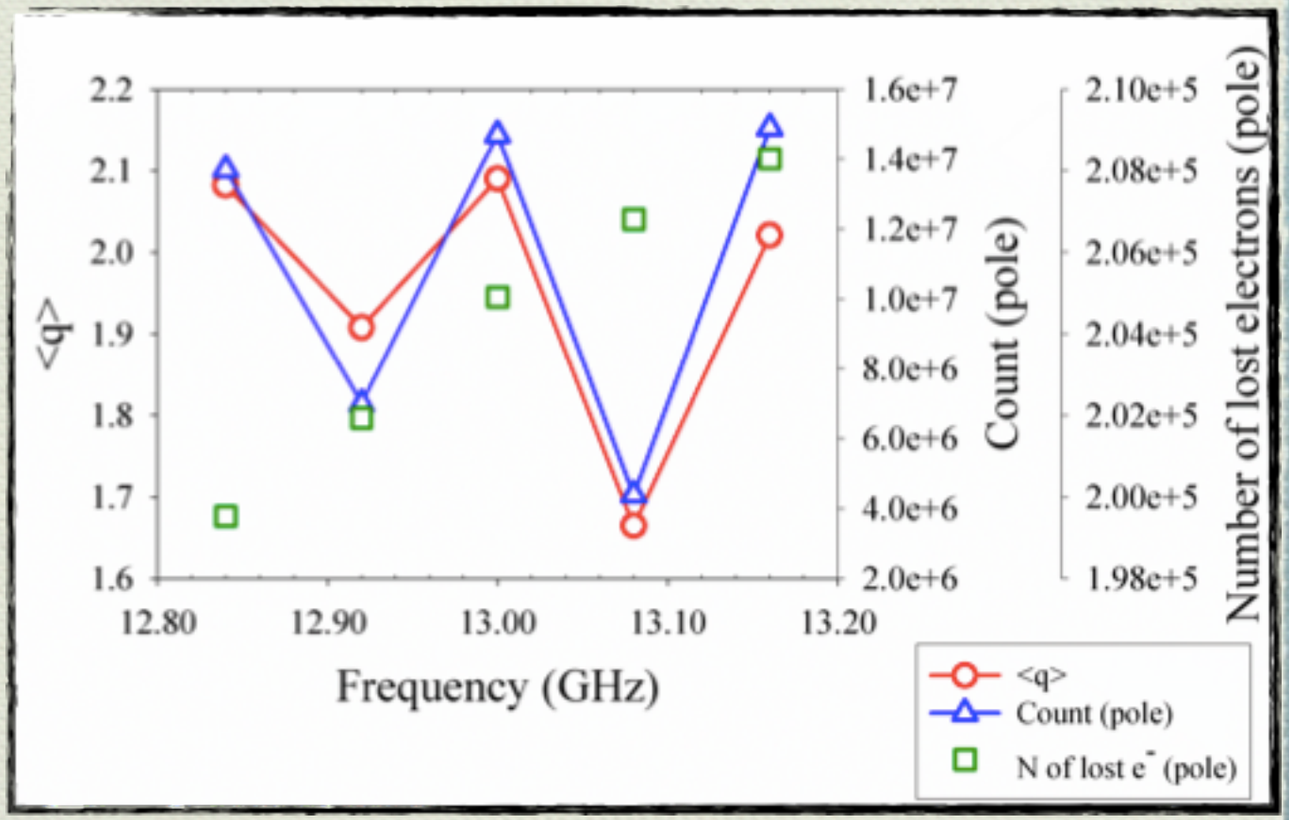

Plasma inspection by energy filtering

Selection of fluorescence lines for the extrapolation of the various elements displacement into the plasma → ***selection of the lines***

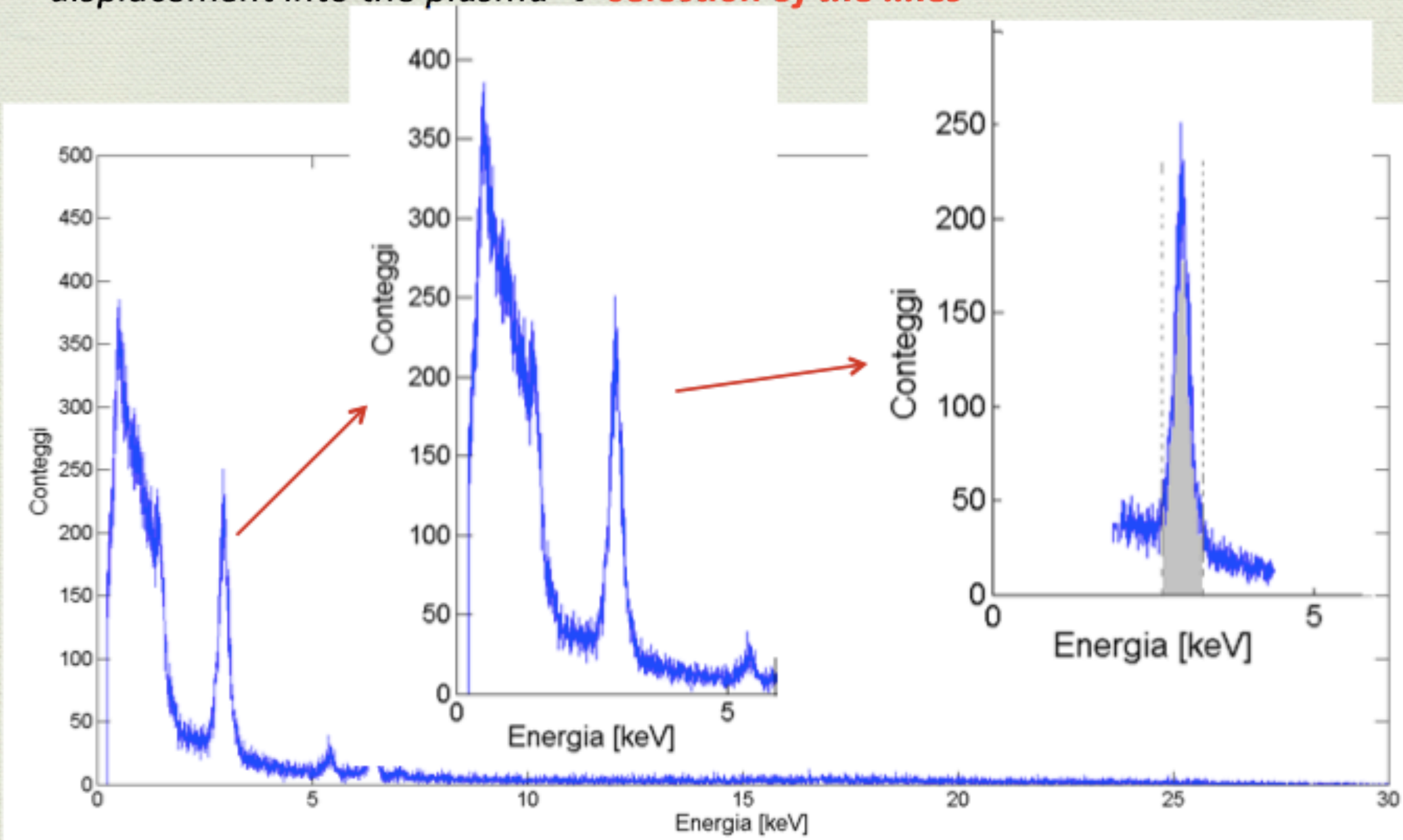

Plasma inspection after energy filtering

12.84 GHz - distribution at different energies

(equalized pseudocolor maps)

E<1.5 keV

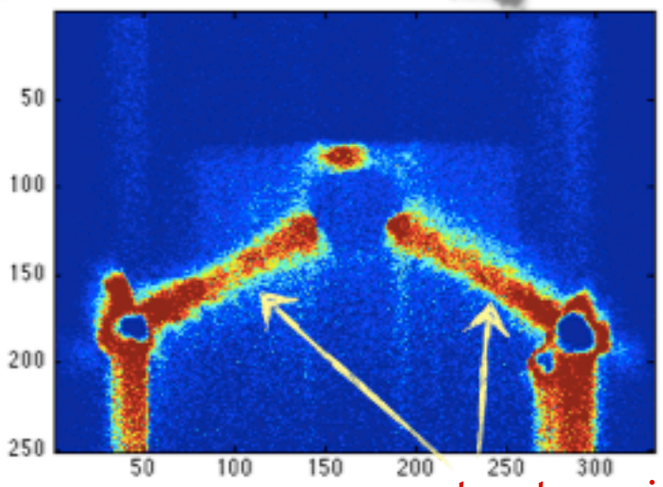

structures in the "arms"

1.5<E<2.5 keV

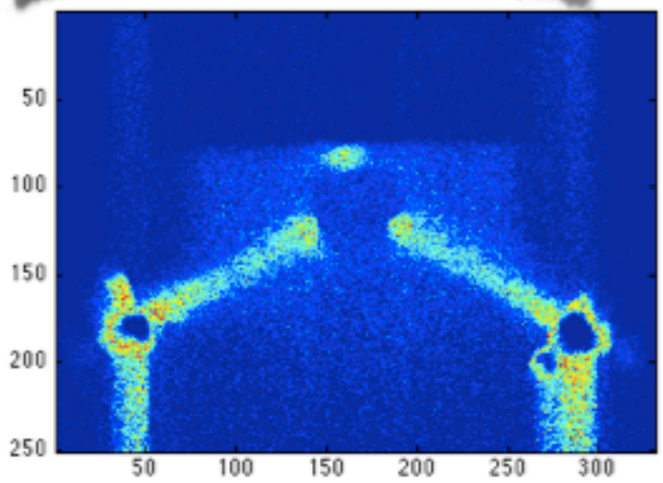

2.5<E<3.5 keV - Ar ions

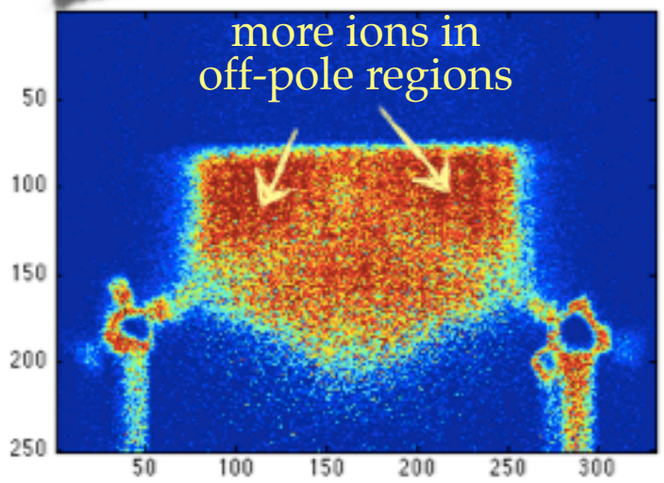

3.5<E<6.5 keV

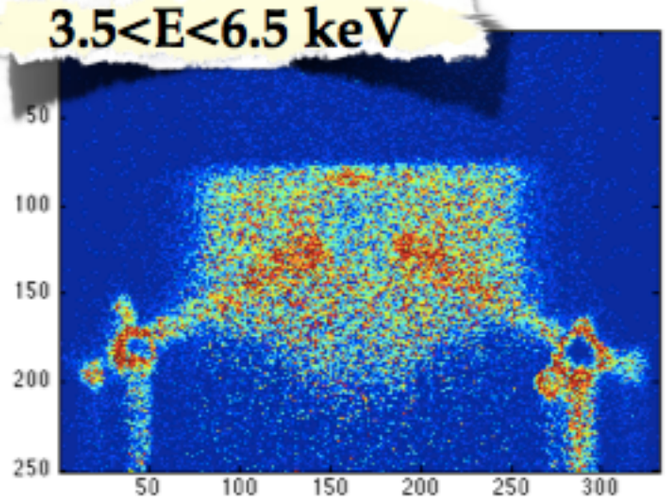

E>6.5 keV

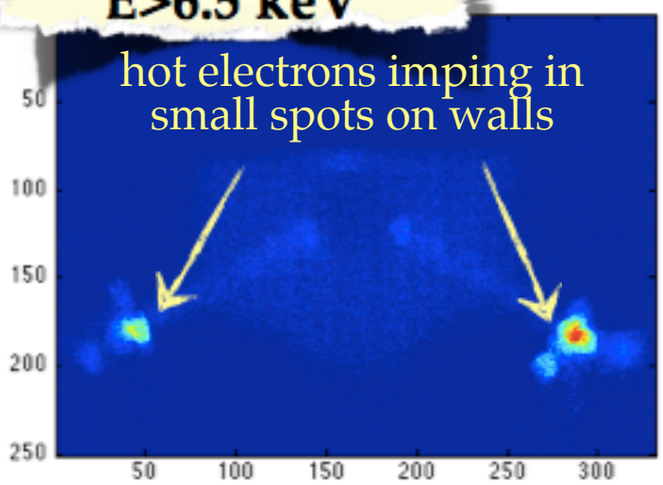

Whole plasma

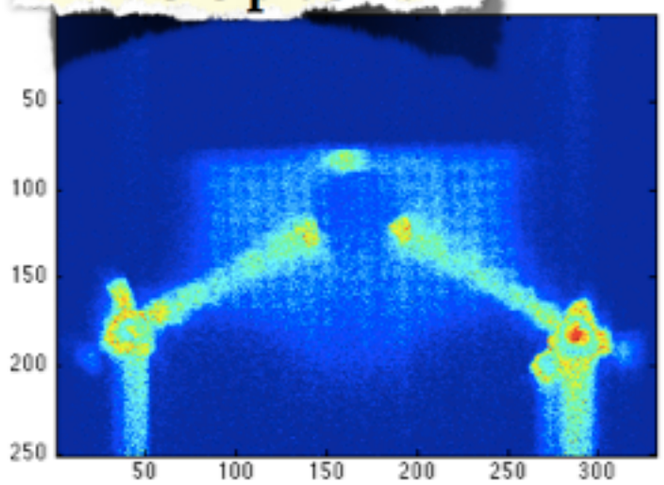

Plasma inspection after energy filtering

12.92 GHz - distribution at different energies

(equalized pseudocolor maps)

E<1.5 keV

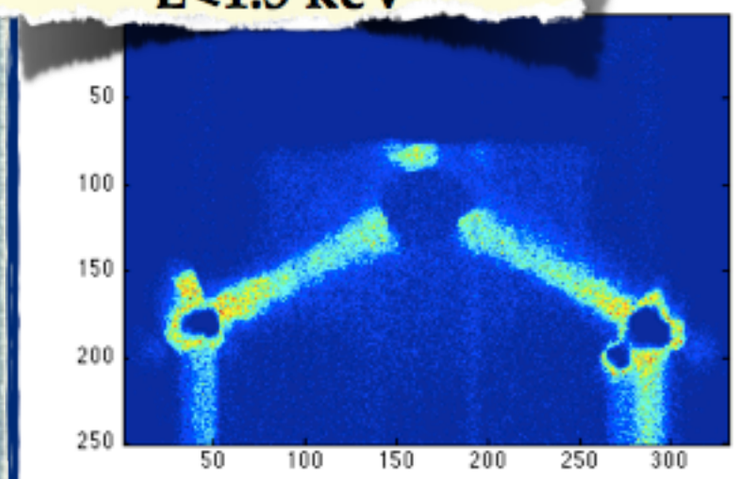

1.5<E<2.5 keV

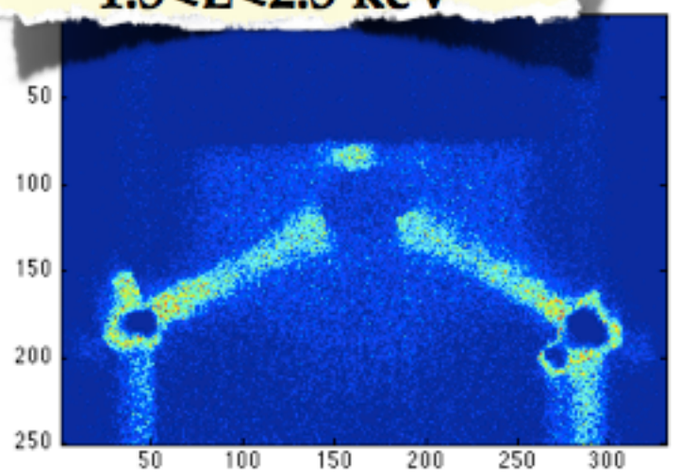

2.5<E<3.5 keV - Ar ions

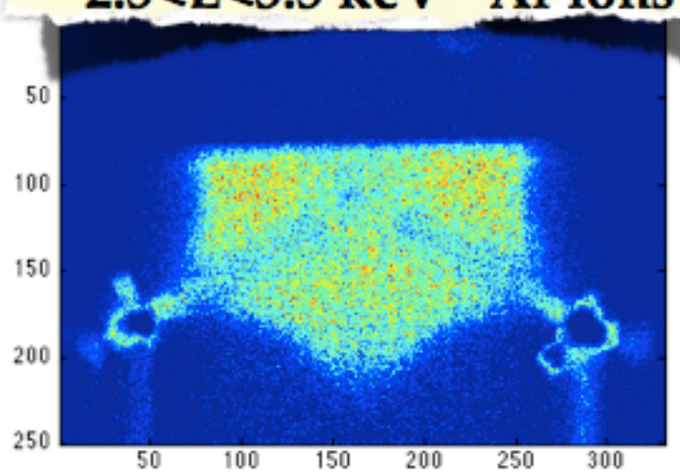

3.5<E<6.5 keV

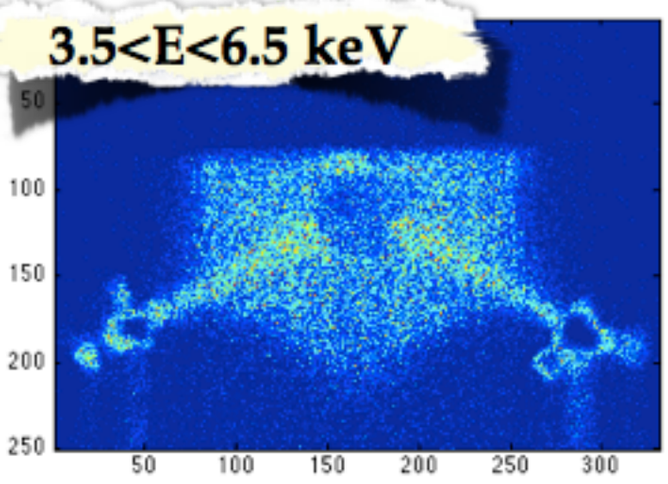

E>6.5 keV

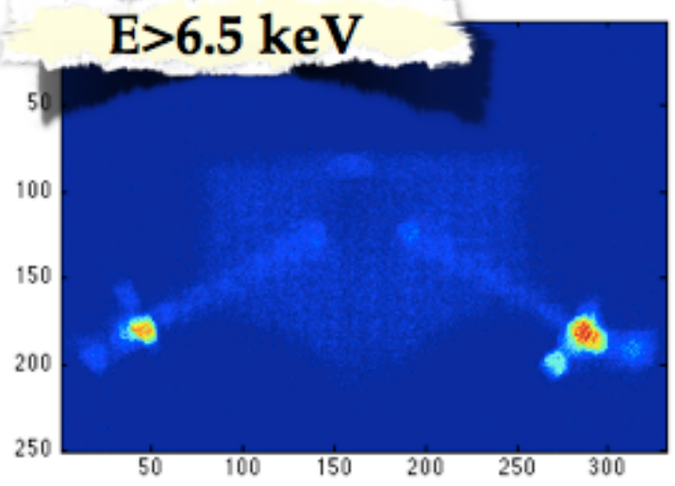

Whole plasma

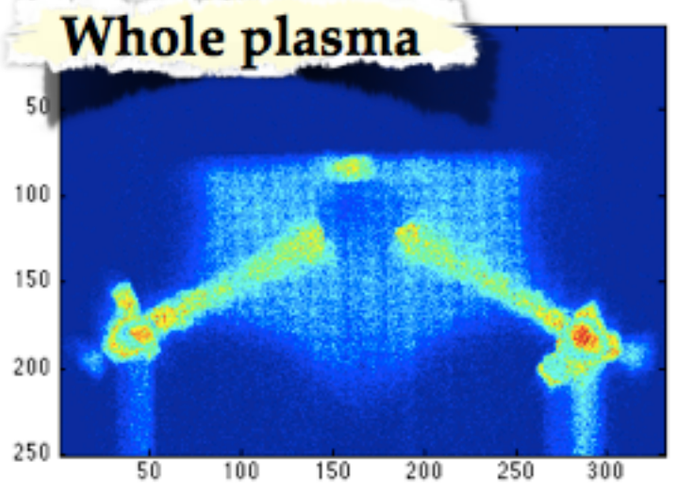

Plasma inspection after energy filtering

13.24 GHz - distribution at different energies

(equalized pseudocolor maps)

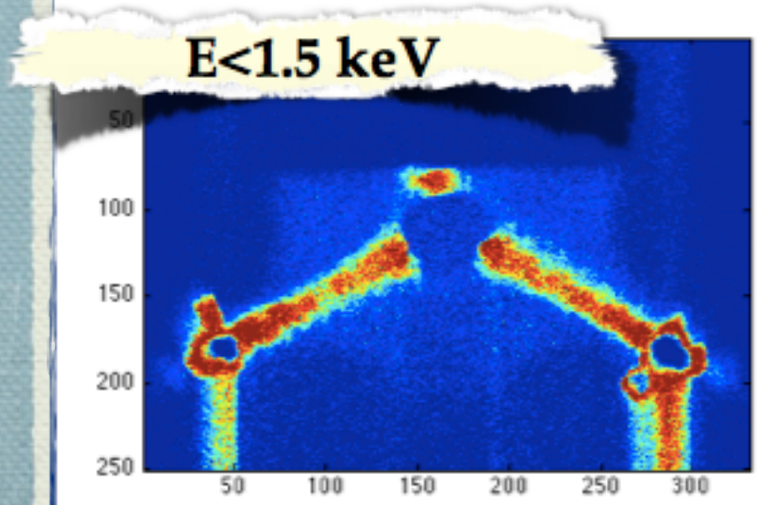

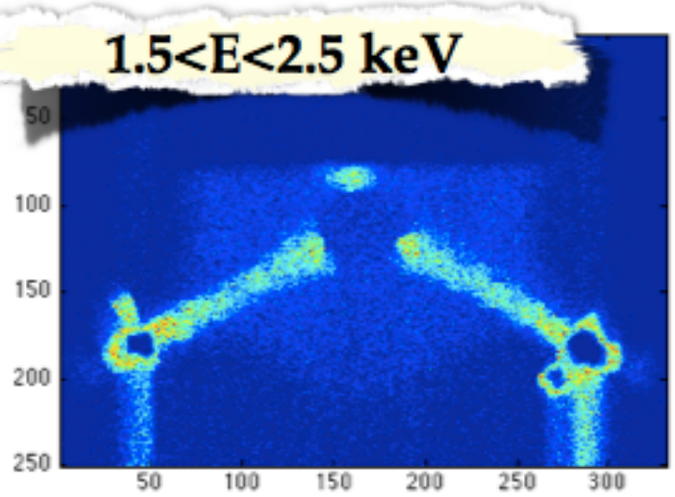

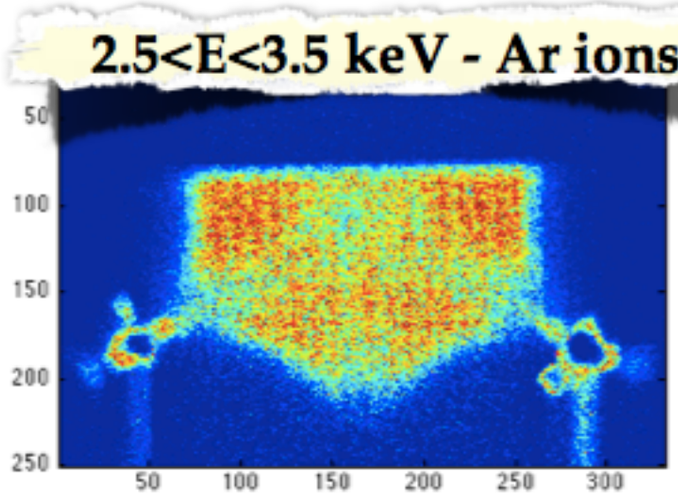

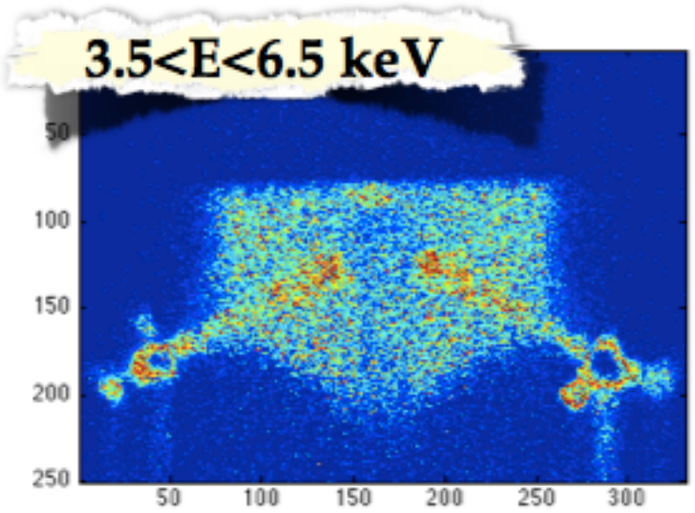

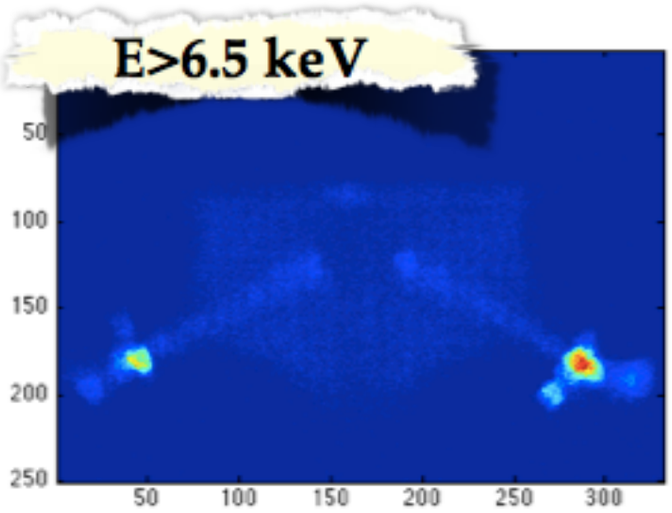

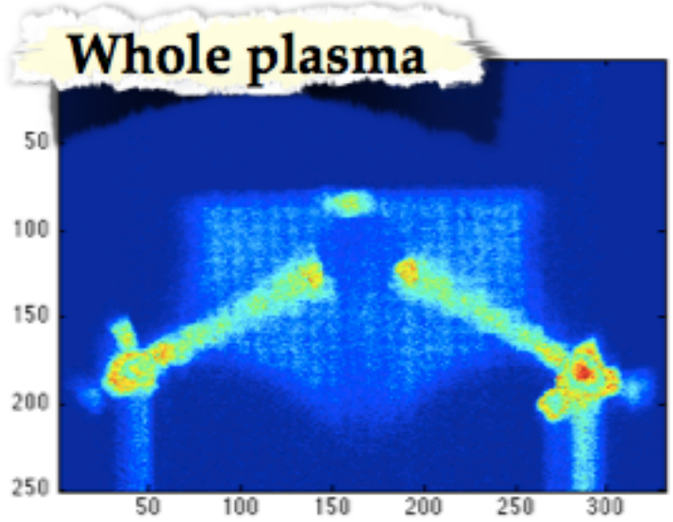

Analysis of plasma morphology

2.8<E<3.5 keV

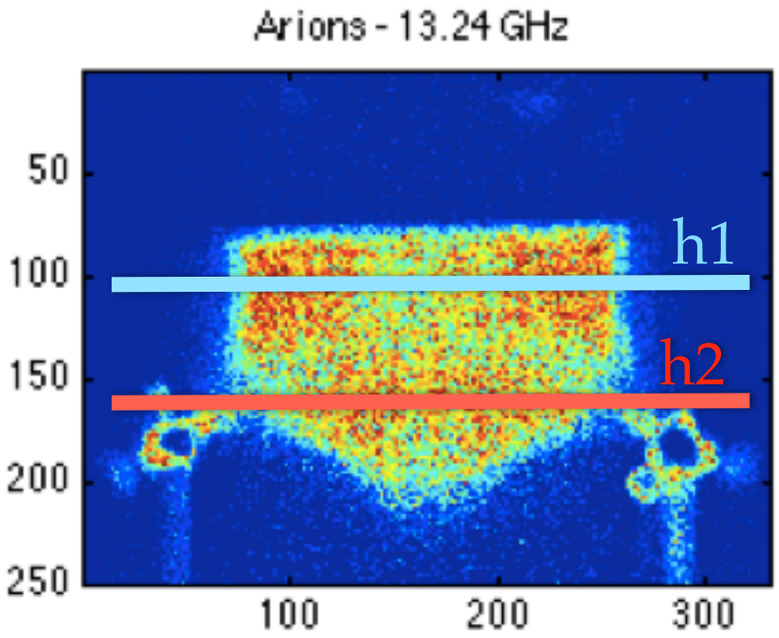

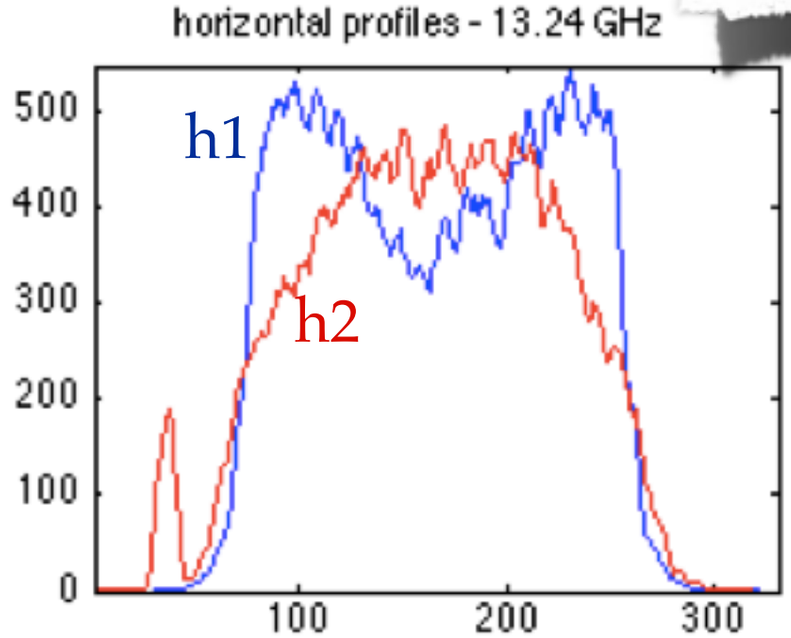

- A more detailed analysis of Ar distribution through 1D profiles
  - 2+2 horizontal/vertical profiles
  - Evidence of "hollow plasma" with axial density depletion
  - Very good spatial resolution (profiles show grid-elements)

Analysis of plasma morphology

2.8<E<3.5 keV

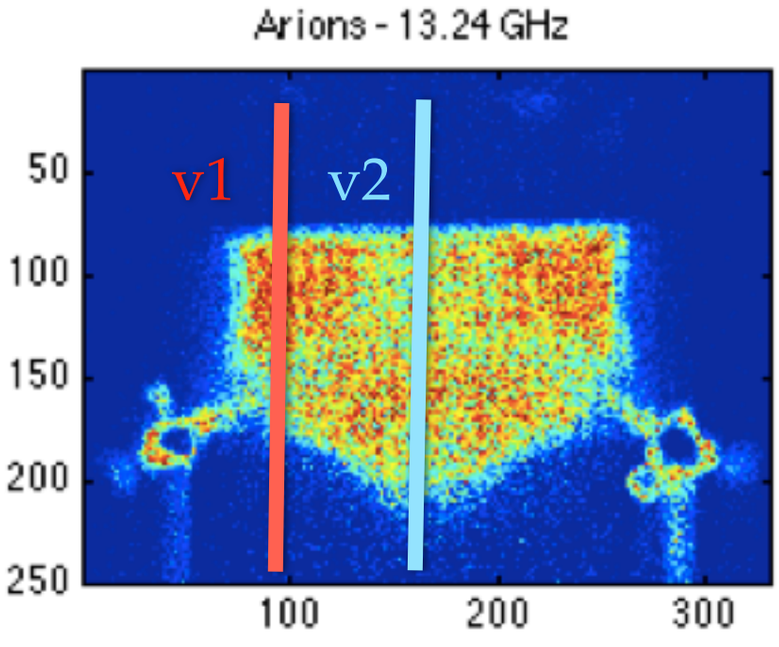

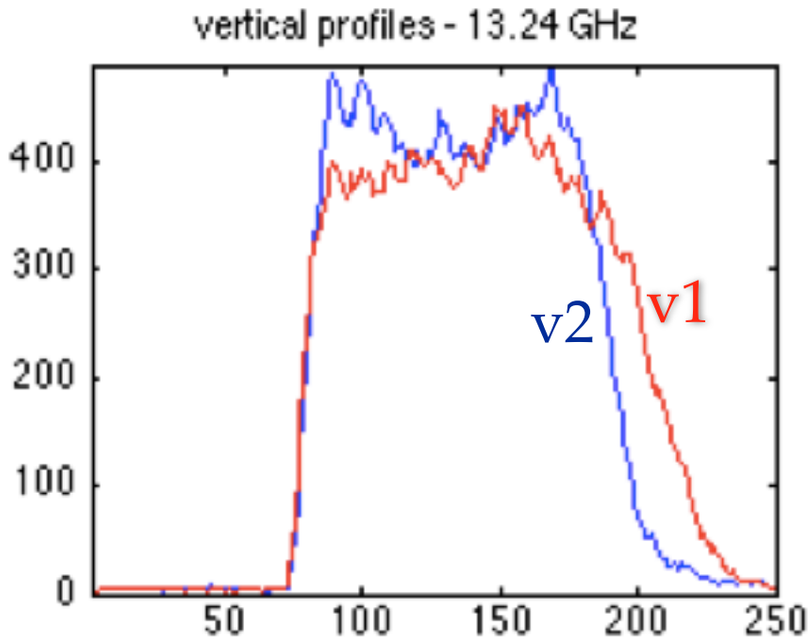

Analysis of plasma morphology

2.8<E<3.5 keV

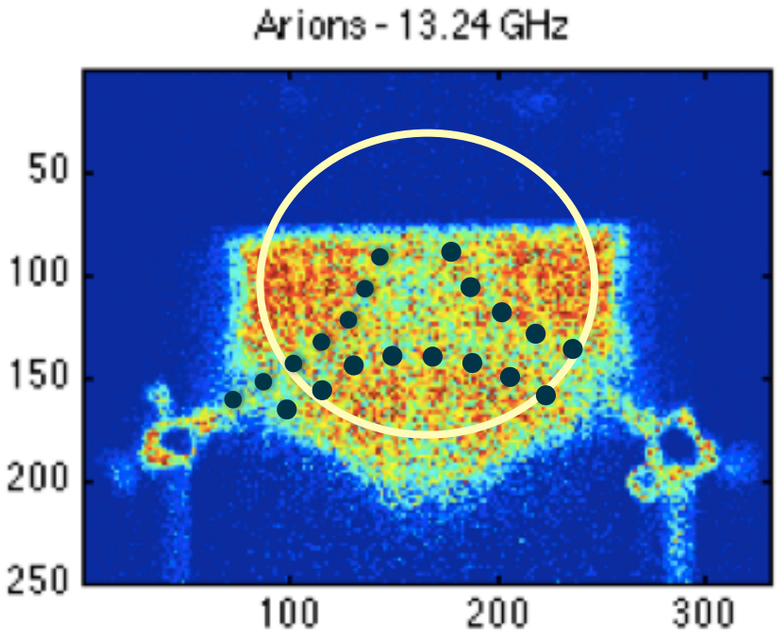

Pole depletion

azimuthal density profile

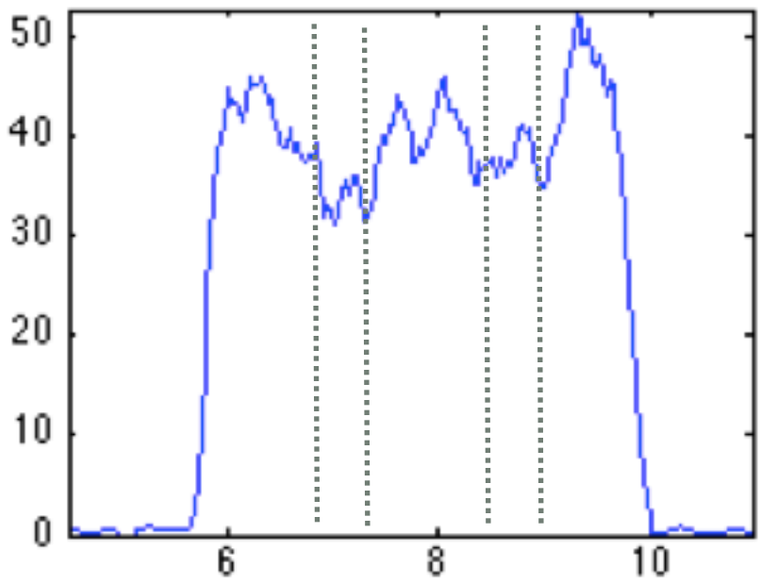

- Azimuthal profile
- Asimmetric plasma
- Magnetic brench depletion

Analysis of shape factors

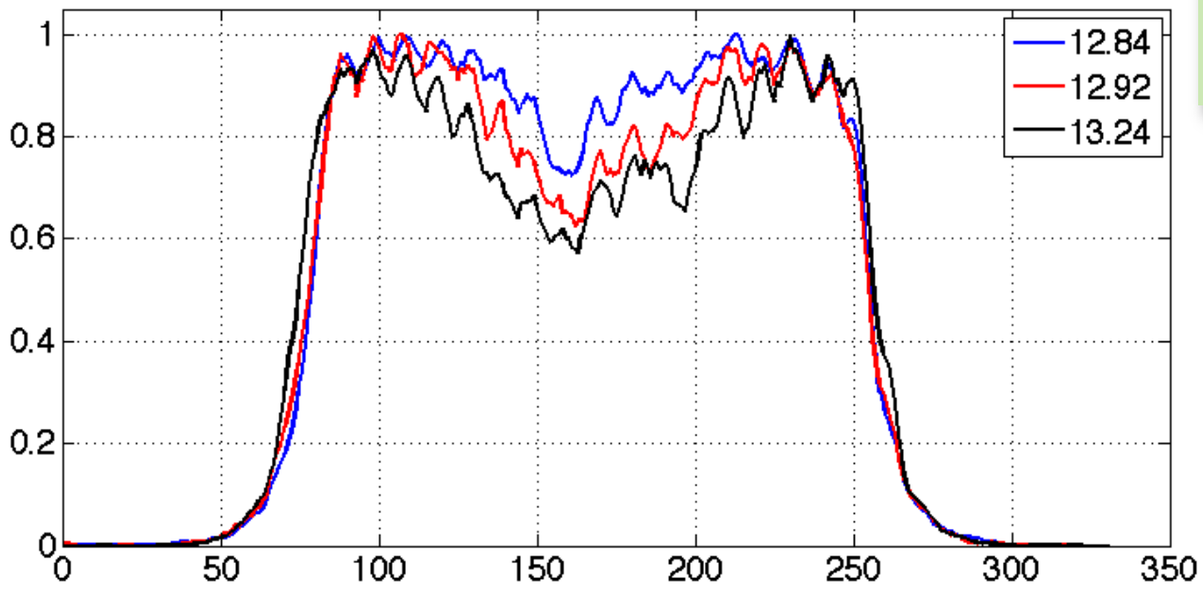

horizontal profiles

- SHAPE FACTOR: regardless from absolute intensity, the "hollow type" profile is affected by the RF freq.

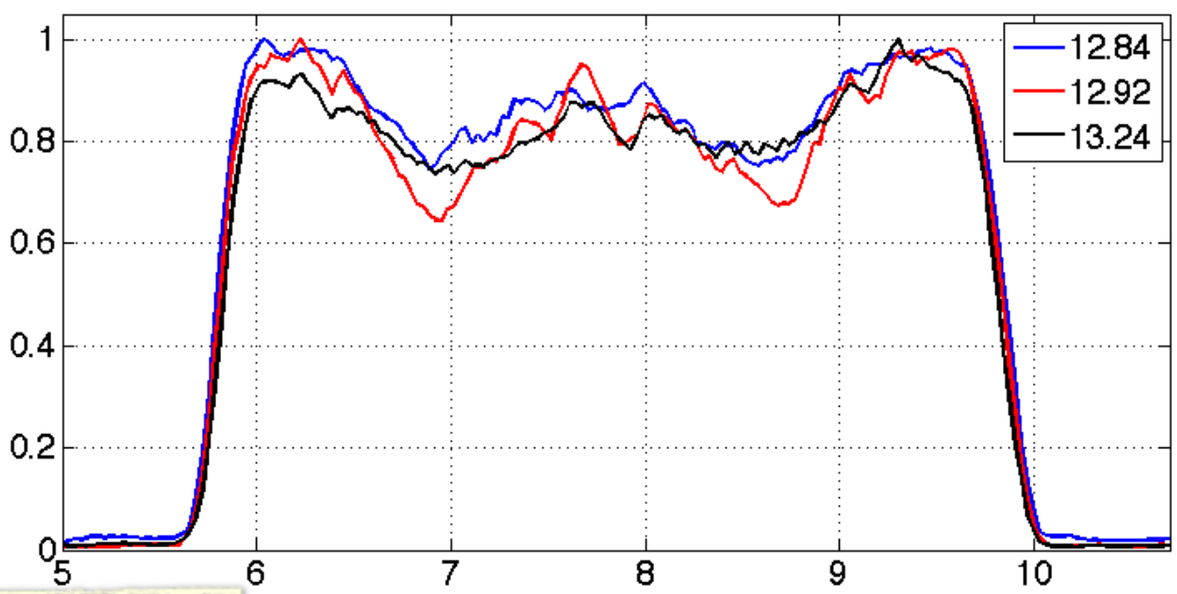

azimuthal profiles

- depletion in "poles" regions also varies with RF frequency

Analysis of plasma morphology

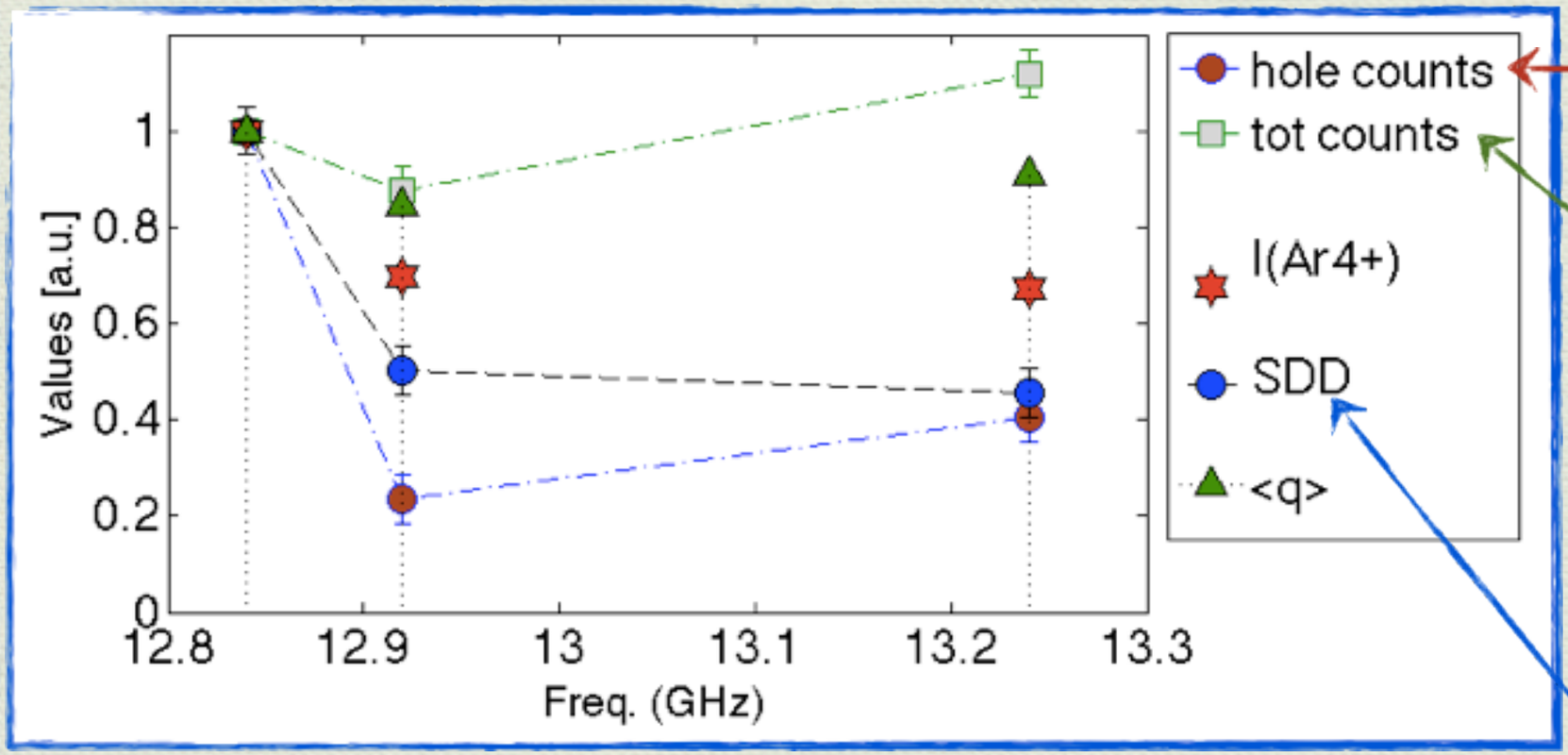

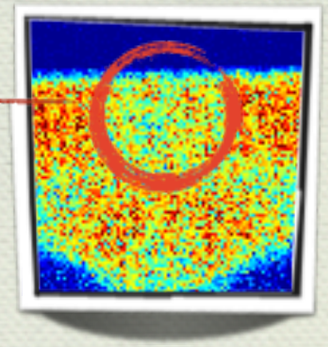

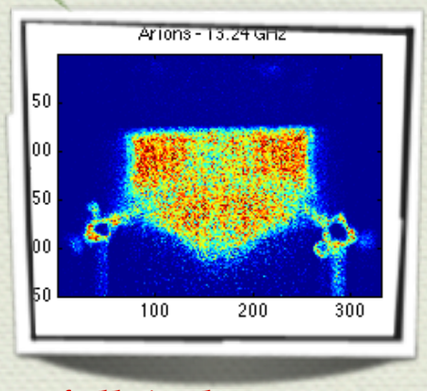

full Ar-lines image integration

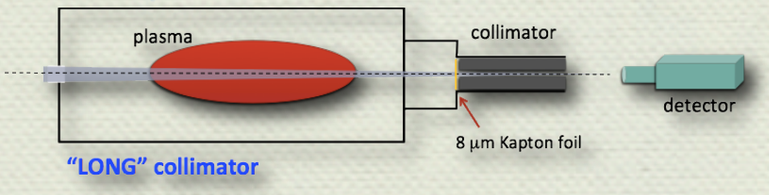

X-rays along the SDD sightline

- **Relative (to 12.84 GHz) comparisons:** Despite 13.24 GHz has the highest number of counts in the full-frame image, but its "near-axis" density is lower than 12.84 GHz case

- Strict interplay between total density and – especially – concentration in near axis region comes out.

Comparison with self-consistent simulations

*Solving the **time-dependent Vlasov equation**, including single particle collisions*

$$\frac{\partial f_\alpha}{\partial t} + \vec{v}\cdot\vec{\nabla} f_\alpha + \frac{q_\alpha}{m_\alpha}\left(\vec{E} + \frac{\vec{v}\times\vec{B}}{c}\right)\cdot\vec{\nabla}_{\vec{v}} f_\alpha = 0$$

$$\frac{d\vec{v}}{dt} = \frac{q}{m_0\gamma}\left[\vec{E} + \vec{v}\times B - \frac{\vec{v}\cdot\vec{E}}{c^2}\vec{v}\right]$$

Collisions by Langevin method [jointly A.Galatà LNL]

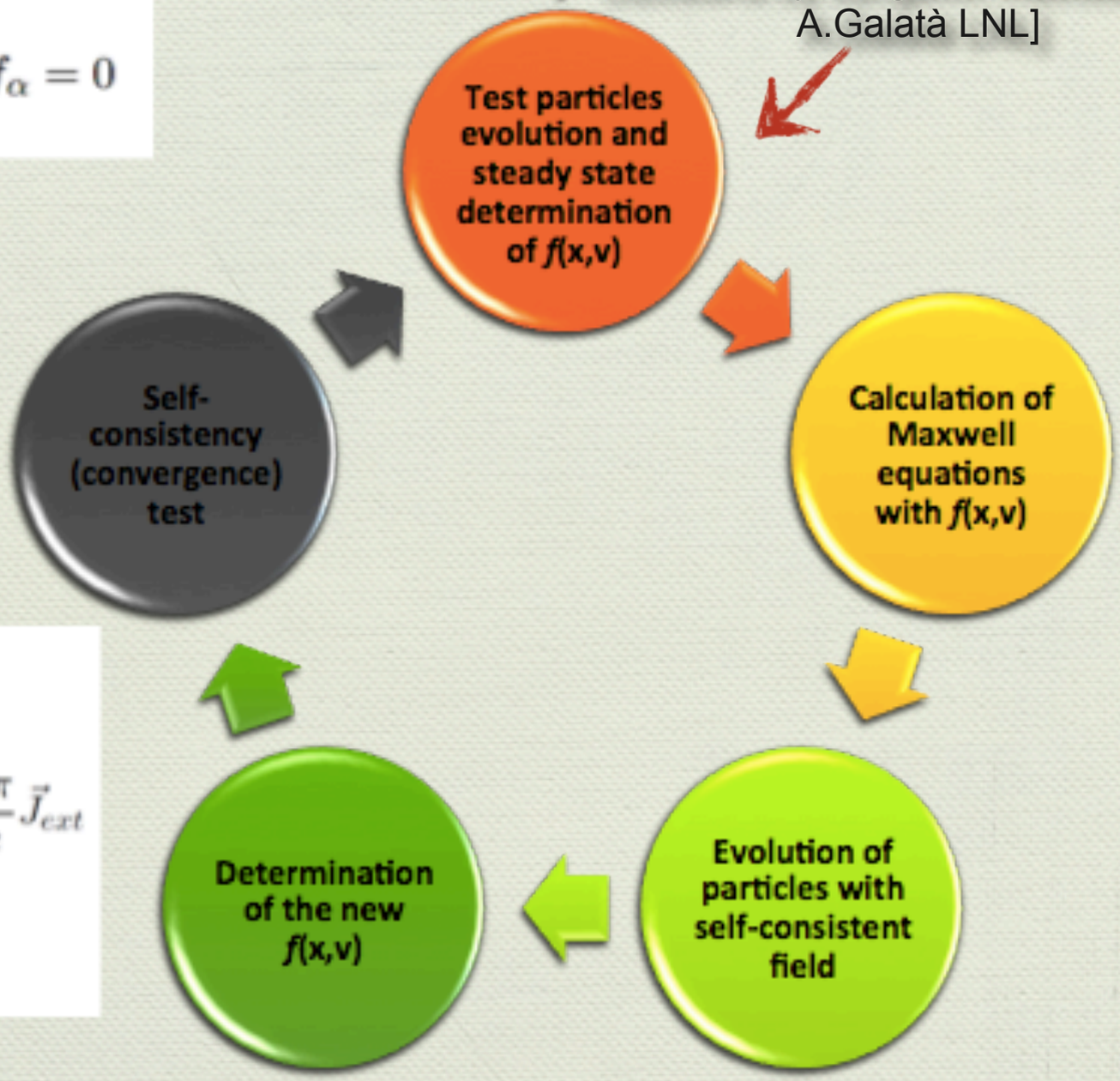

Step-by-step current

Step-by-step plasma density

$$\vec{\nabla}\cdot\vec{E} = 4\pi\sum_\alpha \overline{n}_\alpha q_\alpha \int f_\alpha d\vec{v} + 4\pi\rho_{ext}$$

$$\vec{\nabla}\times\vec{B} = \frac{1}{c}\frac{\partial\vec{E}}{\partial t} + \frac{4\pi}{c}\sum_\alpha \overline{n}_\alpha q_\alpha \int \vec{v} f_\alpha d\vec{v} + \frac{4\pi}{c}\vec{J}_{ext}$$

$$\vec{\nabla}\times\vec{E} = -\frac{1}{c}\frac{\partial\vec{B}}{\partial t}$$

Comparison with self-consistent simulations

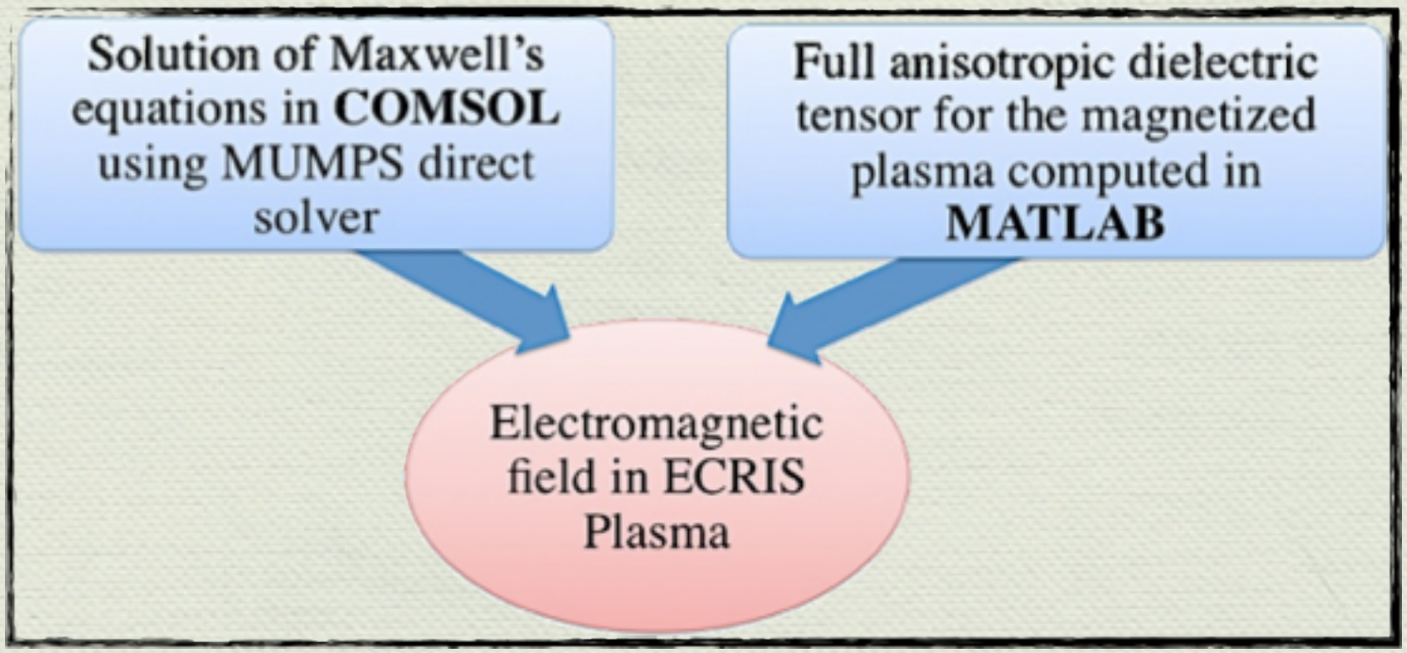

$$\nabla \times \nabla \times \boldsymbol{E} - \frac{\omega^2}{c^2}\overline{\overline{\epsilon_r}} \cdot \boldsymbol{E} = 0$$

Wave equation with tensorial permittivity

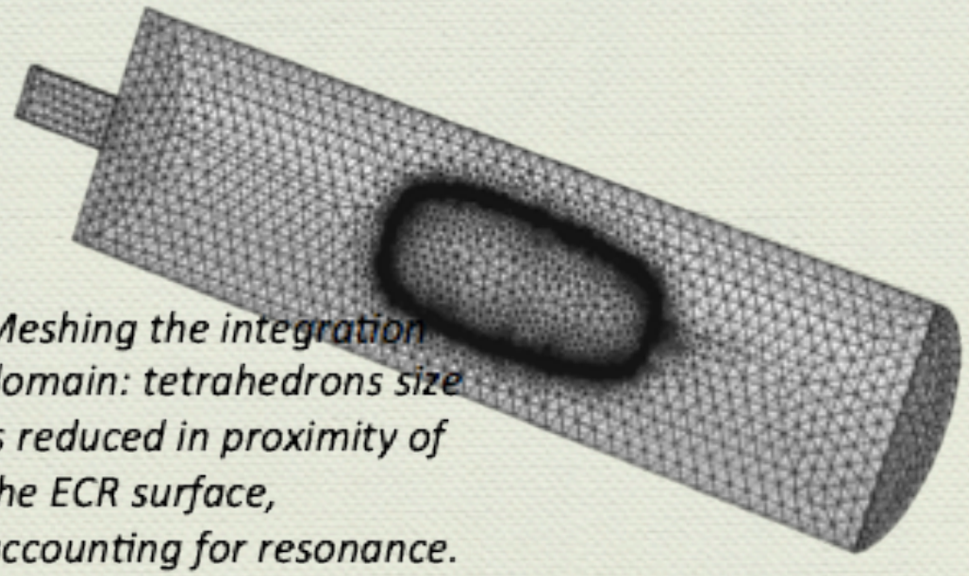

Meshing the integration domain: tetrahedrons size is reduced in proximity of the ECR surface, accounting for resonance.

$$\overline{\overline{\epsilon}} = \epsilon_0 \overline{\overline{\epsilon}}_r = \epsilon_0 \left(\overline{\overline{\epsilon'}} - i\overline{\overline{\epsilon''}} \right) = \epsilon_0 \left(\overline{\overline{I}} - \frac{i\overline{\overline{\sigma}}}{\omega\epsilon_0} \right)$$

$$= \epsilon_0 \begin{bmatrix} 1 + i\frac{\omega_p^2}{\omega}\frac{a_x}{\Delta} & i\frac{\omega_p^2}{\omega}\frac{c_z + d_{xy}}{\Delta} & i\frac{\omega_p^2}{\omega}\frac{-c_y + d_{xz}}{\Delta} \\ i\frac{\omega_p^2}{\omega}\frac{-c_z + d_{xy}}{\Delta} & 1 + \frac{i\omega_p^2}{\omega}\frac{a_y}{\Delta} & i\frac{\omega_p^2}{\omega}\frac{c_x + d_{yz}}{\Delta} \\ i\frac{\omega_p^2}{\omega}\frac{c_y + d_{xz}}{\Delta} & i\frac{\omega_p^2}{\omega}\frac{-c_x + d_{zy}}{\Delta} & 1 + i\frac{\omega_p^2}{\omega}\frac{a_z}{\Delta} \end{bmatrix}$$

Full-3D non homogeneous dielectric permittivity
Tensor depends on local density and B-field

Full-wave solution of the electromagnetic field

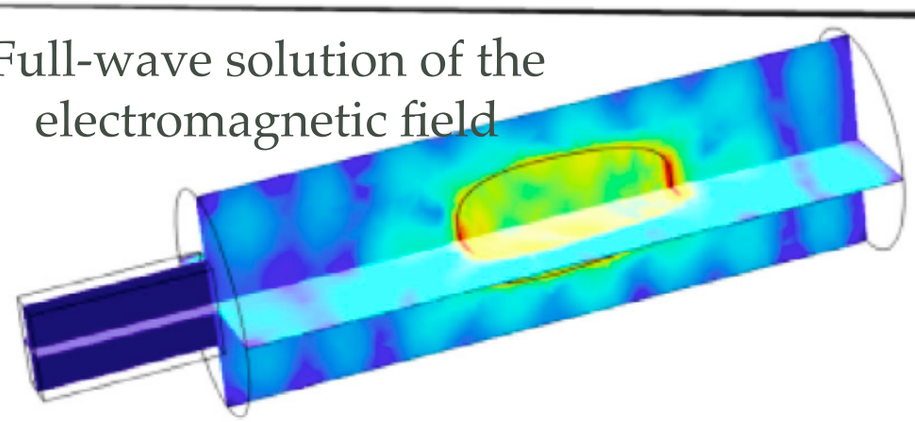

Searching self-consistency

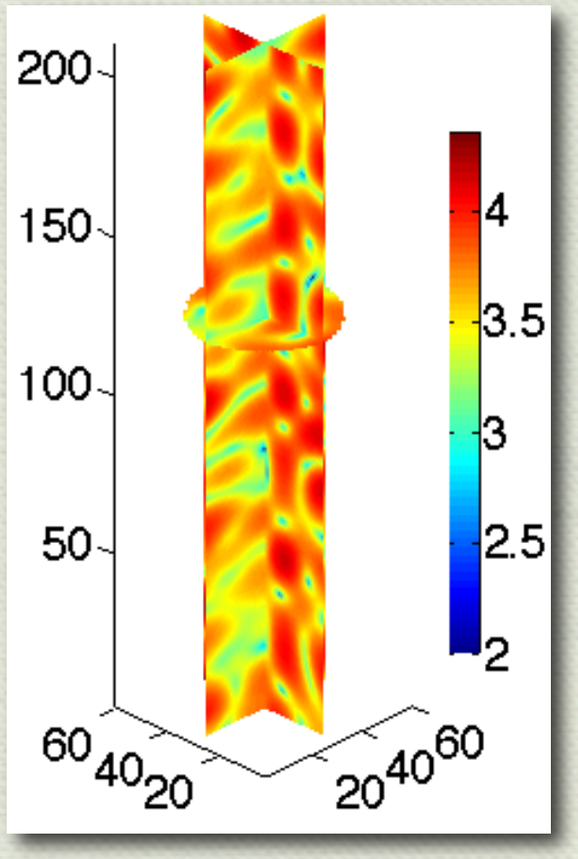

Freq. dom. solution step 0 (vacuum cavity)

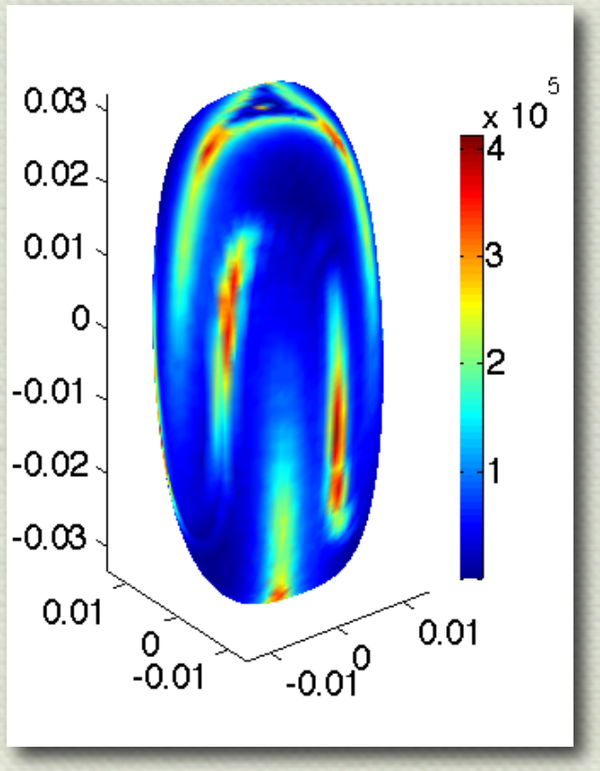

Particle Tracking step 1 (vacuum field +plasmoid-halo initial density distr.)

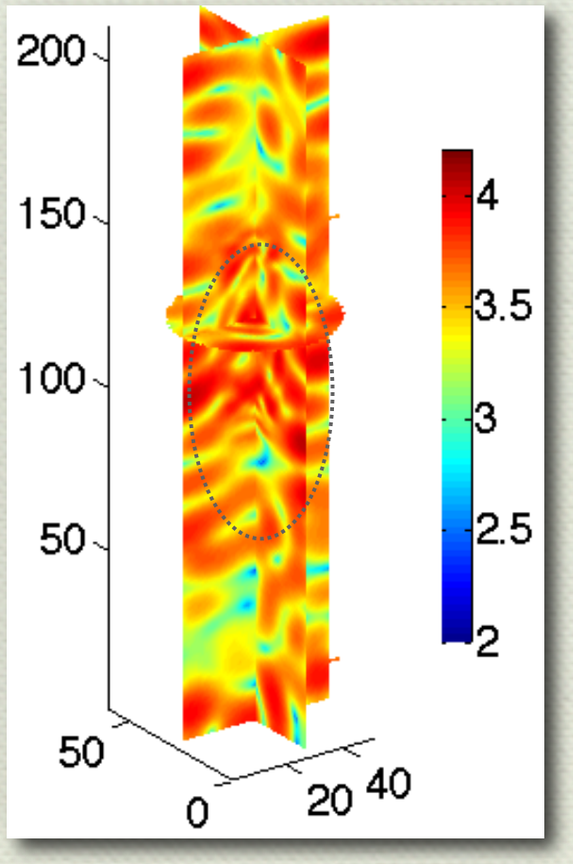

Freq. dom. solution step 1 (70% density from plasmoid halo model +30% step-1 density structure)

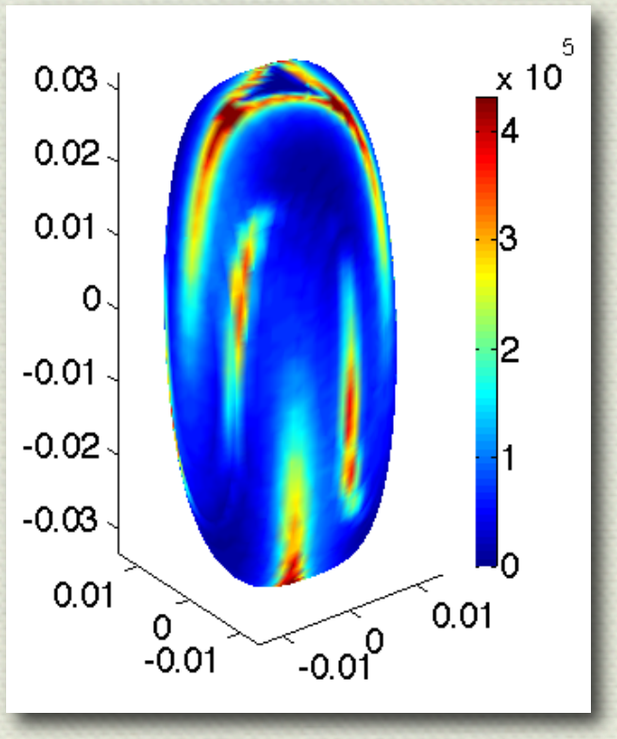

Particle Tracking step 2 (70% vacuum field + 30% step-1 full-wave calculated field)

Plasma shape at different energy domains

12.84 GHz

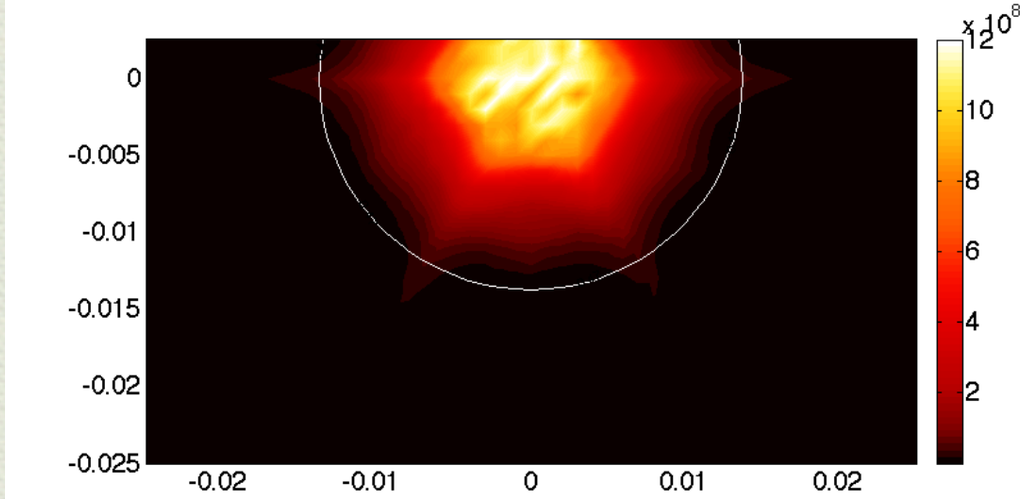

Cold Electrons

E<1 keV

concentration in the near axis region

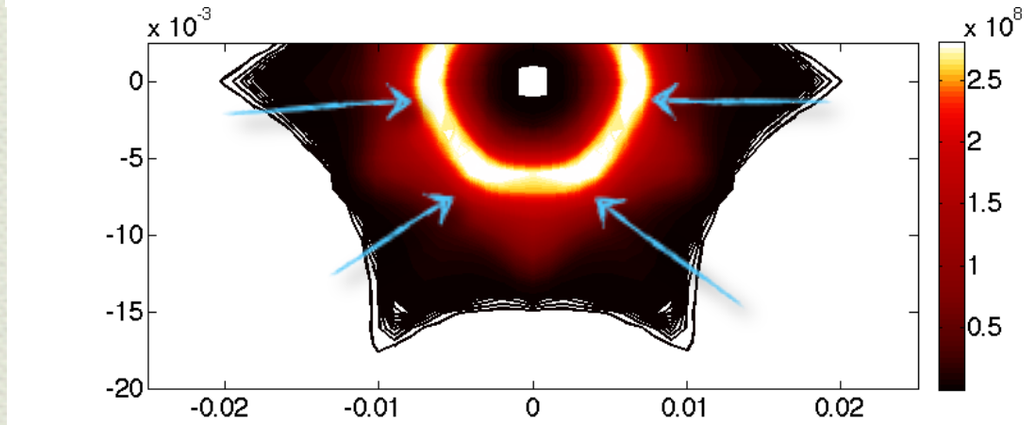

Warm electrons

2 keV<E<30 keV

bright annulus with intense spots in off-pole region

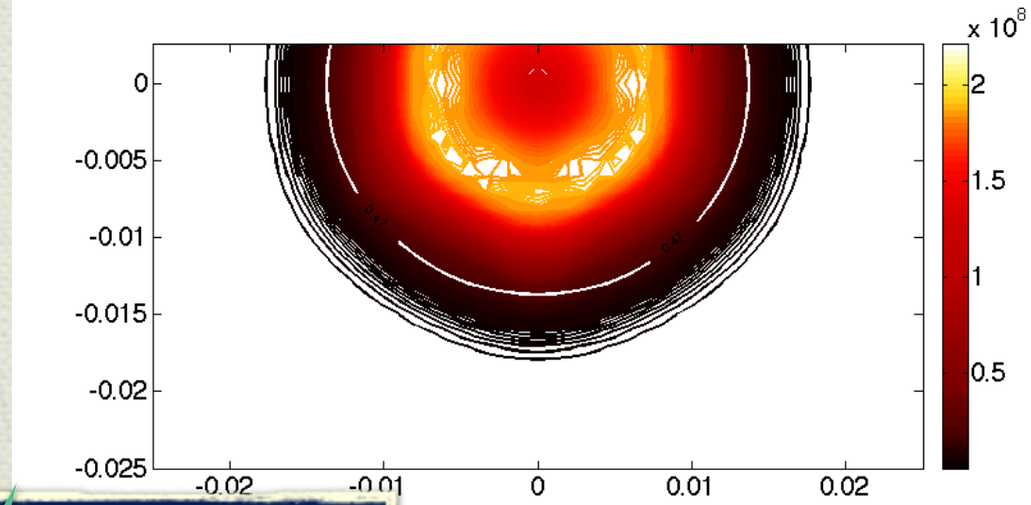

Hot electrons

E>30 keV

broad annulus well inside the resonance layer

Comparison to self-consistent simulations

12.92 GHz

Experimental result Ar-fluor. 3 keV

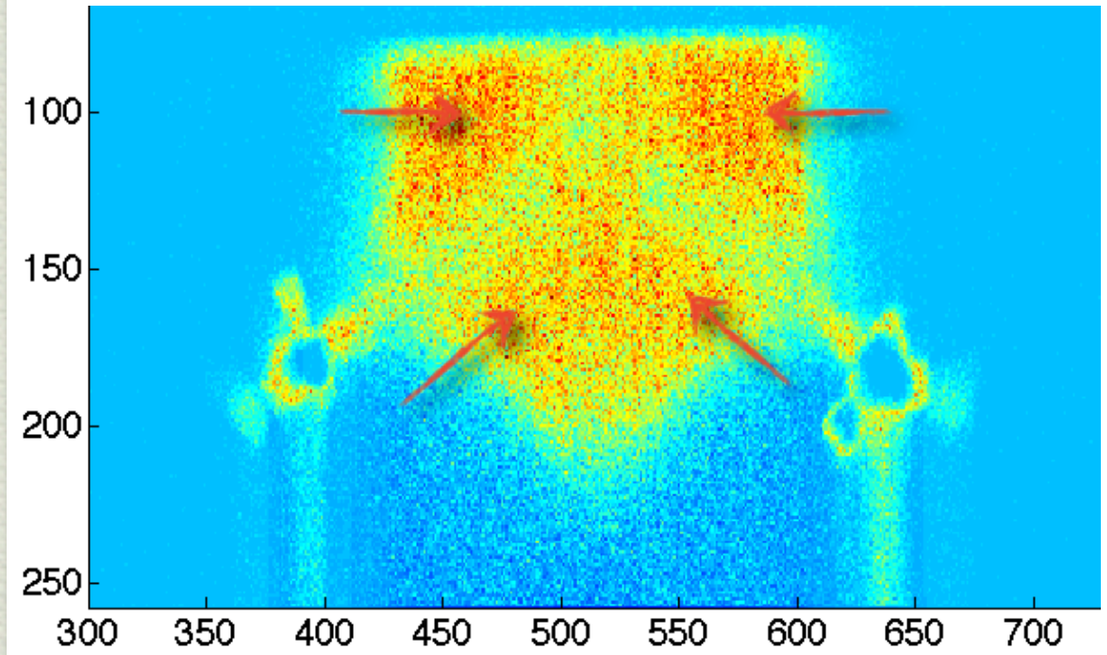

Simulations - warm electrons at 2<E<30 keV

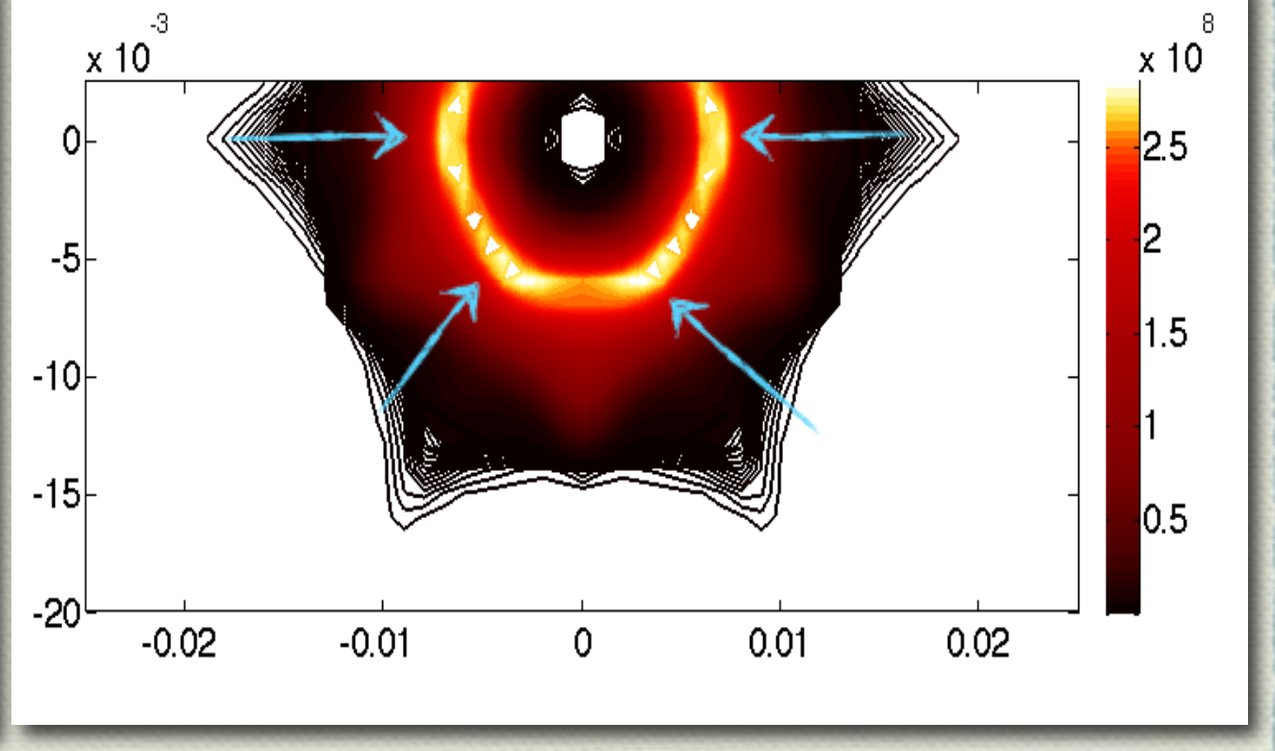

- **Argon ions occupy far-from-poles positions:** from comparison to simulations it comes out there warm electrons (having enough energy for ionisation and excitation) are placed

- **Next step:** comparison of two frequencies

Comparison to self-consistent simulations
12.84 + 12.92 GHz

12.92 GHz
warm-electrons

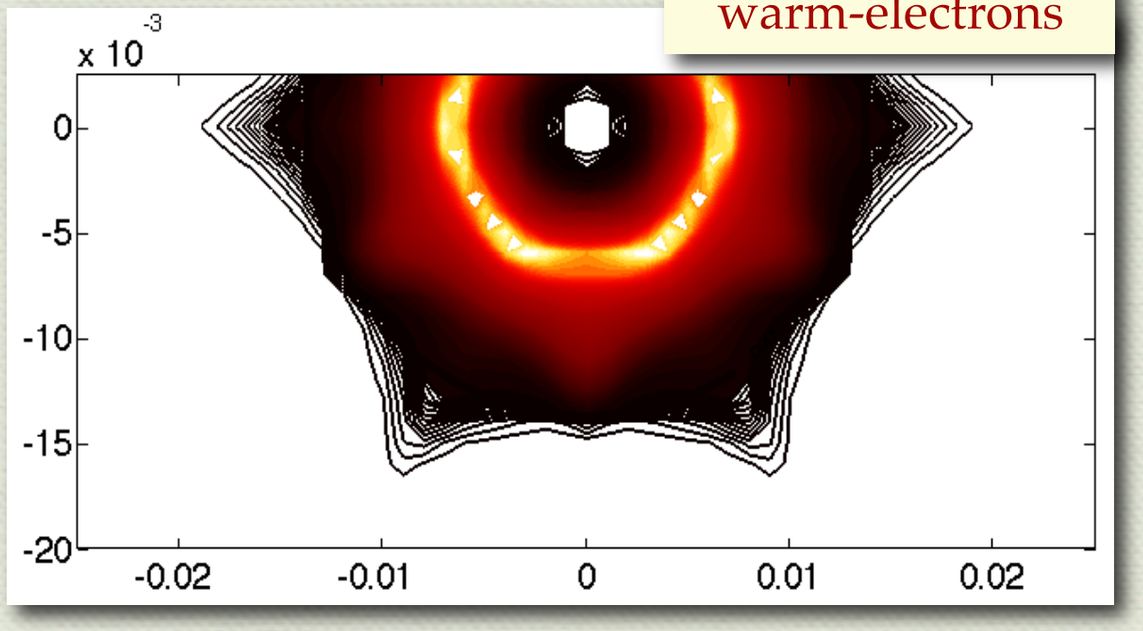

12.84 GHz
warm-electrons

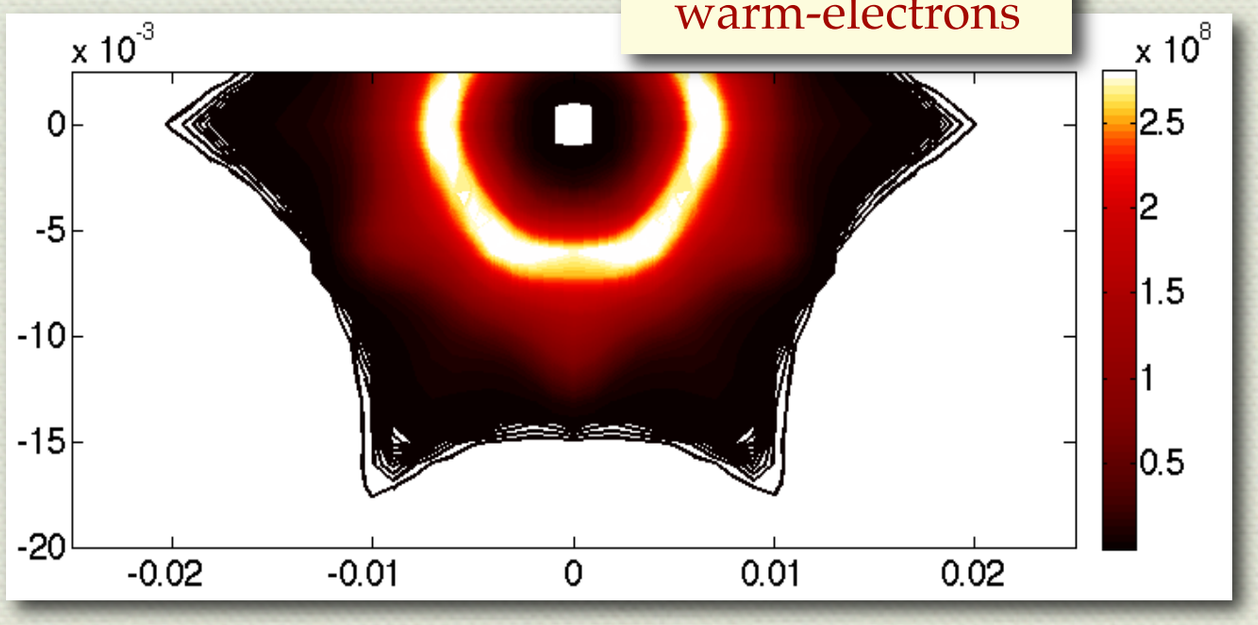

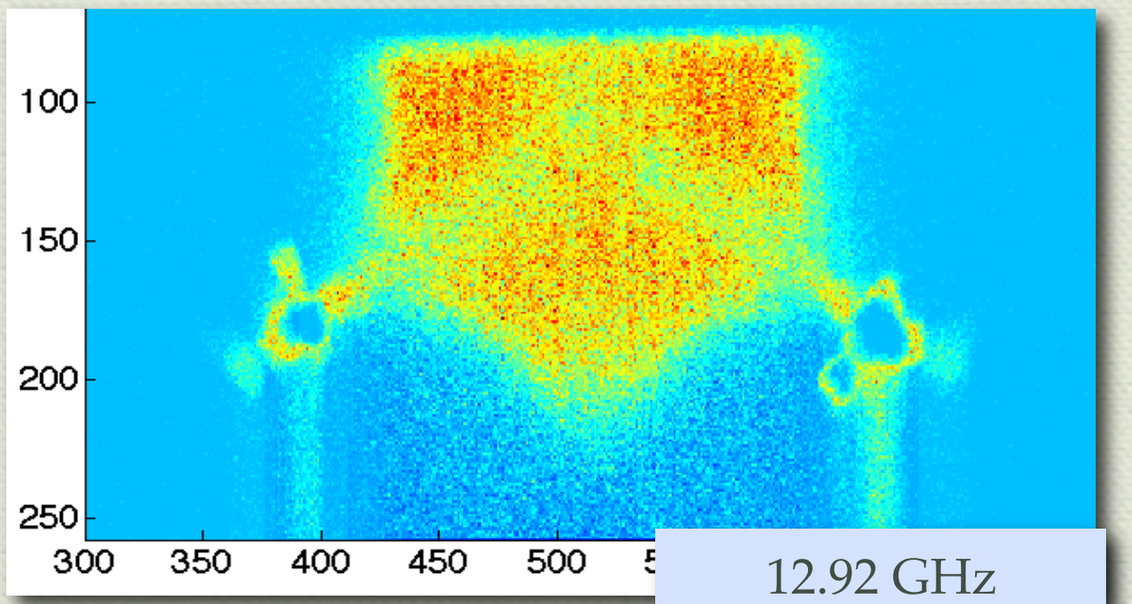

12.92 GHz
Ar fluor. lines

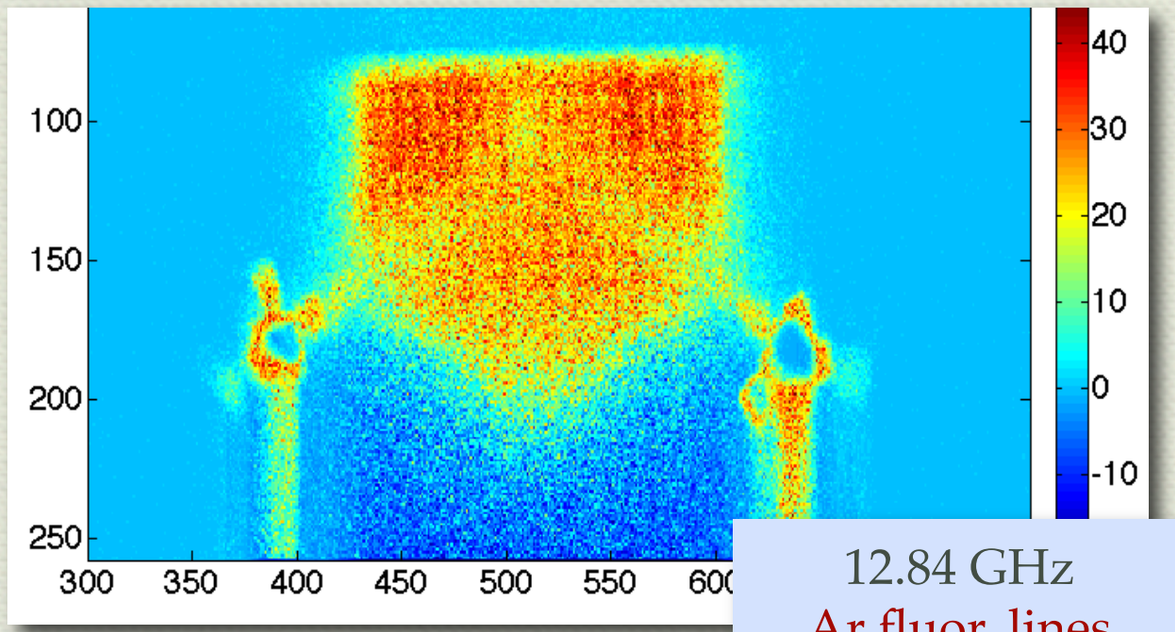

12.84 GHz
Ar fluor. lines

Comparison to self-consistent simulations

12.84 GHz

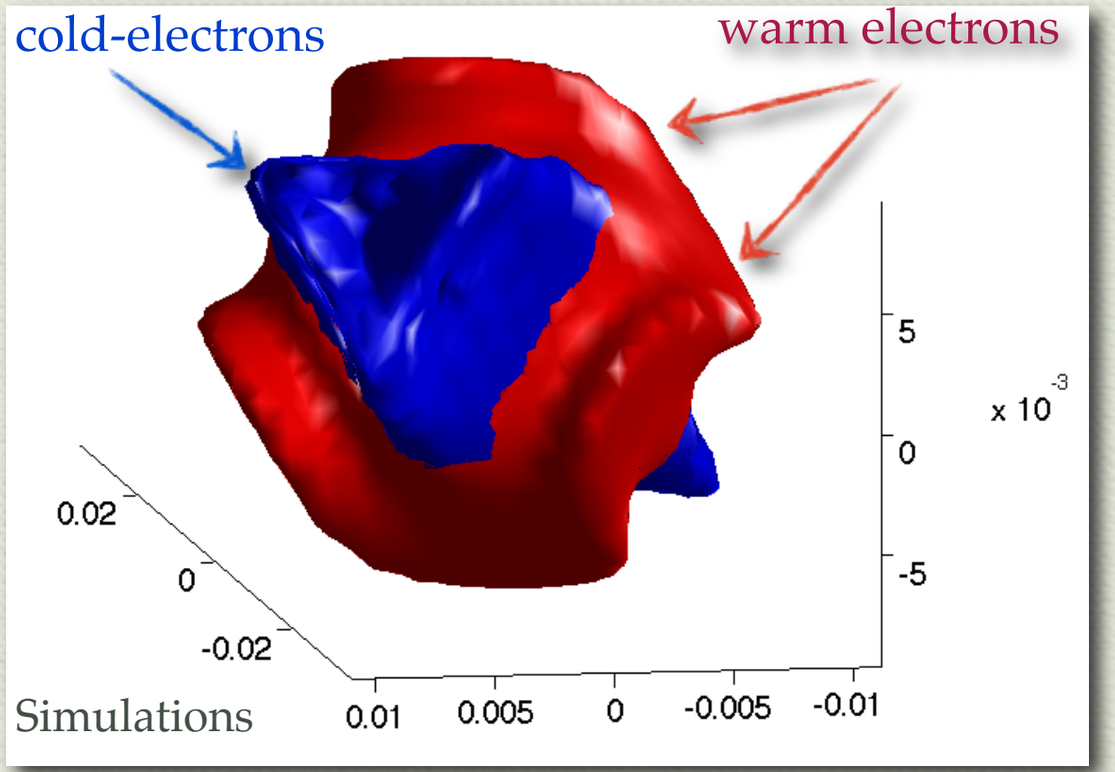

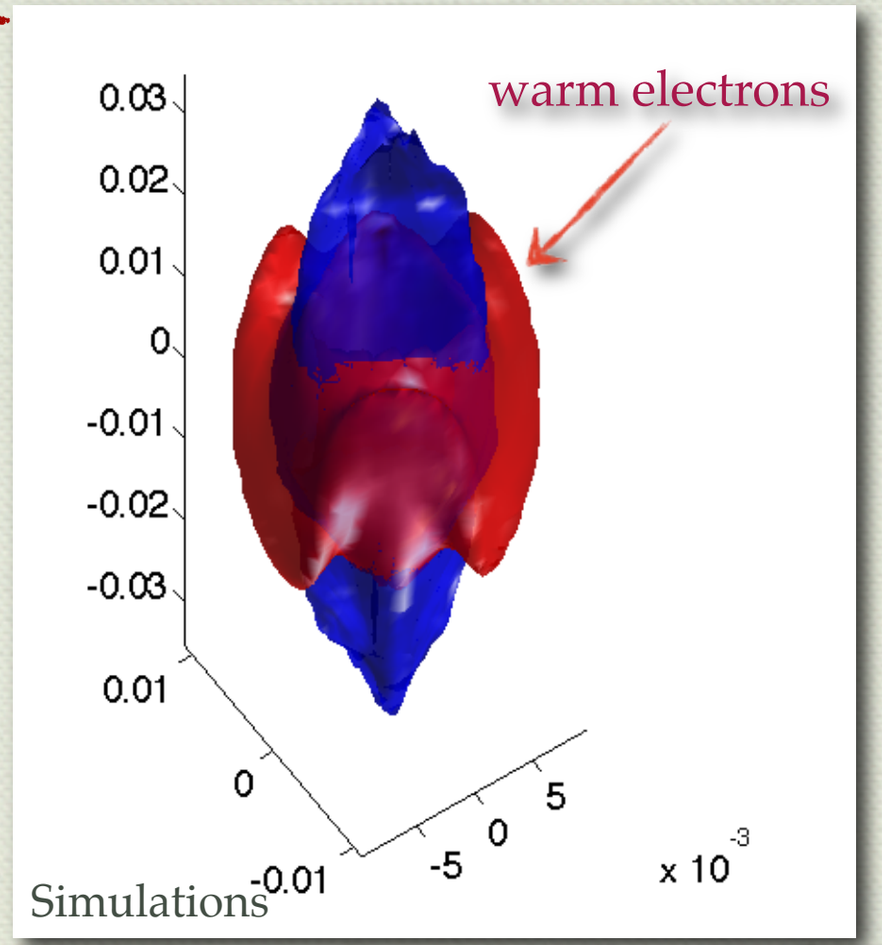

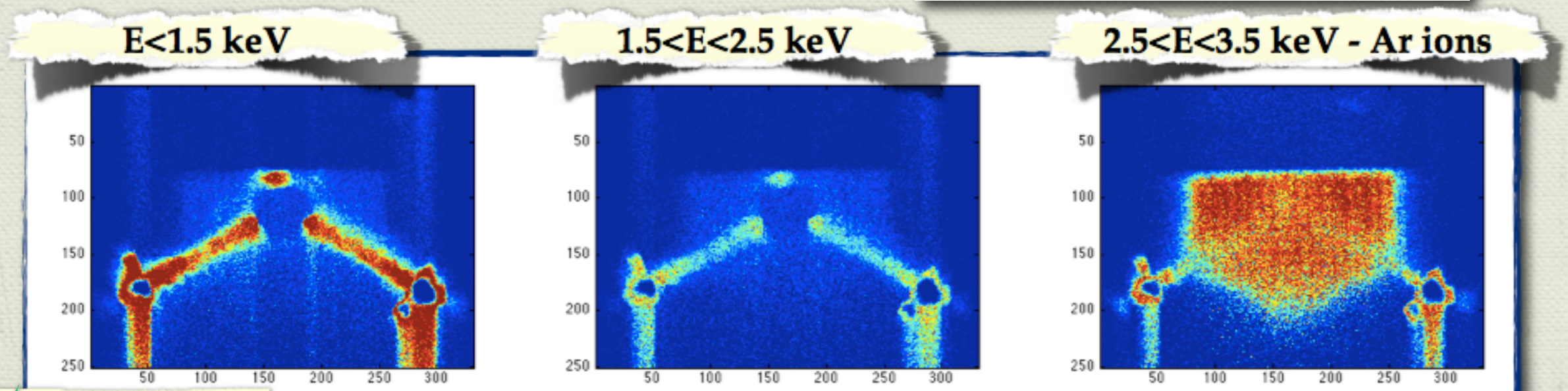

Comparison to self-consistent simulations

12.84 + 12.92 GHz

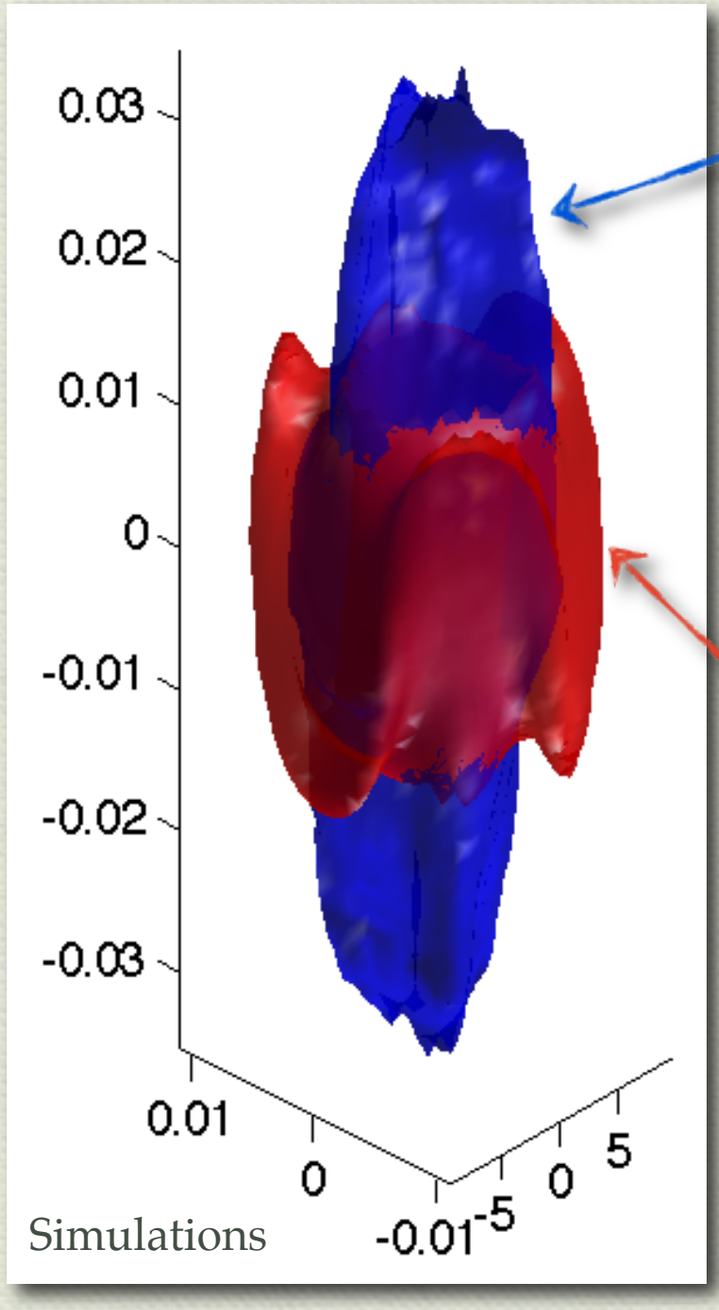

cold-electrons

warm electrons have different morphology

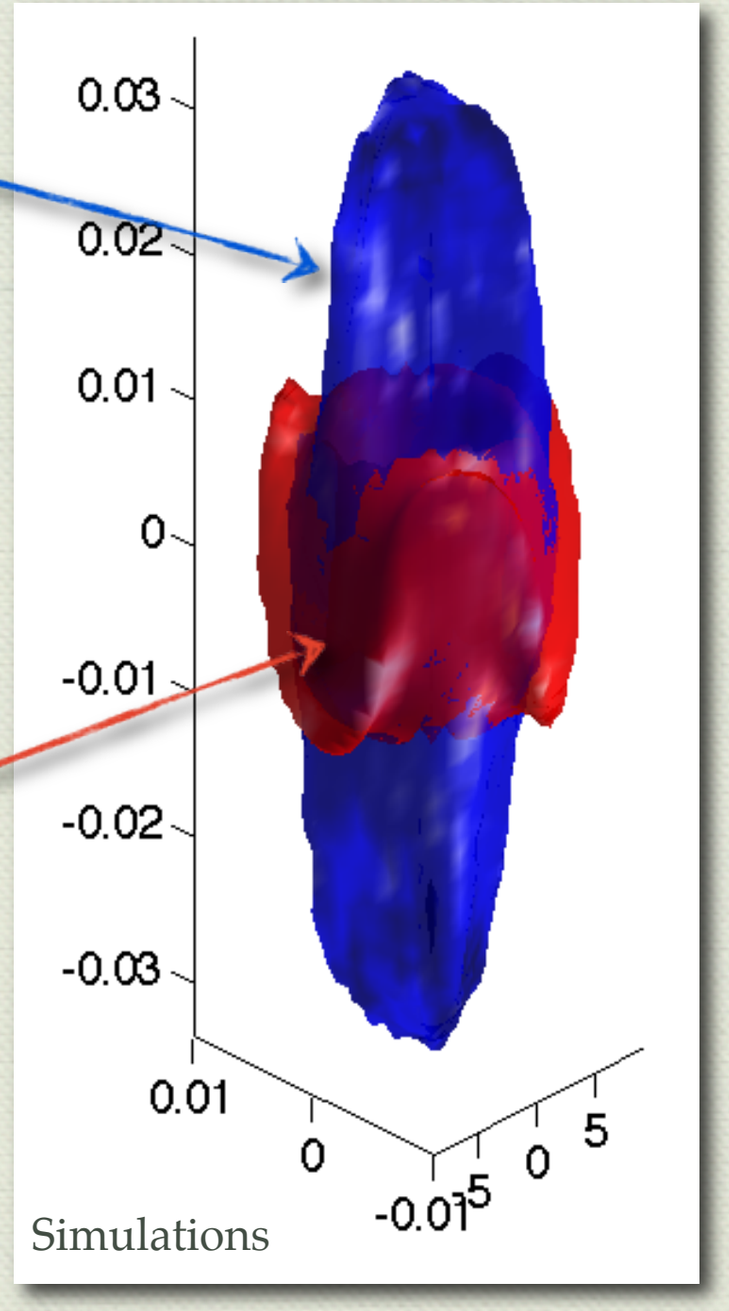

12.84 GHz
cold & warm electrons

12.92 GHz
cold & warm electrons

Achievements and Perspectives

- We are now able to see what happens into the plasma and to model through numerical simulations how it could be happen differently (and in a better way)

- Microwave absorption oriented design is needed: Power deposition into the plasma must be performed in a highly controlled way

→ Single pass absorption

Some ideas

- STILL IN ECR-heating paradigm: are cylindrical shapes of the plasma chamber still mandatory ?

- OVERCOMING ECR-heating paradigm: on-purpose design of microwave launchers for inner plasma modal conversion

Modal Conversion for overdense plasma production

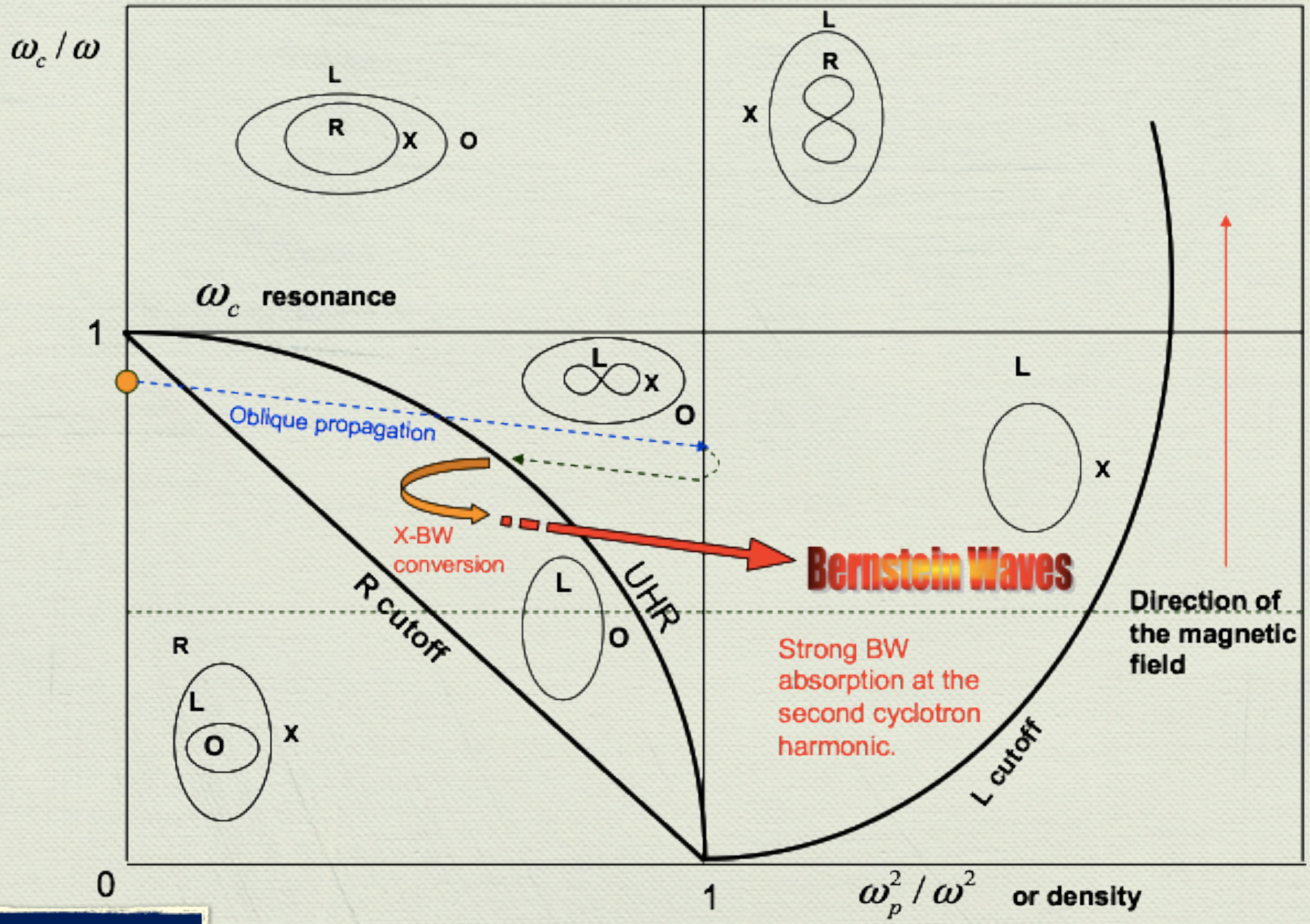

Mechanical Implementation at LNS

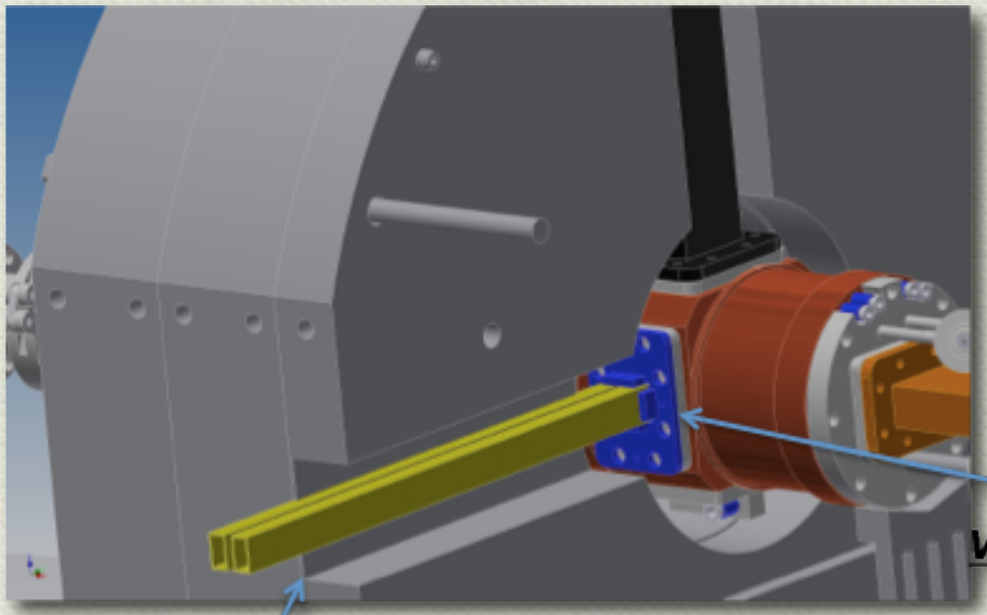

Courtesy of S. Passarello

Vacuum Break window

ARRAY of two waveguides

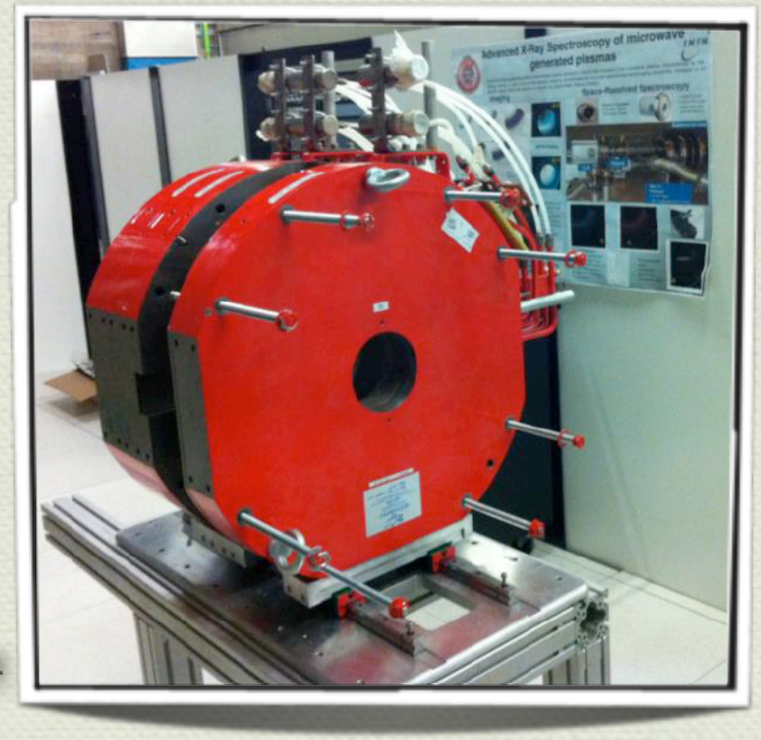

A new setup developed at LNS for fundamental studies: RF launcher construction is ongoing

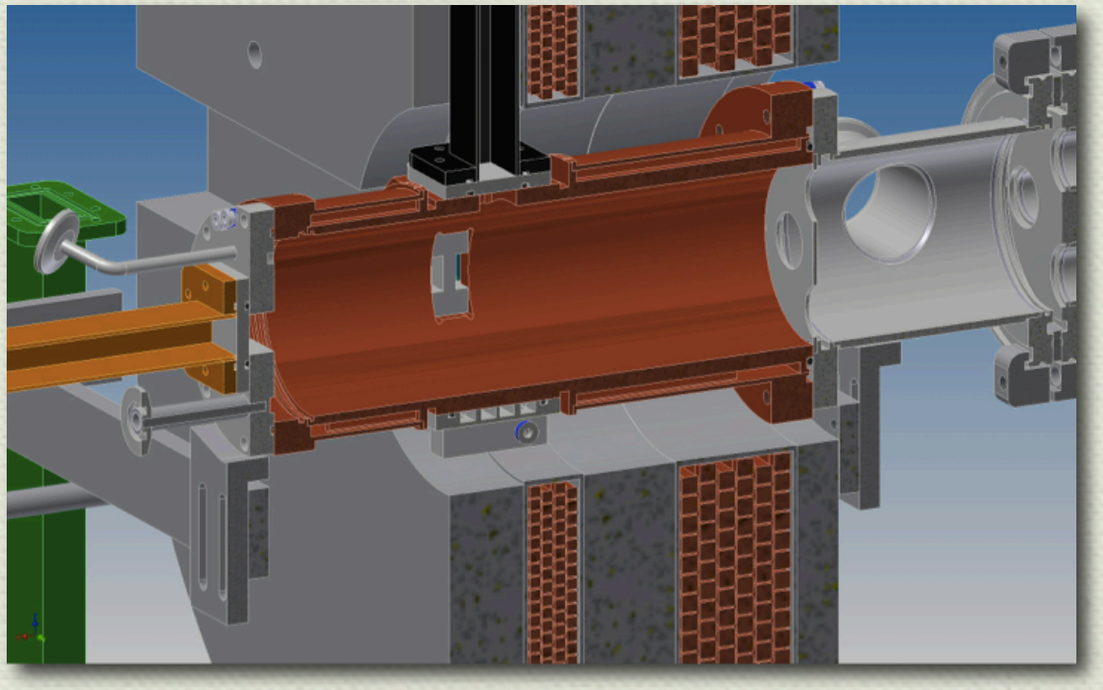

"Microwave-absorption-oriented" design

Launcher by "two-waveguides-array": lobe tilt by phase shift for obtimizing oblique coupling of O-modes --> modal conversion

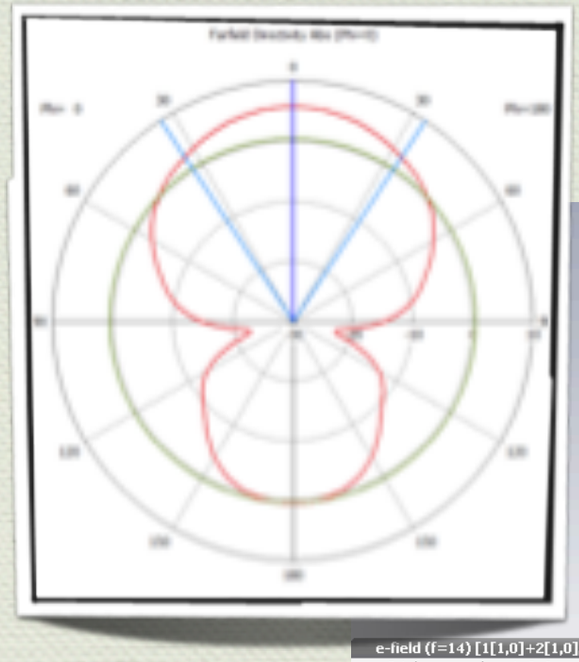

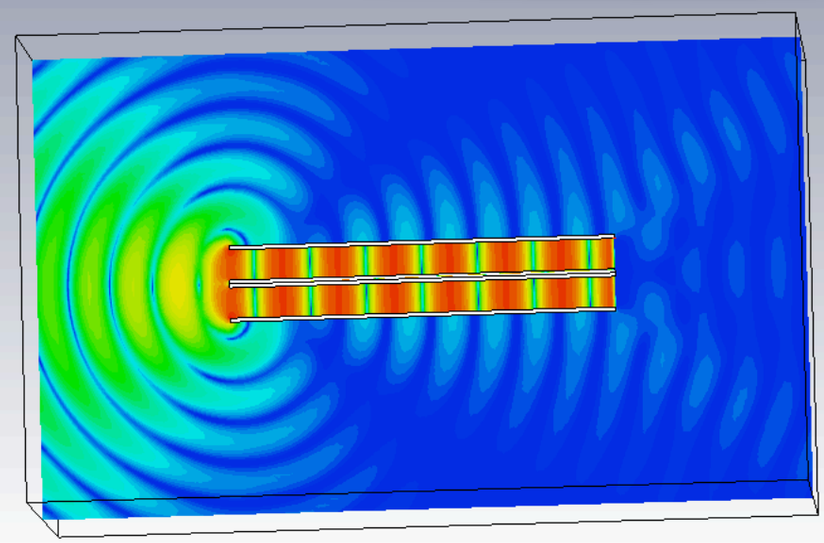

e-field (f=14) [1[1,0]+2[1,0],[15.2]] (peak)
Cutplane normal: 1, 0, 0
Cutplane position: 0
Component: Abs
2D Maximum: 4977

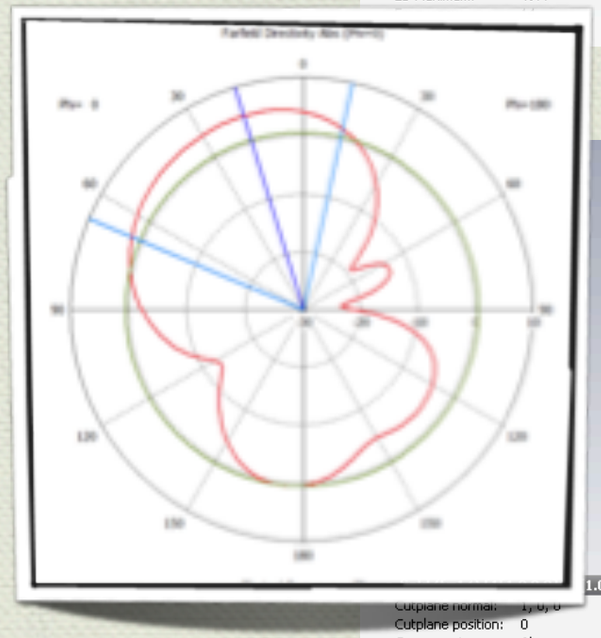

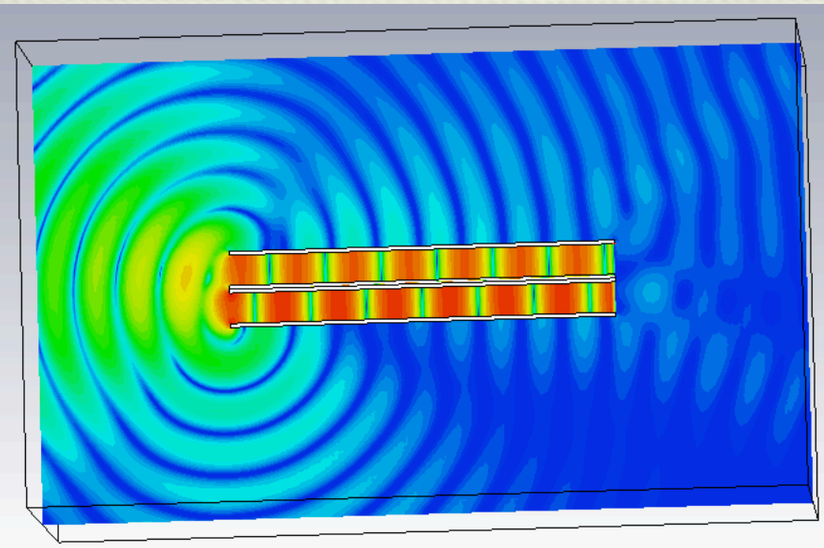

1.0,45],[15.2]] (peak)
Cutplane position: 0
Component: Abs
2D Maximum: 5031
Frequency: 14
303.75

Mechanical Implementation at LNS

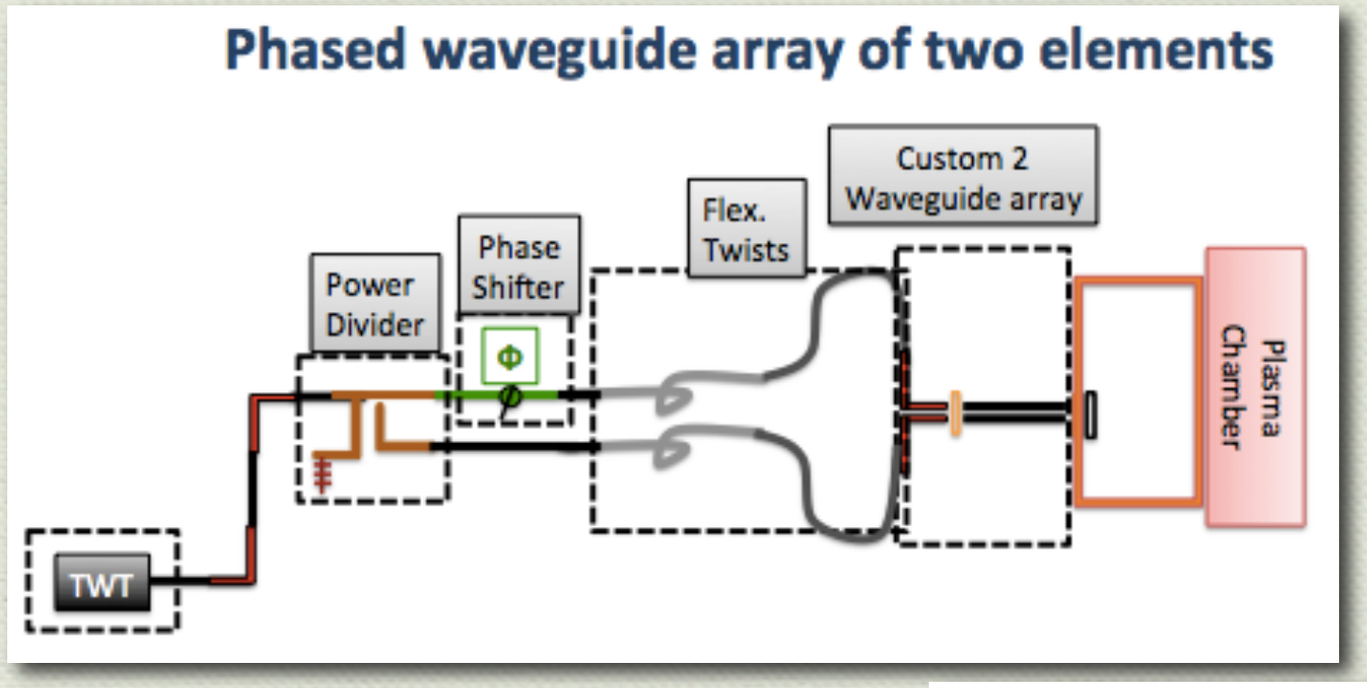

microwave launcher: proposed setup

- TWT ampl. 13.75-14.5 GHz
- Power divider
- Phase shifters
- flexible waveguides

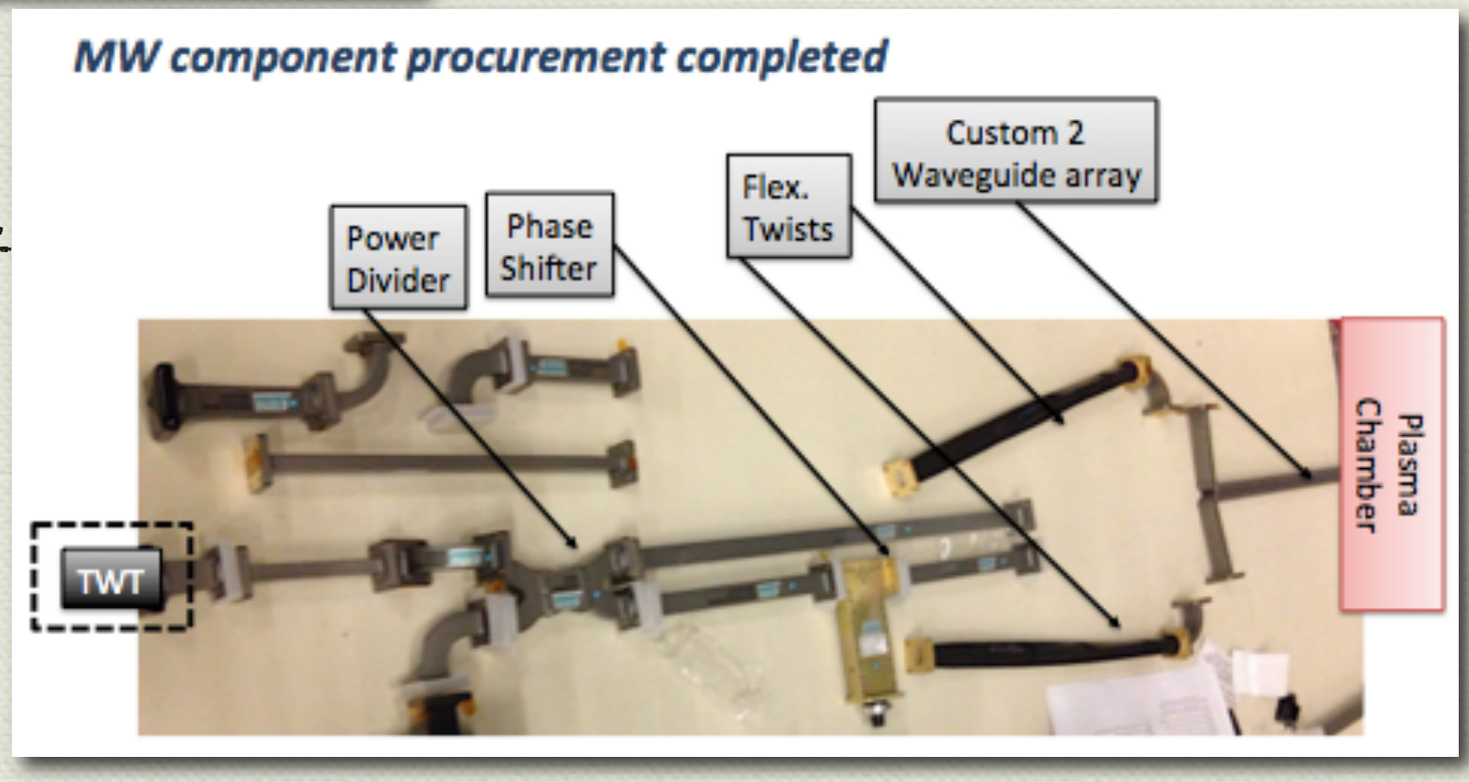

Charge breeding process

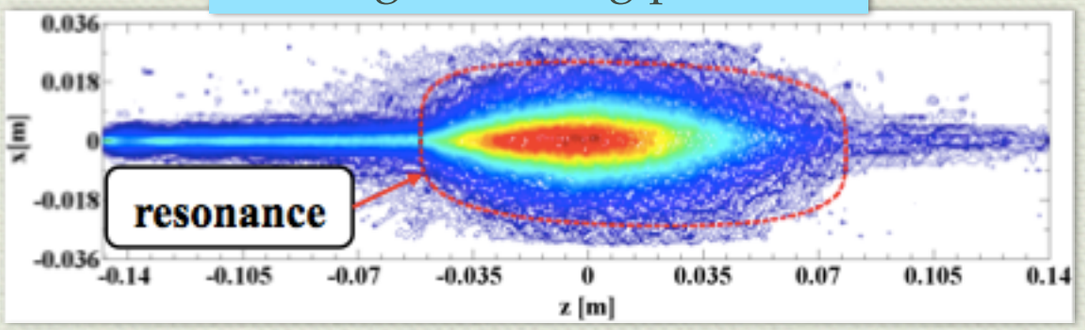

A. Galatà et al. ThuM08

Beam diagnostics

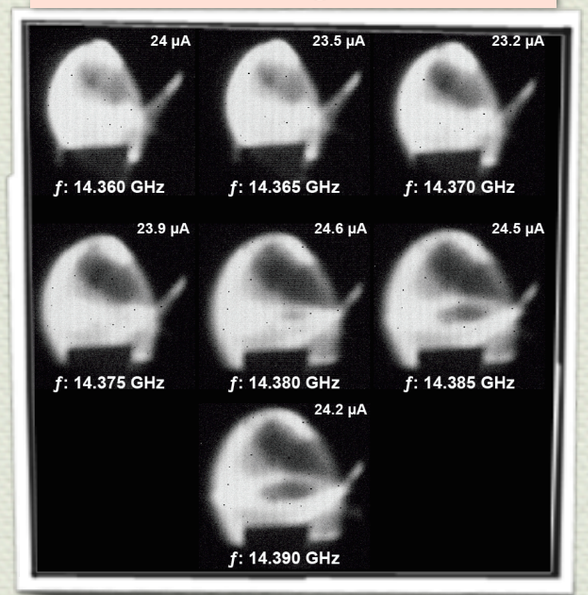

D. Nicolosi et al. MonPE21

H+ formation in MDIS

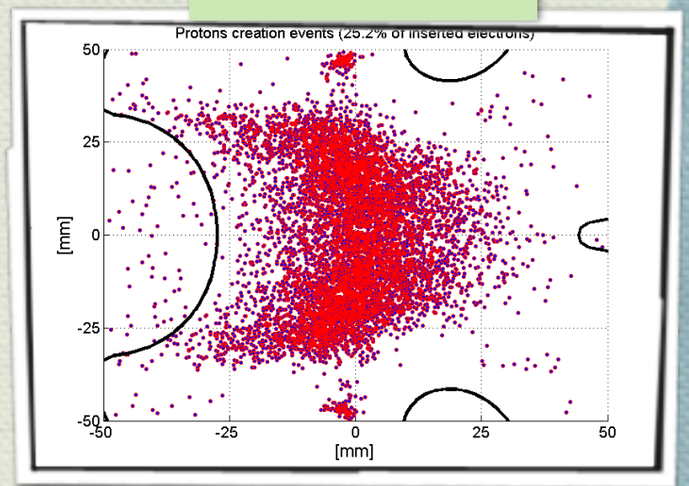

L. Neri et al. TuePE11

wave-plasma interaction

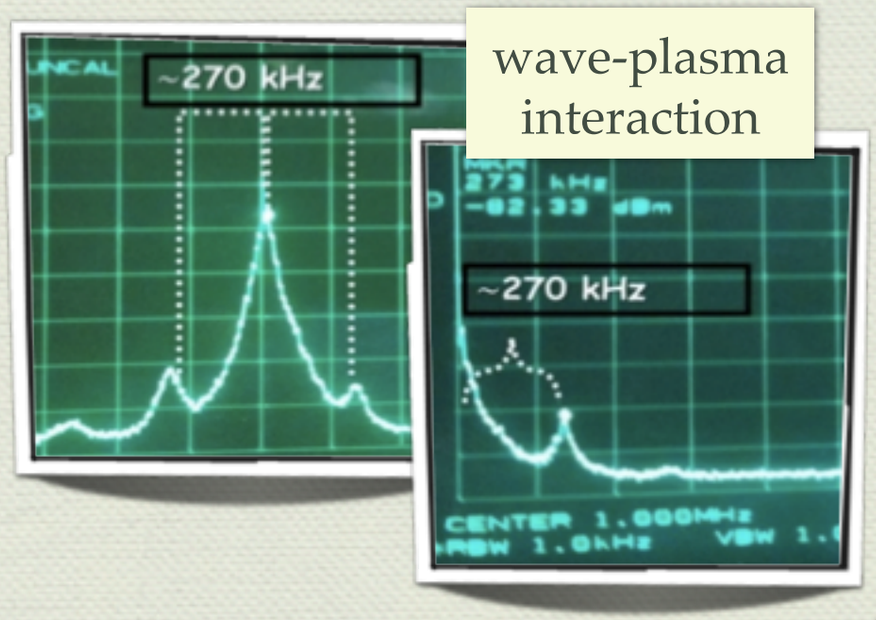

G. Castro et al. TuePE05

Several efforts in diagnostics and modelling

pin-hole camera setup

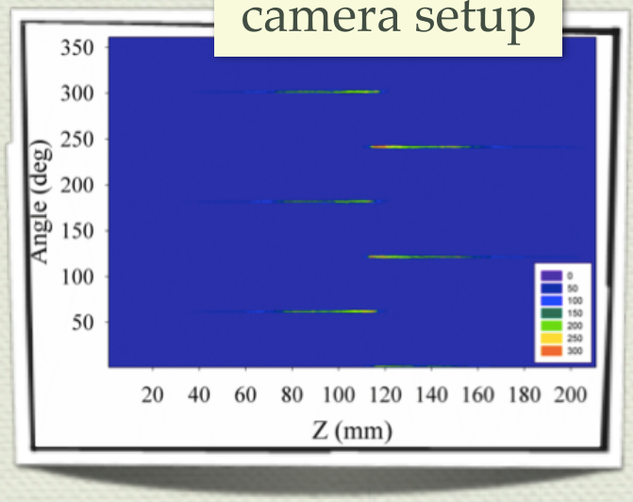

R. Rach et al. ThuPS09

THANK YOU FOR YOUR ATTENTION!!

interferometry

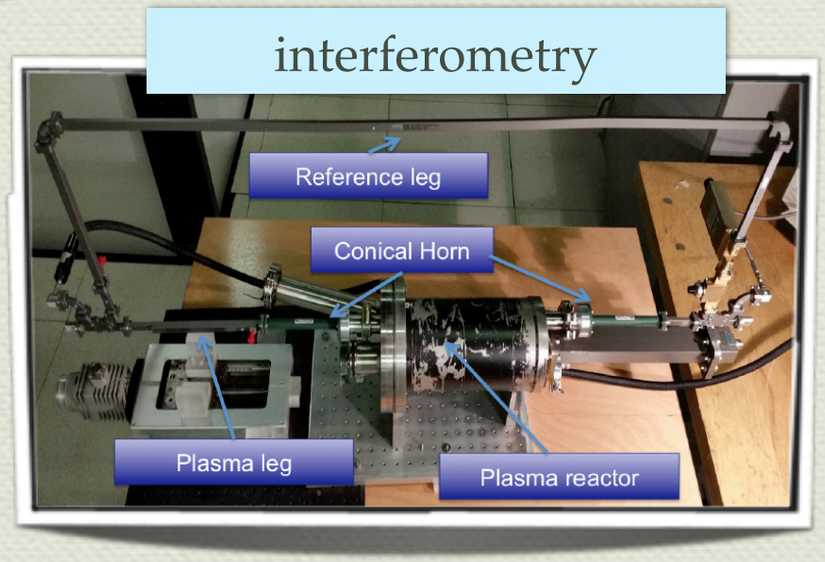

G. Torrisi et al. TuePS27

THANK YOU FOR
YOUR
ATTENTION!!

Boosting plasma density in a Two-Pumping-wave Scenario

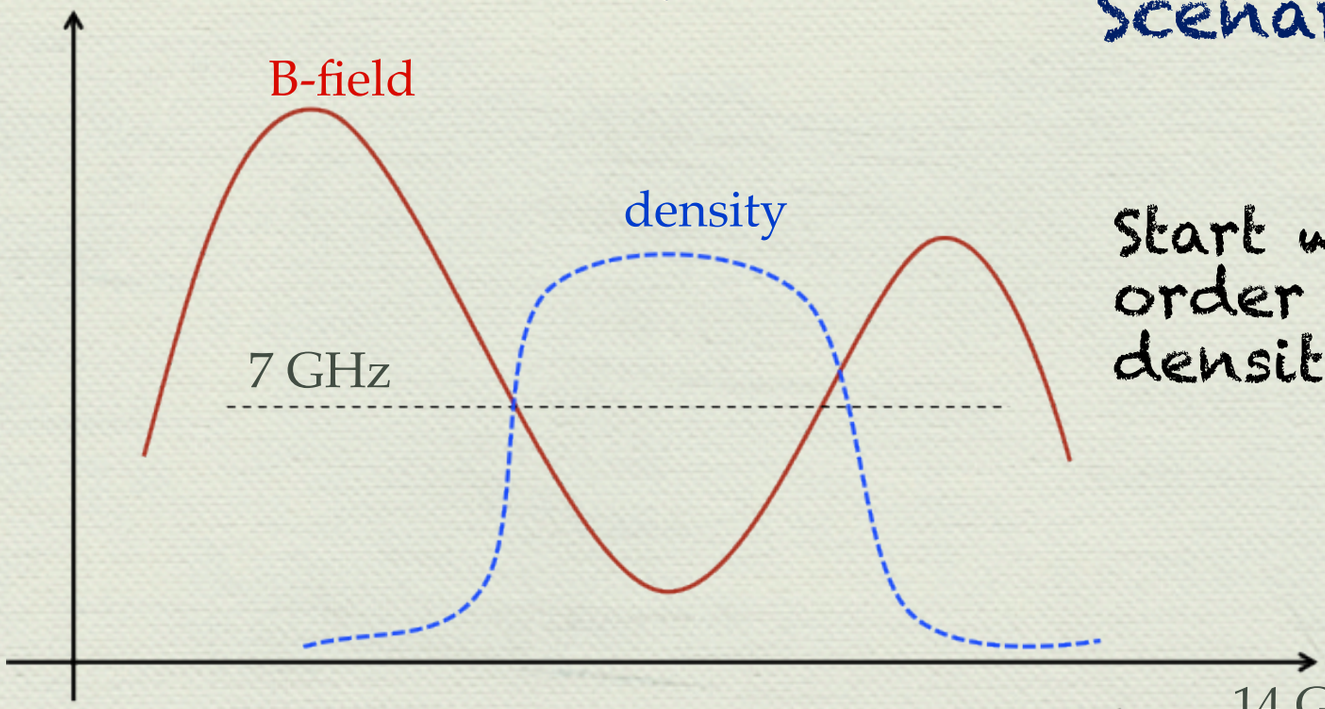

Start with one frequency in order to establish a proper density profile

Launch a second wave for modal conversion and second harmonic heating

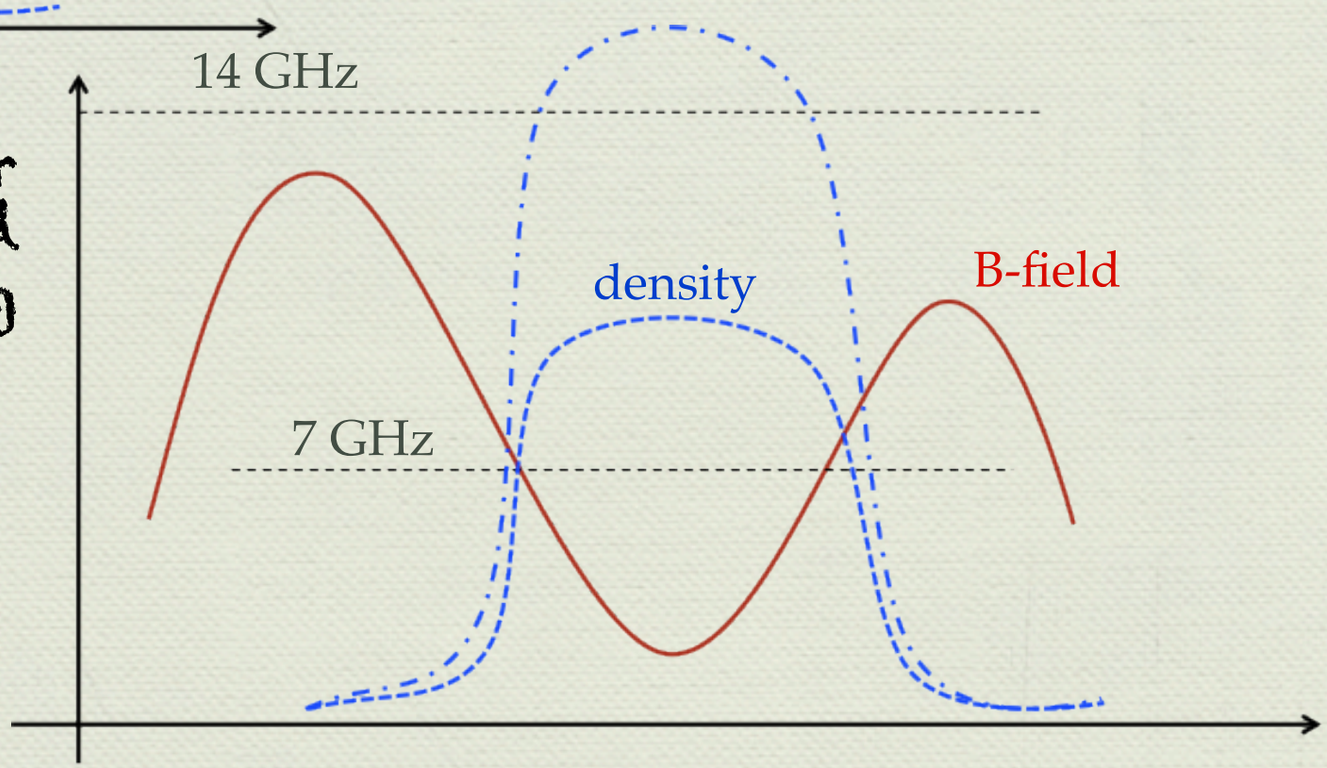

- the modal conversion is a density-magnetic field profiles dependent process
- -> mastering plasma structure is mandatory for conversion optimisation

Mastering of plasma density structure

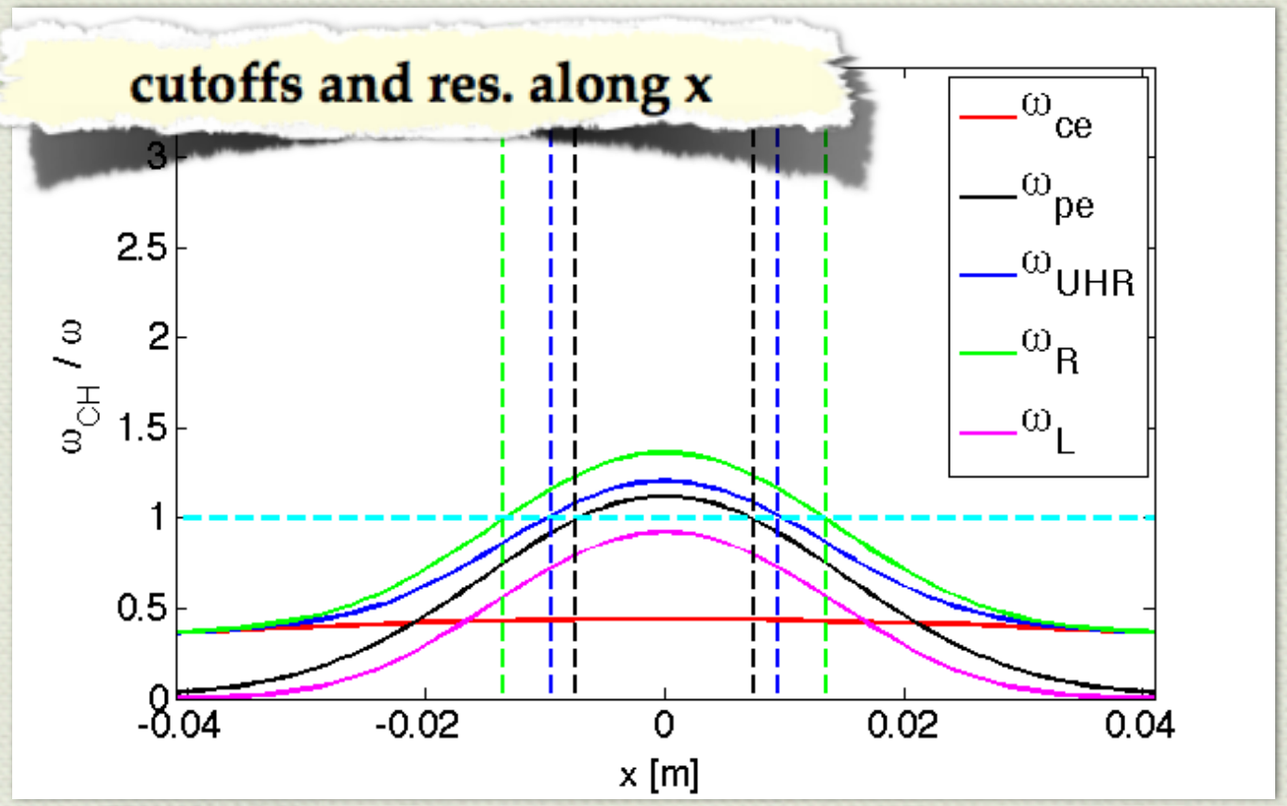

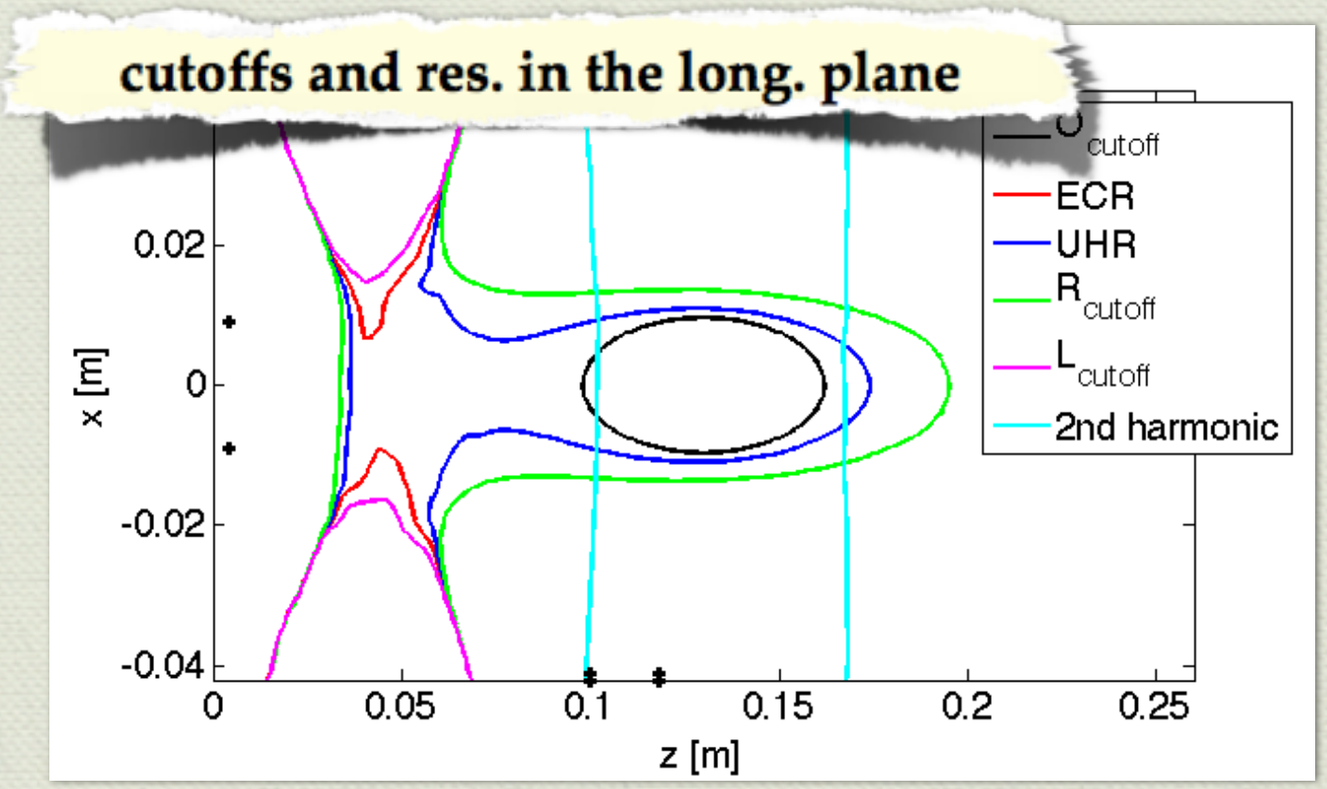

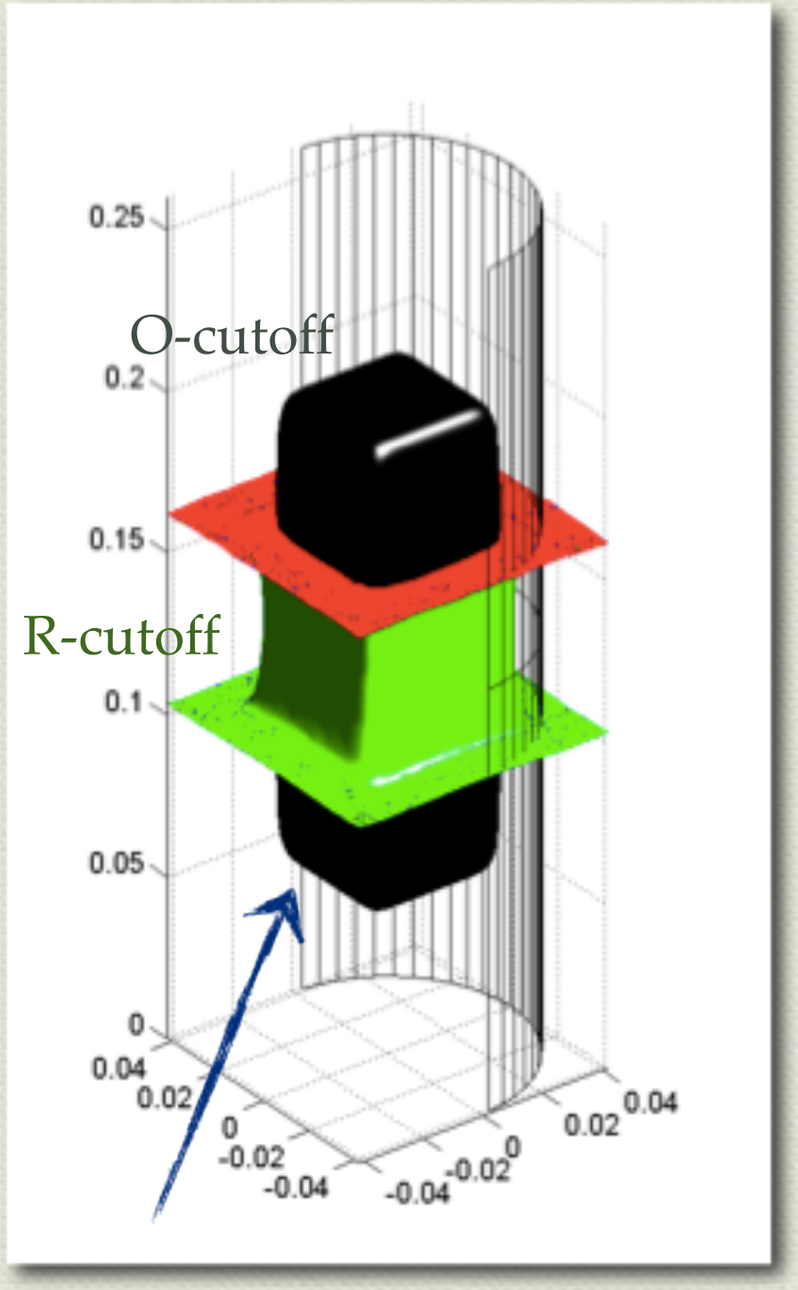

Cut-offs and resonances in 3D view

"Microwave-absorption-oriented" design

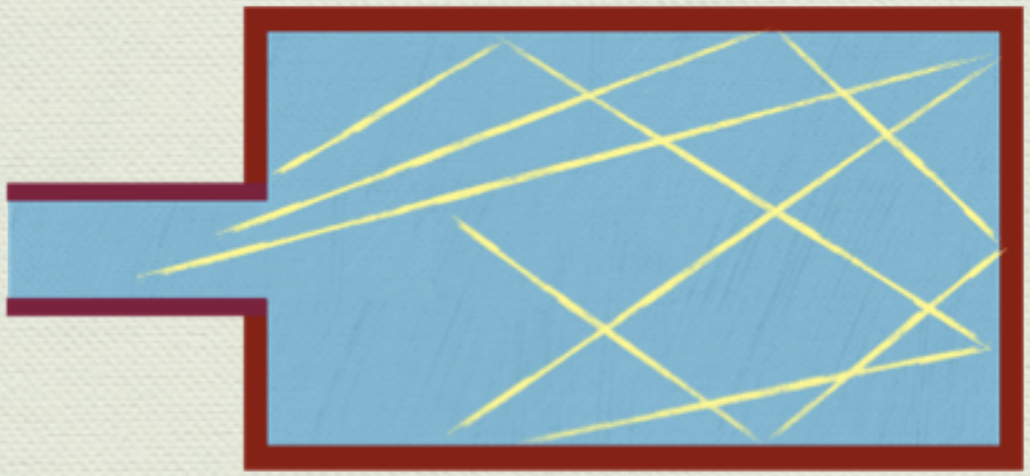

M.A. + guiding + resonator scheme

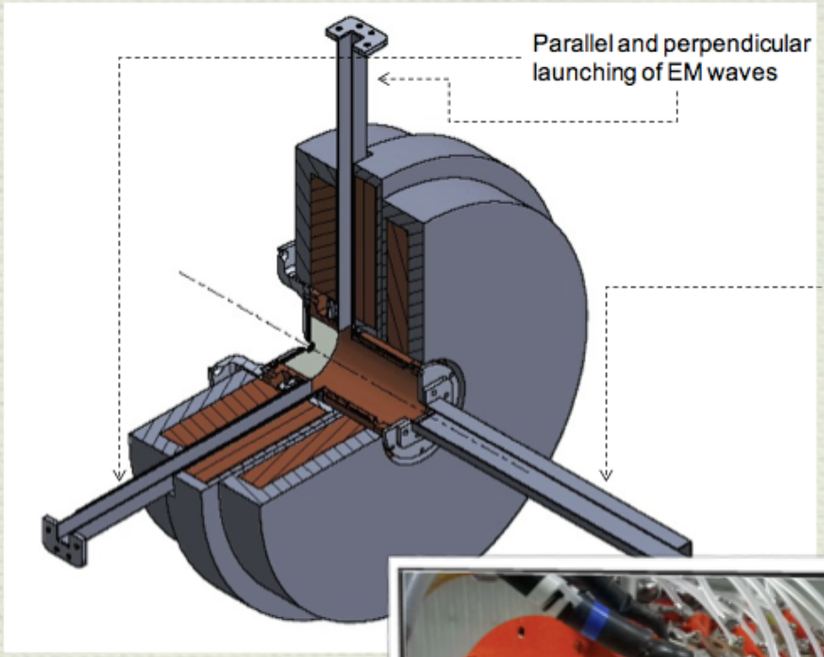

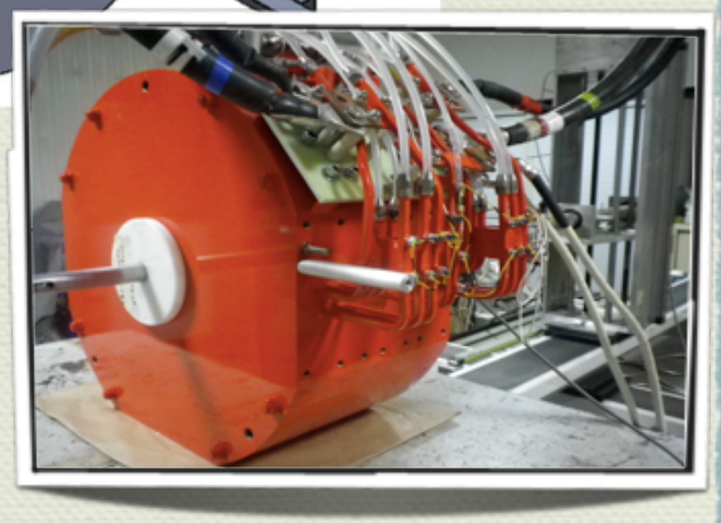

Full-wave calculation of the electric field distribution inside the new Flexible Plasma Trap at INFN-LNS

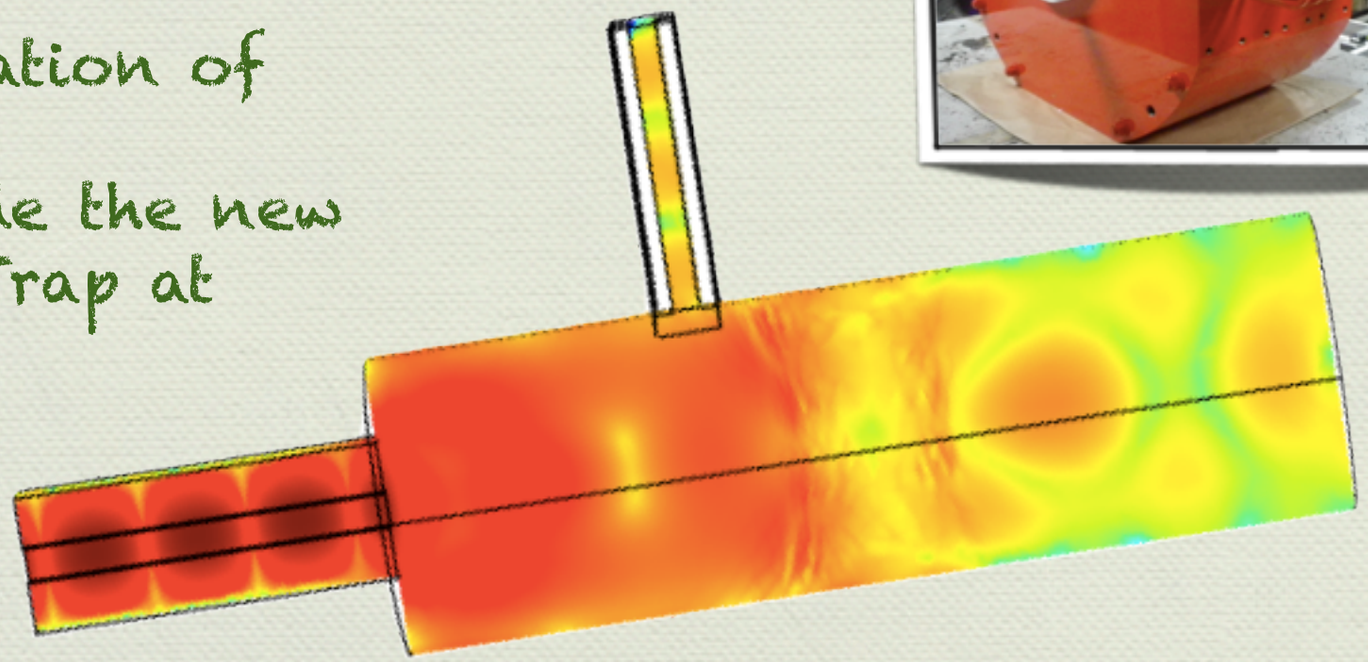

Plasma inspection after energy filtering

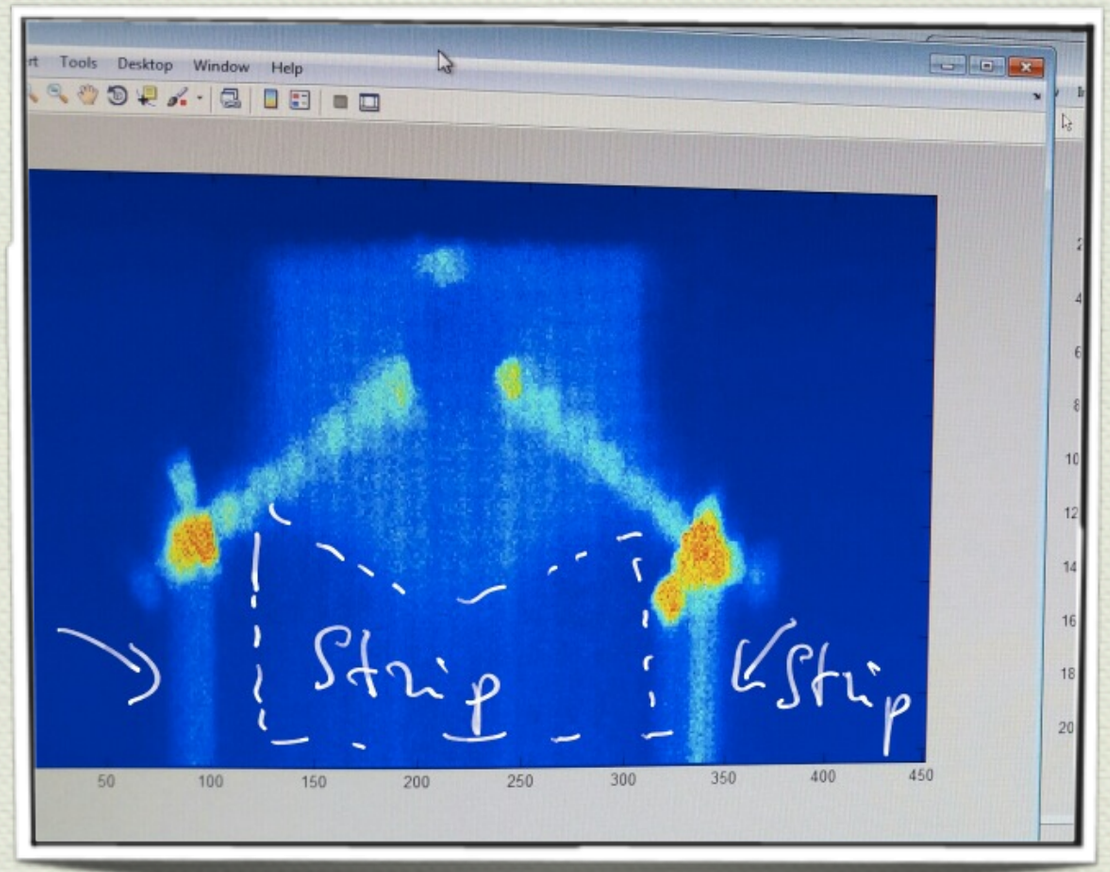

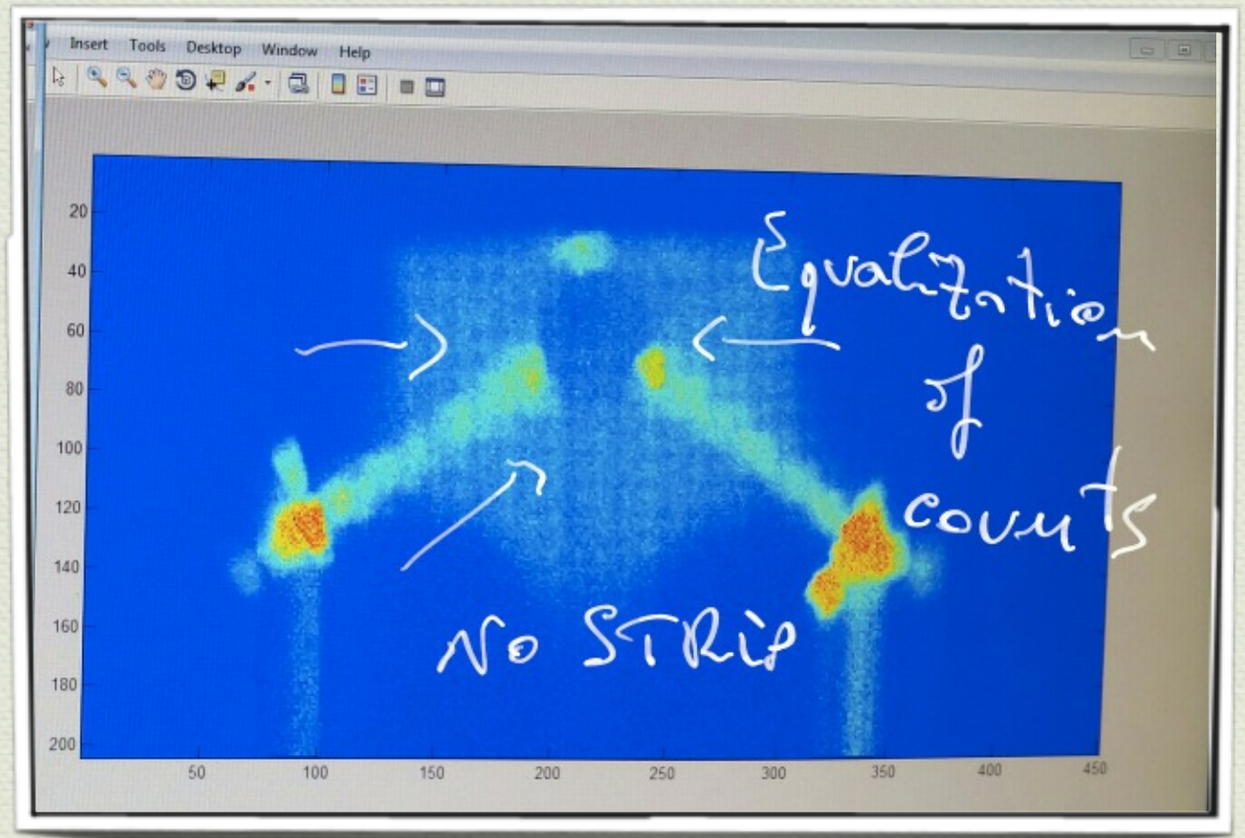

The image is given by the exposure time plus the CCD data transfering across the vertical registers (still active sensor). A "strip" similar to well-known astronomical photigrphy drawbacks, appeared. Post-processing eliminated most of the unwanted counts in the photon counting images

Plasma inspection by energy filtering

Photon Counting – each picture frame is a matrix of pixels where single photons have impinged

1. A single photon can excites a group of pixels;

2. Hence, the local maximum is a 9x9 pixels submatrix is searched → in case of multi-maxima, the submatrix is not considered;

3. Each analysed frame is then summed to the others (>1000);

4. The counts frequency histogram is therefore retrieved, determining also the overall 2D image.

$$E(eV)=\text{n.of counts} \times E^{e\text{-}h}(eV) \times \text{sensitivity}$$

3.65 eV **1.3**

Excellent energy resolution
137 eV@Fe-Kα

SDD and HpGe Set-up

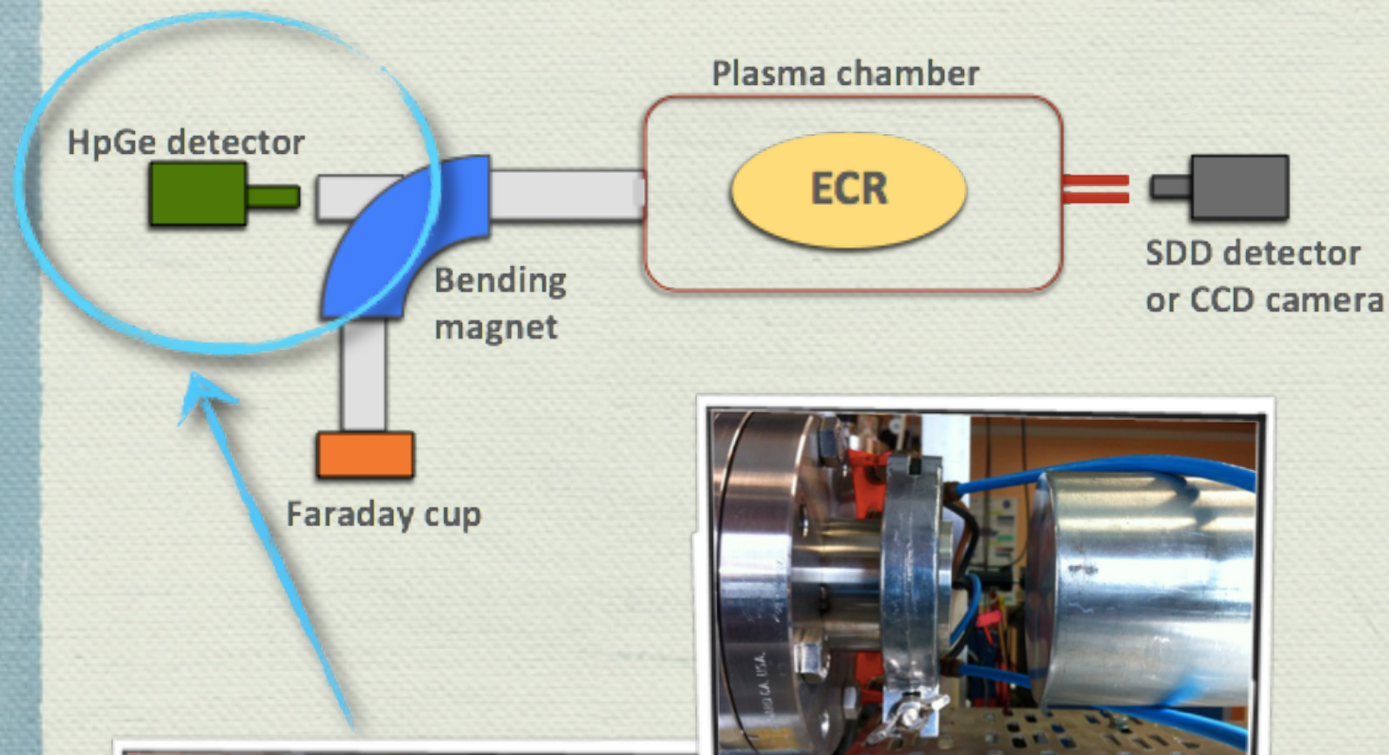

SDD - Silicon Drift Detector (SDD - 80 mm² active area) for measuring **warm X-rays** in the 2.5-30 keV domain.

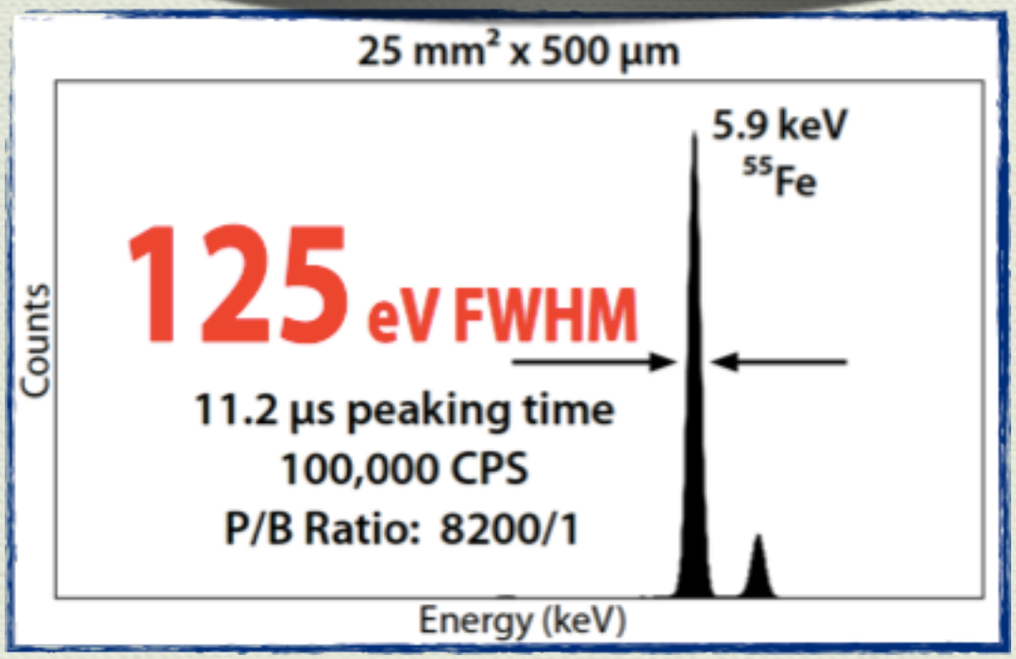

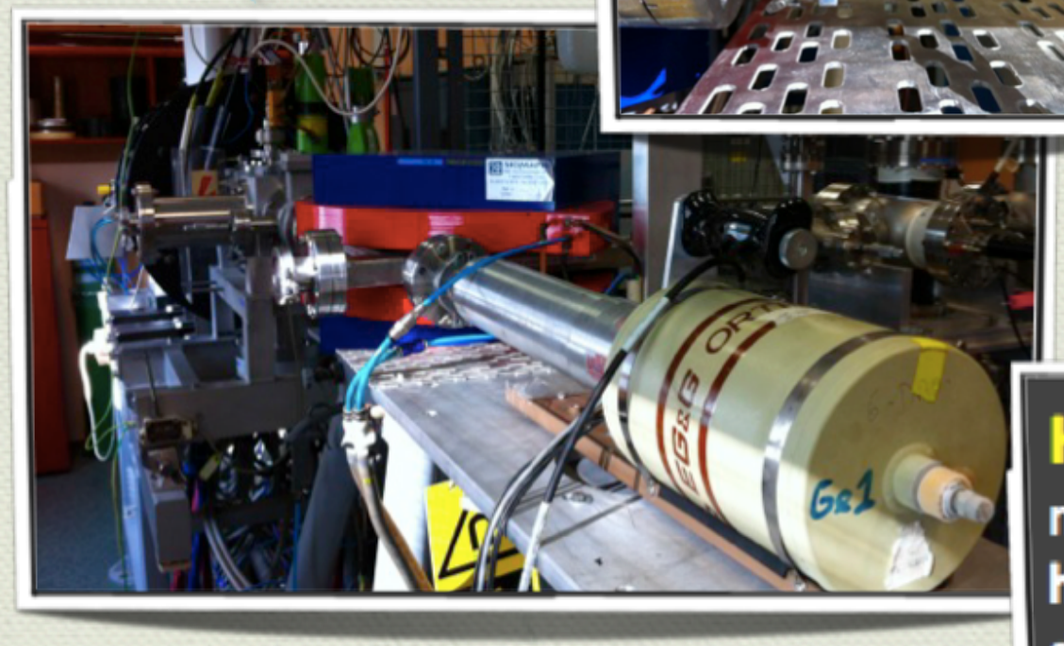

HpGe - HeGe Detector (3000 mm²) active area for measuring **hot X-rays** in the energy domain 30-400 keV

SDD/HpGe - Data Analysis

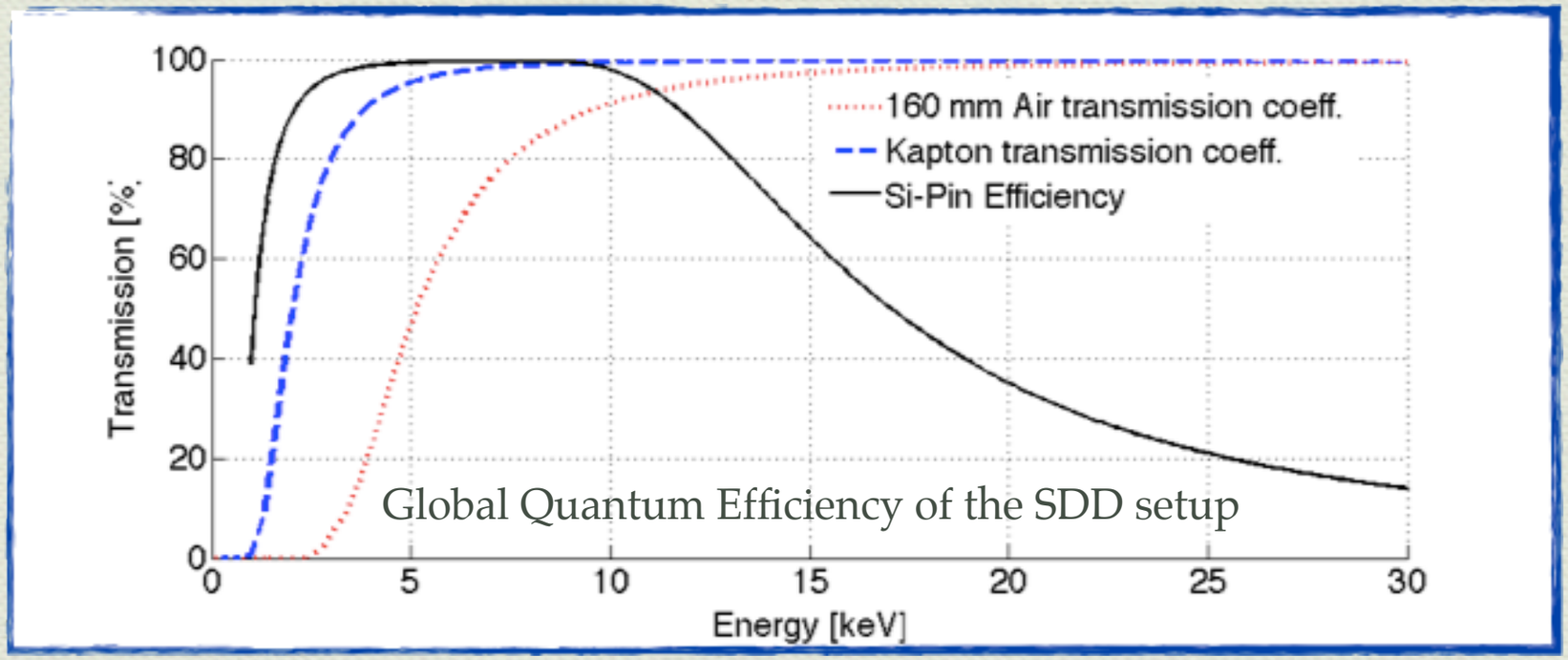

Global Quantum Efficiency of the SDD setup

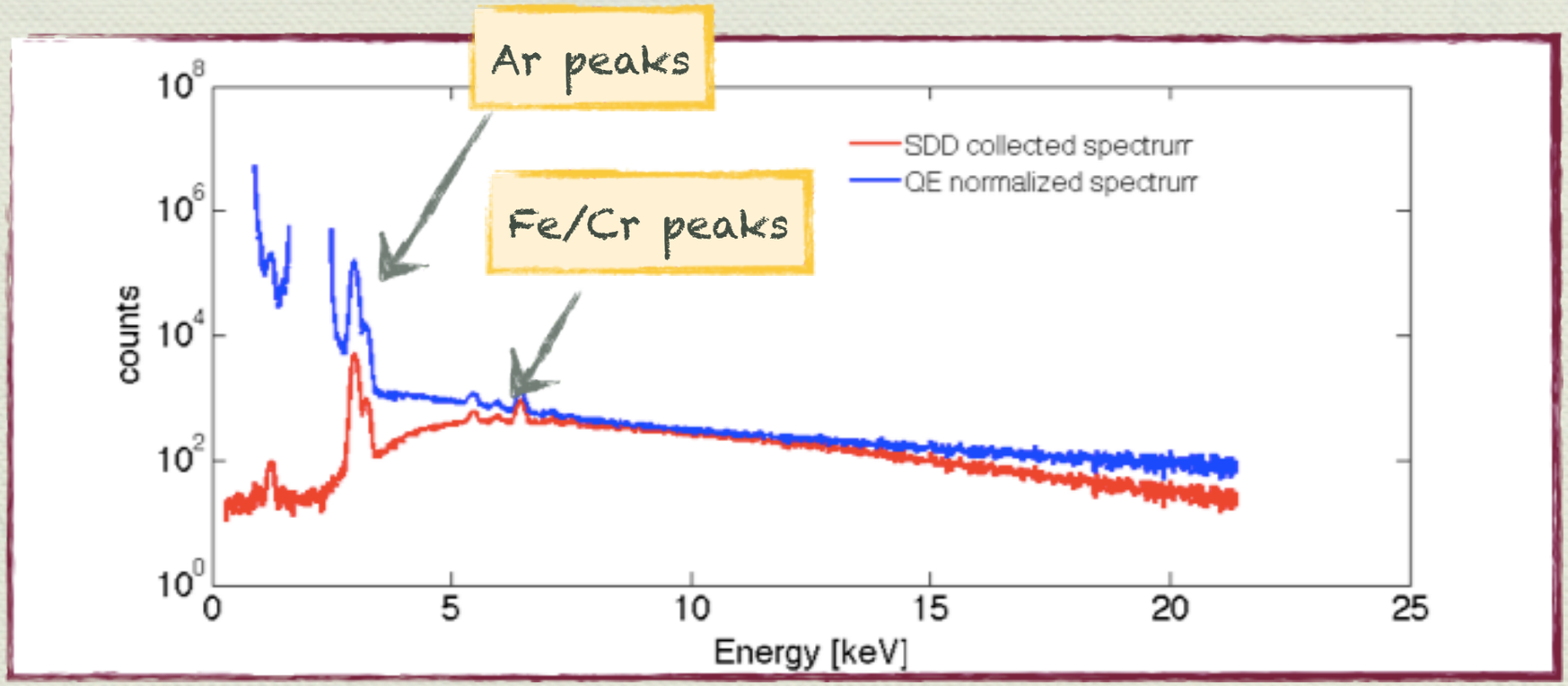

Spectral renormalization for the SDD setup

X-ray imaging

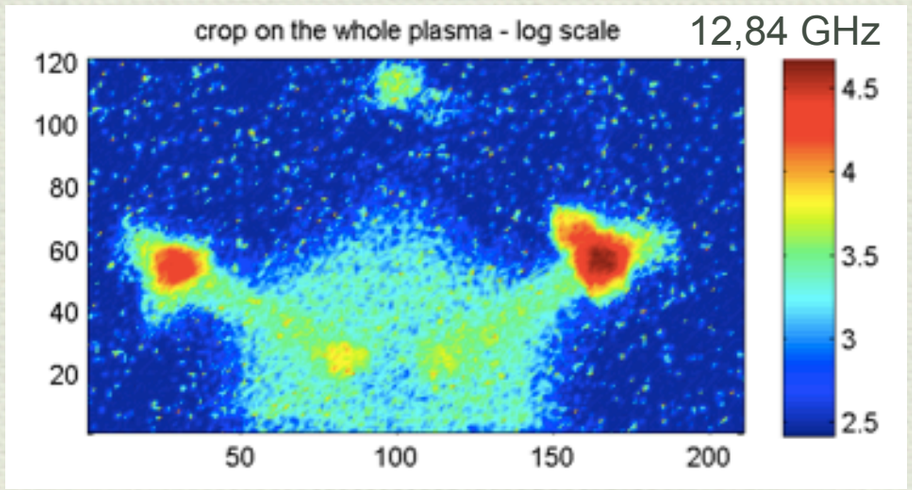

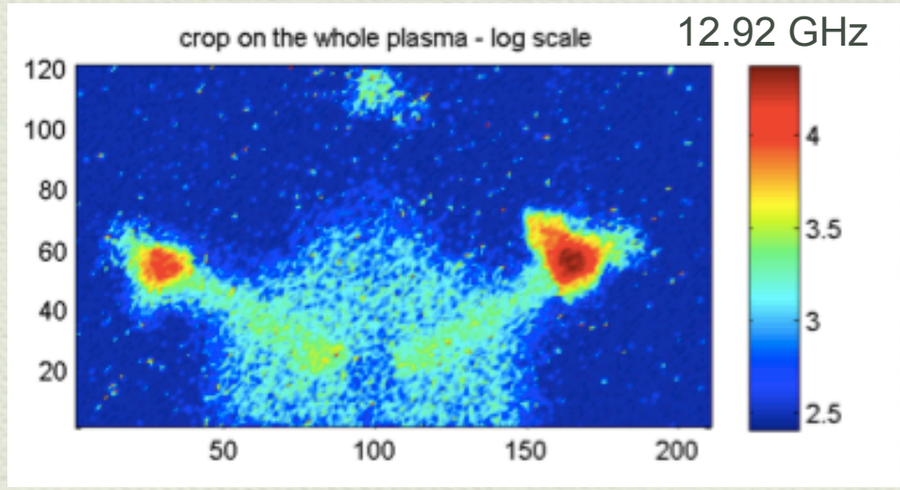

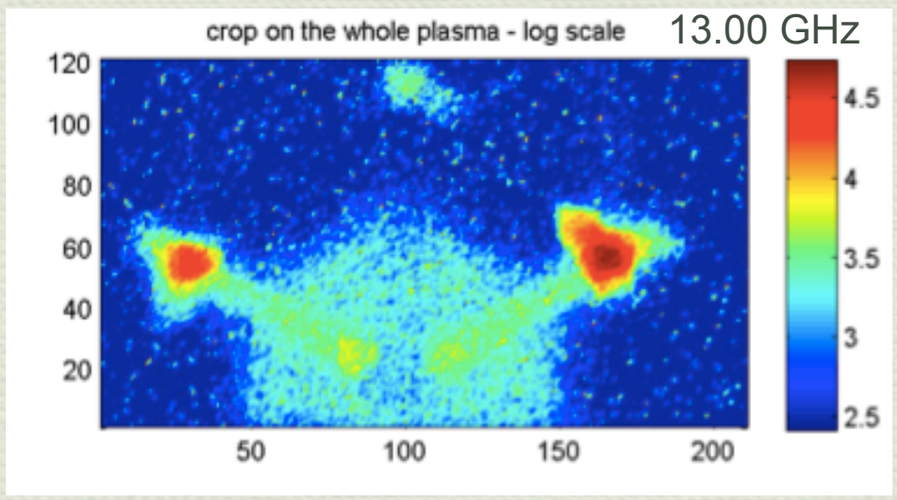

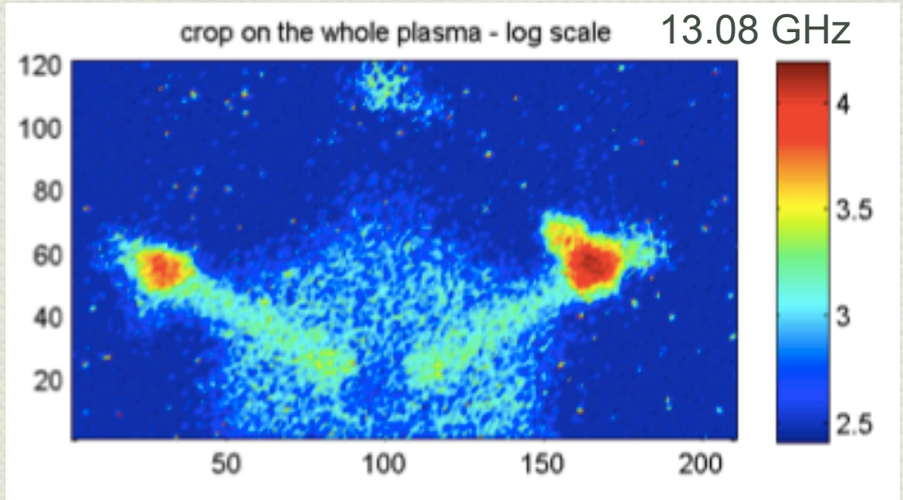

X-ray Imaging

Preliminary results

- ✓ **Magnification= 0,09**
- ✓ **Al-window= 6 µm**

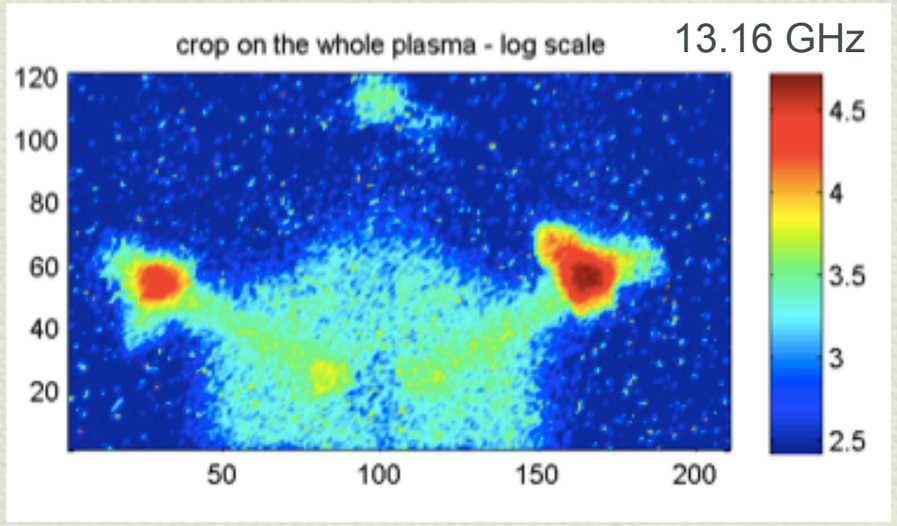

a first rough characterization was done with a low magnification: Regions of Interest were settled and the set of frequencies for investigating FTE was restricted to 12.84 12.92 13.24 Gigaherts

Mechanical Implementation at LNS

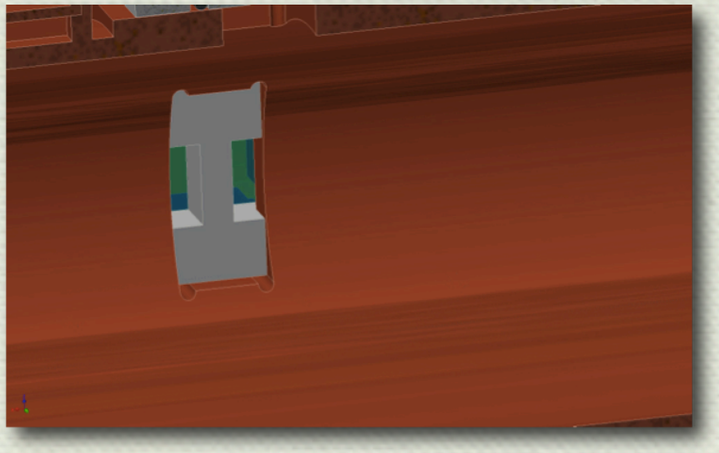

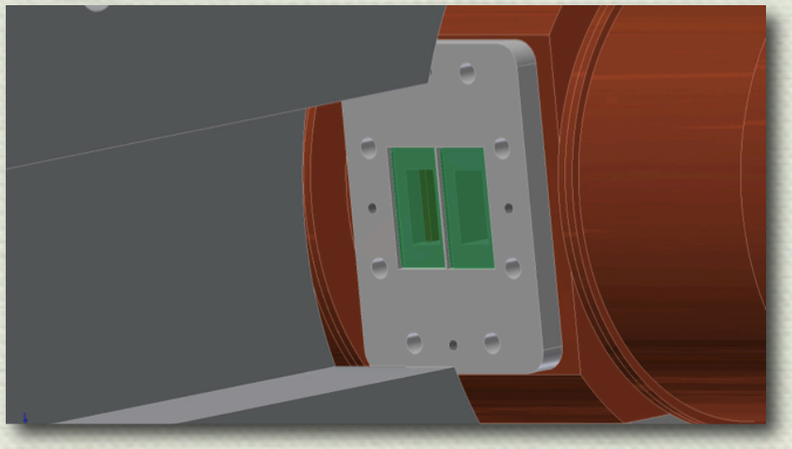

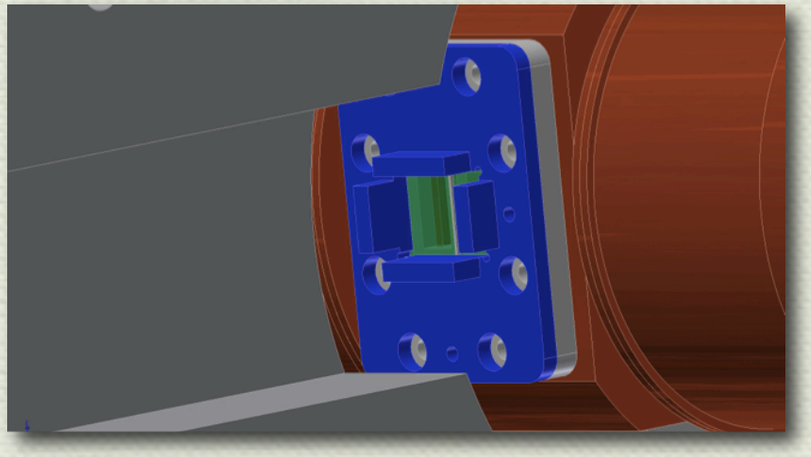

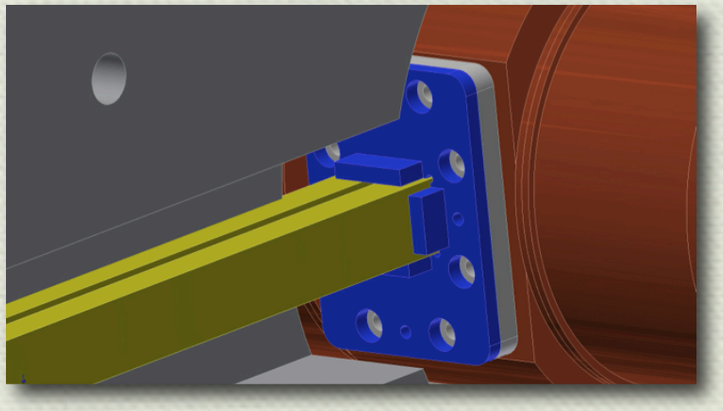

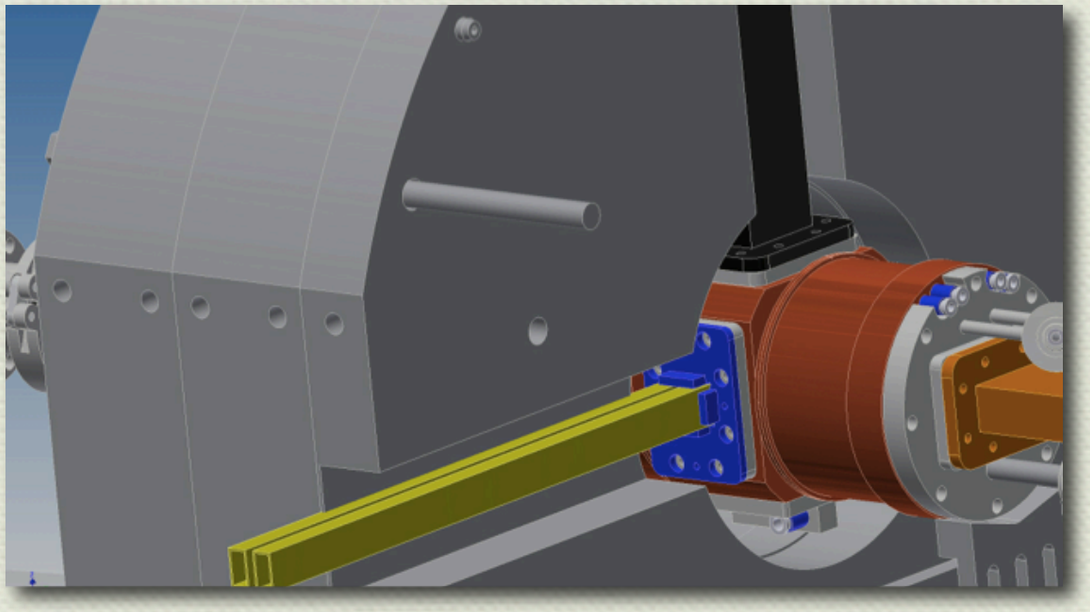

Parallel and Perpendicular access to the plasma chamber in order to operate in double frequnecy/double heating mode: axial ---> ECR, radial ---> EBW-heating